EPRI

DEVELOPMENT OF SEISMIC HAZARD INPUT FOR THE ADVANCED LIGHT WATER REACTOR SEISMIC PRA

Revision 1

Prepared by

Martin W. McCann, Jr.
John W. Reed
Auguste C. Boissonnade

Jack R. Benjamin and Associates, Inc.
444 Castro Street, Suite 501
Mountain View, California 94041

Prepared for

Electric Power Research Institute
3412 Hillview Avenue
Palo Alto, California 94304

EPRI Project Manager

S. Gray
Nuclear Power Division

February 1990

DEVELOPMENT OF SEISMIC HAZARD INPUT FOR THE

ADVANCED LIGHT WATER REACTOR SEISMIC PRA

Revision 1

Prepared by

Martin W. McCann, Jr.
John W. Reed
Auguste C. Boissonnade

Jack R. Benjamin and Associates, Inc.
444 Castro Street Suite 501
Mountain View, California 94041

Prepared for

Electric Power Research Institute
3412 Hillview Avenue
Palo Alto, California 94304

EPRI Project Manager

S. Gray
Nuclear Power Division

February 1990

EXECUTIVE SUMMARY

This report presents the results of an evaluation to define the seismic hazard input for the Advanced Light Water Reactor (ALWR) seismic probabilistic risk assessment (PRA). The ALWR seismic hazard (ALWR SH) consists of two parts. The first is a hazard curve that defines the mean frequency of exceedance of peak ground acceleration (PGA). The second part is a response-spectrum shape, which scaled to a PGA level defines the ground response spectral acceleration input to a plant. Using the results of the Electric Power Research Institute (EPRI)/Seismicity Owners Group (SOG) seismic hazard project, the ALWR SH has been evaluated for the Eastern United States (EUS), east of 105°W longitude. For possible ALWR sites located in the Western United States (WUS), a site-specific seismic hazard analysis must be performed to provide input to the PRA.

The development of the ALWR SH considered a number of factors. These included a target risk level for seismic events which is defined in terms of the mean frequency of core damage, an estimate of the ALWR core-damage fragility and the seismic hazard in the EUS. Each of these factors contributed to the development of the ALWR SH such that the combination of the ALWR SH curve and the system level fragility (e.g., conditional fraction of core damage as a function of PGA) to determine the frequency of core damage is exactly equal to the ALWR target seismic risk level of 10^{-6} events per year.

The ALWR SH is specified for five site (rock/soil) conditions so as to be applicable to a range of possible plant locations in the EUS. The ALWR SH is applicable to all locations in the EUS (east of 105° W longitude) with certain exceptions. Because the ALWR SH is a bounding curve, a site-specific hazard analysis is not required for the majority of locations in the EUS. The exceptions are areas that may have hazard levels that exceed the ALWR SH (e.g., New Madrid). At these locations the ALWR seismic risk may exceed the target risk level. Areas in this category are identified for each site category. Potential ALWR sites located in these areas may require a site and plant specific evaluation to demonstrate that the seismic risk is acceptable

TABLE OF CONTENTS

LIST OF TABLES

LIST OF FIGURES

1.0 INTRODUCTION

1.1 Overview

As part of the probabilistic risk assessment (PRA) for the Advanced Light Water Reactor standardized power plant design (ALWR), the risk of core damage due to seismic events is evaluated. The objectives of the seismic risk portion of the PRA are to assure that the standardized plant at the certification stage has a balanced design from a seismic risk standpoint and to demonstrate that the ALWR Requirements Document risk goals can be met.

In order to evaluate the seismic risk of core damage for the ALWR, the following inputs are required:

- seismic hazard,
- component (i.e., structure and equipment) fragility information, and a
- seismic systems model.

To the extent that the ALWR seismic fragility (e.g., median capacity and variability) can be determined from the plant design, the seismic risk associated with the ALWR can be computed. The plant systems model (e.g., event trees and fault trees) can be used to evaluate the plant level fragility (e.g., conditional fraction of core damage as a function of ground motion level). Given an estimate of the plant seismic capacity, the mean frequency of core damage can be determined by integrating the plant mean fragility curve and the ALWR seismic hazard (ALWR SH).

1.2 Objectives

The objective of this evaluation is to determine the seismic hazard input to the ALWR seismic PRA. The ALWR seismic hazard (SH) consists of two parts. The first is a hazard curve that defines the mean frequency of exceedance per year of peak ground acceleration (PGA). The second part is a response-spectrum shape, which scaled to a PGA level defines the ground response spectral acceleration input to a plant. The ALWR SH is defined in terms of a bound on the mean frequency of exceeding levels of PGA. The ALWR SH curve is a bounding curve such that, when integrated with the mean plant fragility for core damage, the resultant mean frequency of core damage is equivalent to the ALWR seismic risk goal. By this definition the notion of a 'bounding' seismic hazard curve is applicable only in the sense, when integrated with a plant level fragility curve. In this evaluation a target seismic risk level is specified in terms of an achievable mean frequency of seismically induced core damage.

By examining the seismic hazard in the U.S., an evaluation is made to determine if a bound on seismic hazard can be defined that does not result in a mean frequency of core damage that exceeds the target risk level. If the ALWR SH bounds the seismic hazard everywhere, then a bound on the ALWR seismic risk can be determined and site-specific hazard analyses would not be required (since all sites have a hazard level equal to or less than the ALWR SH). If the mean hazard curve at certain locations exceeds the ALWR SH, the risk of core damage may be to high (i.e., higher than the target risk level).

To account for the range of possible site (soil) conditions that may exist at ALWR locations, the ALWR SH is developed for five site categories. These include rock and four soil categories. Note, that only ground shaking hazards are considered in this study. Other seismic hazards such as liquefaction or soil failure are not addressed.

The purpose of this study is to define the ALWR SH based on a consideration of the seismic hazard in the U.S. As discussed later, the ALWR will be applicable to the majority of locations in the Eastern U.S. (EUS) (east of 105° W longitude). Areas where the seismic hazard is anticipated to be higher than the ALWR SH (e.g., Western U.S. (WUS)) are identified.

1.3 Report Scope

In Section 2 the procedure that is used to develop the ALWR SH is described. A detailed discussion is given that defines the ALWR SH and the factors considered in its development. The process that was used to evaluate the seismic hazard in the entire EUS is also discussed.

Based on past seismic PRA experience for commercial power reactors, it is anticipated that high levels of ground motion (greater than 1.0g) that may be generated by moderate- to large-magnitude earthquakes will be important contributors to the frequency of core damage. In this case, the estimation of the likelihood of high-ground motion levels must be considered.

Section 3 discusses the approach that is used to assess the seismic hazard in the EUS. The discussion includes an overview of the EPRI/SOG methodology to perform seismic hazard assessments. The EPRI/SOG methodology and data are used to perform site-specific hazard evaluations for sites in the EUS.

Section 4 presents the ground motion models that are used in the hazard assessment. In addition a review of information in the literature was conducted to gather information on the variability and limits of strong ground motion. The results of this review were used to specify the logarithmic standard deviation on attenuation and a truncation of the probability distribution on ground motion.

As part of the effort to determine a measure of seismic hazard throughout the EUS, regional-hazard calculations are performed. These calculations provide an estimate of the hazard for a closely-spaced grid of sites that covers the entire EUS. Coupled with site-specific hazard assessments for selected locations using the EPRI/SOG seismic hazard methodology and data, a robust measure of the seismic hazard virtually throughout the EUS is obtained. The results of these analyses and the development of the ALWR SH response spectra are reported in Section 5.

Section 6 describes the development of the ALWR mean core damage fragility curve, which is used to calculate the frequency of core damage.

In Section 7 the results of ALWR seismic risk calculations for sites in the EUS are compared to the ALWR seismic risk goal. These evaluations are used to determine the ALWR SH and to identify areas where the ALWR seismic risk goal may be exceeded.

Section 8 summarizes the results of this study and defines the ALWR SH, including areas where site-specific hazard analyses are required.

2.0 ALWR SEISMIC HAZARD EVALUATION

2.1 Introduction

The ALWR SH is being developed to define the seismic hazard input to the ALWR seismic PRA. A primary objective of this evaluation is to establish a measure of the seismic hazard that ideally, is applicable to all locations in the U.S. and possible site conditions. For those locations and site conditions where the ALWR SH is applicable, a site-specific hazard assessment would not be required since the actual hazard at the site is by definition, bounded. For locations where the ALWR SH does not apply, a site-specific hazard assessment is required.

In this section the procedure that is followed to develop the ALWR SH is described. Section 2.2 defines the factors that are considered in the evaluation. As part of this discussion the definition and interpretation of the ALWR SH curve is provided. Section 2.3 describes the procedure to calculate seismic risk. In Section 2.4 the method to evaluate the seismic hazard in the U.S. is discussed. In Section 2.5 the basis for the ALWR SH is described. Section 2.6 defines the ALWR target seismic risk level. Section 2.7 considers the level of seismic hazard that satisfies the target risk level.

2.2 ALWR SH Assessment

The ALWR SH is being developed for use in the seismic PRA being performed for the ALWR at the certification stage. The input to the seismic PRA consists of a seismic hazard curve that quantifies the mean frequency of exceedance of levels of PGA and a ground-response spectrum shape (normalized to 1.0g). Figure 2-1 illustrates the form of these two parts of the ALWR SH. The ground-response spectrum characterizes the response of structures and equipment items as a function of their dynamic response frequency and is used in the assessment of component seismic fragility data.

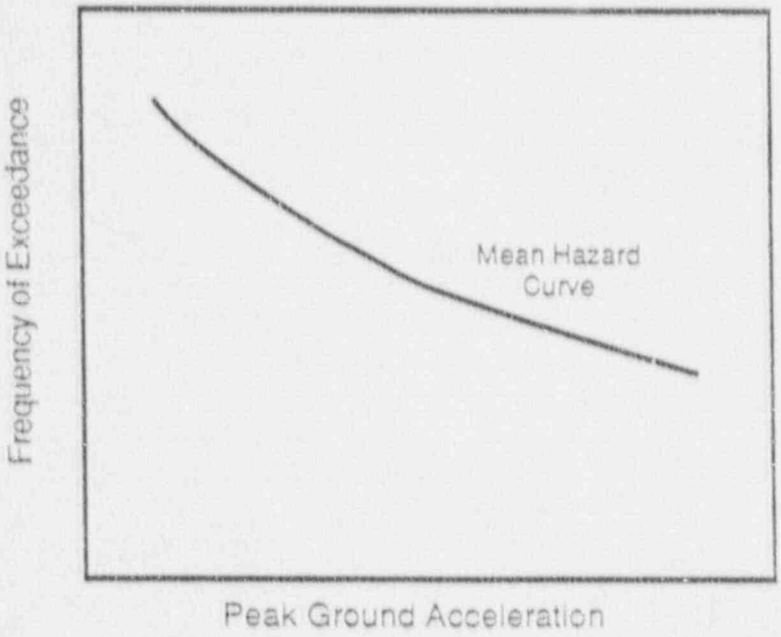

(a)

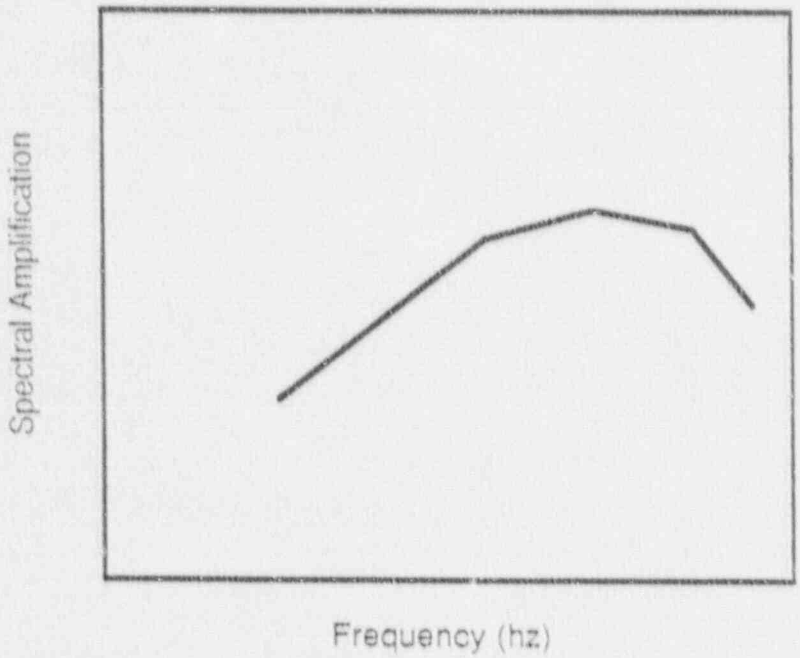

(b)

Figure 2-1 Illustration of the format of the ALWR SH which consists of, (a) mean frequency of exceedance of peak ground acceleration and a (b) ground response spectrum shape.

At this stage of the ALWR development, specific locations for the plant have not been selected. Consequently, it is not possible to define the ALWR SH on the basis of a site-specific hazard assessment. Alternatively, an approach is taken such that a level of seismic hazard is determined that will be applicable to the majority of locations in the U.S. As discussed below, this is possible only for the EUS.

To develop the ALWR SH a number of factors are considered. First, the ALWR SH should be applicable to the majority of locations and possible site conditions in the U.S. Secondly, when the ALWR SH is used in the seismic PRA there should be a reasonable assurance that the ALWR seismic risk goal is satisfied. The first consideration suggests that the ALWR SH curve should represent some sort of a bound on the seismic hazard. It also requires that the ALWR SH be developed for different soil conditions that may exist at ALWR sites. The second factor requires a consideration of the seismic risk that is determined using the ALWR SH as input.

Combining these concepts, the ALWR SH curve is defined as a limiting mean hazard curve such that for sites whose hazard is less than this bound, there is a reasonably assurance that the frequency of seismic core damage is acceptable (e.g., is low enough that the target risk level is satisfied). The definition of the ALWR SH curve requires that the seismic risk associated with potential candidate curves be considered. In this way the risk associated with the ALWR SH is known.

To determine the ALWR SH, the following steps are taken:

- determine the limiting seismic hazard curve which combined with the ALWR system fragility equals the target seismic risk level,

- systematically survey the seismic hazard in the U.S. to determine where the ALWR SH is applicable,

- delineate areas, if any, where the ground shaking hazard may result in an ALWR seismic risk that exceeds the target risk level, and

- develop the ALWR SH for a range of possible site conditions.

To calculate the frequency of core damage the ALWR system or plant-level fragility must be defined and integrated with the seismic hazard. As described in Section 6, the ALWR plant level fragility is developed for a range of possible site conditions. As part of the fragility development, different response-spectrum shapes that correspond to each site condition are used.

2.3 Evaluation of Seismic Risk

The frequency of seismic core damage is computed by integrating the seismic hazard and system level fragility. This is calculated according to:

$$P_f = \int P(f|a)\, G(a)\, da \qquad (2\text{-}1)$$

$P(f|a)$ = conditional fraction of core damage given ground motion level a (e.g., system level fragility curve)

$G(a)$ = annual frequency of occurrence of ground motion in the interval $a \pm \frac{da}{2}$.

To estimate the mean frequency of core damage the mean seismic-hazard curve and the mean core-damage fragility curve are used (see the discussion in Section 2.8).

2.4 Assessing the ALWR Seismic Hazard

2.4.1 U.S. Seismic Hazard

As part of the ALWR SH development an evaluation of the seismic hazard in the U.S. must be available in order to determine the ALWR SH curve and to identify regions where it is applicable. Seismic hazard in the U.S. varies considerably from region to region. In particular there is a major distinction between the WUS and the EUS in terms of the tectonic processes that generate earthquakes and the attenuation of ground motion. The WUS is an intraplate region as represented by the San Andreas Fault system and the subduction zones along the northwest coast. The EUS on the other hand is an intraplate region characterized by a much lower rate of earthquake occurrences than in the west.

The rate of earthquake occurrences in the WUS is approximately a factor of 5 to 10 higher than in the EUS. Also, the likelihood of large magnitude events ($M > 7$) is much greater in the WUS. These factors contribute to a much higher seismic hazard in the WUS. Because of basic differences in the geologic character of crust, the attenuation of ground motion is substantially different in the EUS and WUS. Ground motion amplitudes in the WUS attenuate much more rapidly than in the EUS. As a result, earthquakes of a given magnitude are felt over a larger area in the EUS. On balance, the seismic hazard in the WUS is considerably higher than in the east (1).

Estimates of seismic hazard in the WUS suggest that evaluations are highly dependent on specific tectonic features. As a result, due to the rapid attenuation of ground motions in the west, hazard calculations must be performed on a smaller spatial scale. For purposes of evaluating the ALWR SH, it is not possible to systematically evaluate the hazard in the WUS (west of 105°W longitude). Therefore, due to the generally higher rate of earthquake occurrences and the localized nature of the hazard in the west, the seismic hazard input for the ALWR PRA for sites in the WUS must be considered on a site-specific basis.

Conversely, the seismic hazard in the EUS has been extensively studied in its entirety as part of two different studies (2, 3). In this case site-specific hazard assessments can be made for areas throughout the EUS. As a result, the ALWR SH will be evaluated for the EUS only.

2.4.2 Seismic Hazard Evaluation in the EUS

In the EUS the SOG and EPRI have recently completed a study that provides the capability to evaluate the seismic hazard for locations east of 105° W longitude (2). Ideally, a complete picture of the seismic hazard in the EUS could be obtained by performing hazard calculations using the EPRI/SOG methodology and data for a dense grid of sites. However, to do this at a high enough density (e.g., one quarter to one-half degree spacing) would require an extensive effort. To implement the EPRI/SOG methodology, requires that input to the EQHAZARD software package be prepared on a site-specific basis for each of the thousands of sites in a grid that covers the entire EUS. In addition, extensive computer time would be required to perform these calculations. The task of preparing the necessary input and performing the seismic hazard calculations at a large number of sites is prohibitive and thus eliminates the use of the EPRI/SOG methodology as a viable option.

Alternatively, a simpler approach is used that serves as a surrogate measure of the seismic hazard in the east. When coupled with site-specific hazard results using the EPRI/SOG methodology, a realistic measure of the seismic hazard throughout the EUS can be obtained. This approach is described next.

2.4.3 Regional-Seismic Hazard Calculations

In order to evaluate seismic hazard calculations for a grid of sites that encompasses the entire EUS, a simplified, less computationally intense hazard analysis is performed. A so-called regional-hazard analysis is conducted using the same basic methodology developed in the EPRI/SOG seismic hazard project (see Section 3.0). However, rather than using the input from the six Earth Science Teams (which involves hundreds of seismic sources), a regional assessment is performed that uses a single seismic source that encompasses the entire EUS. For this single source, seismicity parameters are computed and a maximum magnitude is defined. By considering only one source, the number of hazard calculations that must be performed is reduced substantially.

There are two basic reasons why a regional hazard calculation of this type should provide a reasonably accurate measure of the seismic hazard in the EUS. The first reason is that experience suggests that the ground shaking hazard is dominated by the seismicity nearest a site. Secondly, as part of the EPRI/SOG seismic hazard project, an effort was made in the determination of seismicity parameters to be reasonably faithful to the seismicity budget. That's to say the seismicity estimated by the Earth Science Teams should generally be consistent with the overall historic rate of earthquake occurrences in an area, unless there is a particular hypothesis that suggests that the future rate of earthquakes will be different. Assuming that the Earth Science Teams have not systematically considered hypotheses that deviate dramatically from the seismicity budget, the regional-hazard calculations should provide a reasonable measure of the rate of earthquake occurrences. The only parameter that must be defined is the maximum magnitude, m_{max}. Since a single seismic source is used, a maximum magnitude must be defined that is generally applicable to the EUS. Section 5.0 describes the estimation of seismicity parameters and maximum magnitude values that are used in the regional-hazard analysis.

Given the source geometry, seismicity parameters, and the maximum magnitude for this single seismic source and a ground-motion attenuation model, the hazard at each site in the grid can be computed using the EQHAZARD code, EQHAZ (4).

The details of the regional-hazard evaluation are described in Section 5. As the hazard results in Section 5 will demonstrate, the regional-hazard analysis provides an estimate of the seismic hazard that compares favorably with the hazard estimates generated by the EPRI/SOG methodology.

As is the case in the site-specific hazard assessment, the uncertainty in each component of the analysis is considered in the regional-hazard evaluation. As a result, multiple hazard calculations are performed for each site in the grid, considering all possible combinations of alternative parameter values.

2.4.4 Site-Specific Seismic Hazard Calculations

Site-specific seismic hazard calculations are performed using the methodology and data developed as part of the EPRI/SOG seismic hazard project. The input from the six Earth Science Teams are used to define the seismic sources that are active in a region, the seismicity parameters for these sources and the maximum magnitude distribution for each source.

Based on a review of the regional-hazard calculations, areas of relatively high seismic hazard were identified. In each area, specific locations where site-specific calculations are performed. The sites considered include existing nuclear power plant sites as well as other sites located in or near high seismic regions.

2.4.5 Ground Response Spectra

The ALWR SH response spectrum is derived from the uniform-hazard response spectra (UHS) developed as part of the EPRI/SOG project for nuclear power plant sites in the EUS (5). A UHS is used because it provides a realistic measure of the spectral characteristics of the seismic hazard as defined by the likelihood of occurrence of different size earthquakes. Using the results of the EPRI/SOG as a database of UHS shapes, an average spectral shape for the EUS is developed.

2.4.6 Site Conditions

To consider the possible site conditions that may exist at a future ALWR site, five soil categories that were studied in the EPRI/SOG project are considered (6). The categories range from rock to deep soil sites. For each site condition an ALWR SH curve and ground-response spectrum pair is determined. The EPRI/SOG soil categories and the procedure to estimate the seismic hazard for each site condition is described in Section 5.0.

2.5 ALWR Seismic Hazard - Evaluation Procedure

Figure 2-2 illustrates the procedure that is followed to determine the ALWR SH. First, the seismic hazard in the EUS is reviewed to identify areas of relatively high hazard. To do this, regional-hazard calculations are performed for a grid of sites that covers the EUS. The results of these calculations provide a view of the hazard throughout the east. From this, areas of relatively high seismicity are identified.

In the next step, site-specific seismic hazard calculations are performed using the EPRI/SOG methodology and data to obtain a best estimate (best in the sense of using the best available data) of the hazard. The results of these calculations are later used to calibrate the regional-hazard results. The site-specific calculations are performed for areas with high seismic hazard.

Next, seismic risk calculations are performed by combining the ALWR core-damage fragility and the regional- and site-specific hazard results. At this point, two measures of seismic risk have been generated. The first consists of the risk estimates at each site where a site-specific hazard assessment was performed. A second set of seismic risk results consists of the mean core-damage frequency at each site in the grid that covers the EUS. This second set provides a map of the seismic risk for the ALWR throughout the east.

By comparing the estimates of seismic risk based on the site-specific and regional-hazard calculations at locations where the two estimates are available, the seismic risk map can be calibrated.

In the final step, the site-specific hazard results are reviewed to determine which curve produces an estimate of seismic risk that corresponds (or nearly corresponds) to the target seismic risk level. This is the ALWR SH curve. By reviewing the seismic risk estimates throughout the EUS based on the regional-seismic hazard calculations, areas where the target ALWR seismic risk level may be exceeded are identified.

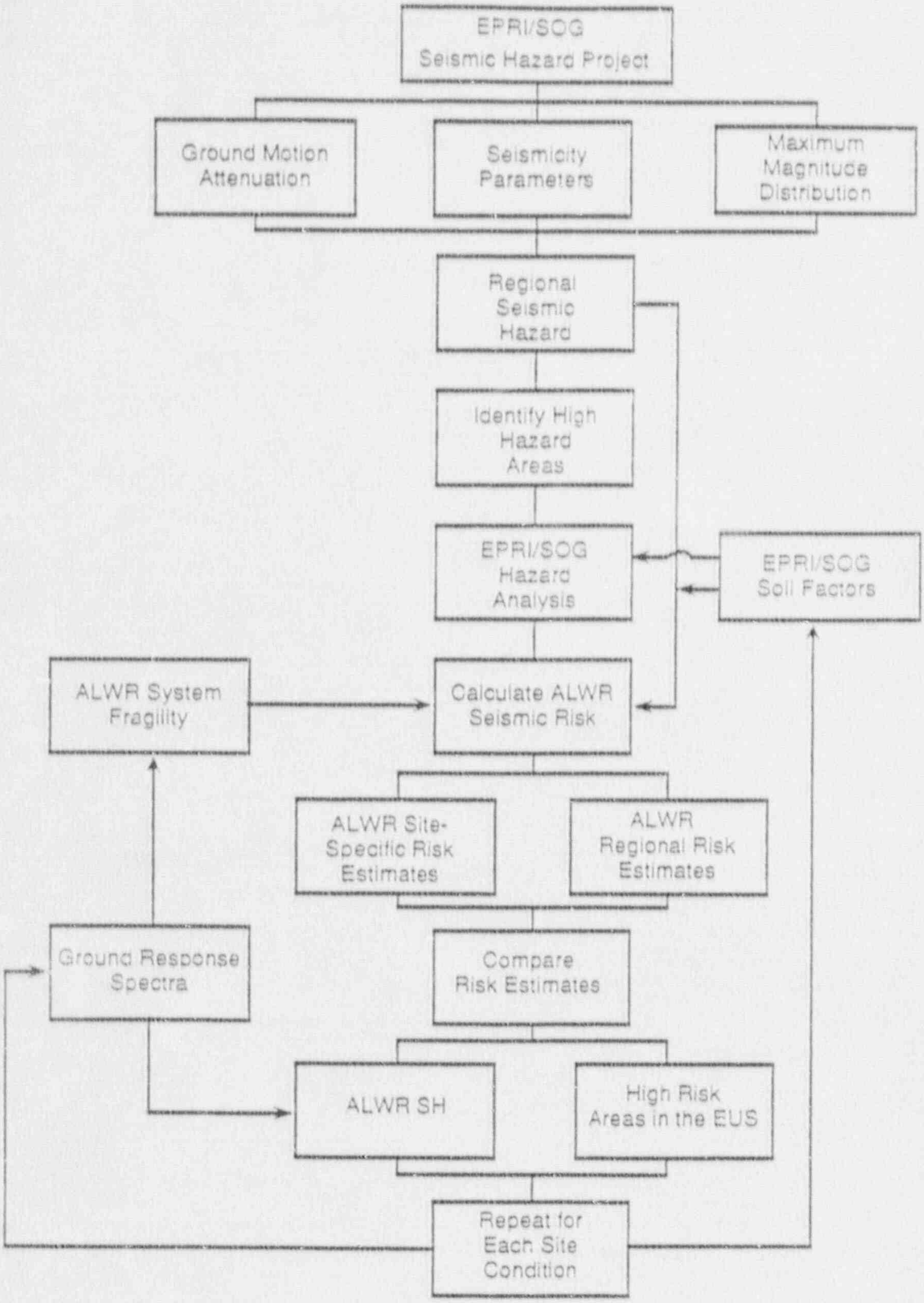

Figure 2-2 Illustration of the steps to develop the ALWR SH.

This procedure is carried out for the seismic hazard results that correspond to rock site conditions. By converting the hazard results for rock to motions that would occur at soil sites (see Section 5.0), this procedure is repeated for each site condition that is considered.

2.6 Target ALWR Seismic Risk Level

An objective of the ALWR PRA is to demonstrate the adequacy of the ALWR design to meet specified safety goals for internal and external events. To meet the safety goal (for all events), a corresponding target for the contribution of seismic events to the likelihood of core damage is defined. For purposes of this evaluation, the limiting mean frequency of core damage for the ALWR design is 10^{-6} per year.

2.7 ALWR Seismic Capacity

The seismic capacity of the ALWR plant is defined in terms of the system level mean core-damage fragility curve. For purposes of estimating the seismic risk associated with the ALWR plant design, a system fragility curve is developed that is assumed to be achievable, given the ALWR seismic design. Note, in a seismic PRA that is performed for an ALWR vendor design, a plant specific core-damage fragility curve will be developed by incorporating individual component fragilities into a seismic systems model.

For purposes of this evaluation the system level fragility is inferred based on the ALWR seismic design level, 0.30g, and design specifications. The ALWR seismic design criteria and procedures provide for considerable margin between the design level and the ground motions required to cause damage. Section 6.0 describes the development of the ALWR mean core-damage fragility curve.

2.8 Consideration of the ALWR Seismic Hazard

The assumed ALWR system level fragility and seismic risk goal imply a limit on the seismic hazard that can be considered for the ALWR. If it is assumed that the seismic hazard from location to location differs in level only (e.g., seismic hazard curves have the same basic shape), it is possible to determine the limiting seismic hazard level that satisfies the ALWR risk goal. Assuming for the moment that the seismic hazard can be described by a function of the form,

$$G(a) = k\, a^{-\alpha} \tag{2-2}$$

where a is the ground motion parameter (PGA), k is a variable that varies by location and α is a shape parameter. Letting the uncertainty in seismic hazard be defined by the uncertainty in k, which is assumed to be lognormally distributed with median $\hat{k}$ and logarithmic standard deviation β_H, the mean seismic hazard is defined by,

$$\overline{G}(a) = \hat{k}_1\, a^{-\alpha}\, e^{0.5\beta_H^2} \tag{2-3}$$

where the overbar denotes the mean.

Assuming the mean hazard is defined by eq. 2-3 and the mean system fragility is lognormally distributed, the mean frequency of seismic core damage is Cornell (7),

$$\overline{P}_f = \overline{G}(\hat{a})\, e^{0.5\beta_c^2\, \alpha^2} \tag{2-4}$$

According to equation 2-4 the mean frequency of core damage is equivalent to the mean frequency of occurrence of the median acceleration capacity of the ALWR system, $\hat{a}$, times a factor that depends on the composite variability of the system capacity, β_c, and the seismic hazard shape parameter, α.

Ellingwood reports that a typical value of α for sites in the EUS is -2.70 (8). For α equal to -2.70 and β_c of 0.50, equation 2-4 becomes,

$$\overline{P}_f = 2.49\ \overline{G}(\hat{a}) \qquad (2\text{-}5)$$

If the ALWR seismic risk goal is 10^{-6}, the bounding value of $G(\hat{a}=1.40g)$ is 4.02-7[1] (10^{-6} / 2.49). Based on the assumptions used in this evaluation (e.g., the shape of the seismic hazard curve, ALWR system capacity and variability, etc.), 4.02-7 represents an upper limit on the mean frequency of occurrence of 1.40g. The sensitivity of this result can be considered by varying the values of β_c and α. Table 2-1 shows the variation of G(1.40g) for pairs of β_c and α values. The results in Table 2-1 can be used as general guidance to assess the ALWR SH.

Because the seismic hazard at different locations may not satisfy the assumptions used in this evaluation, direct consider of the seismic hazard in the EUS must be made.

[1] 4.02-7 = 4.02x10^{-7}

Table 2-1

Summary of G(1.40g) for Alternative Values of β_c and α

Shape Parameter, α	Seismic Fragility Composite Variability - β_c				
	0.30	0.40	0.50	0.60	0.70
2.0	8.35-7	7.26-7	6.07-7	4.87-7	3.75-7
2.5	7.55-7	6.07-7	4.58-7	3.25-7	2.16-7
2.7	7.20-7	5.58-7	4.02-7	2.69-7	1.68-7
2.9	6.85-7	5.10-7	3.50-7	2.20-7	1.27-7
3.1	6.49-7	4.64-7	3.01-7	1.77-7	9.49-8

3.0 SOG METHODOLOGY

3.1 Overview

A probabilistic seismic hazard assessment quantifies the frequency that specified levels of ground motion will be exceeded at a site. The SOG and EPRI have developed a methodology to evaluate ground motion levels with low frequencies of occurrence ($<10^{-3}$ per year) for sites in the EUS (2). As part of the EPRI/SOG methodology, procedures are provided to quantify the uncertainty in hazard estimates that is attributable to uncertainty in the current state-of-knowledge of tectonic processes that generate earthquakes in the EUS (e.g., rate of earthquake occurrences, maximum magnitudes) and in ground motion attenuation. By propagating the uncertainty in individual inputs to the final results, a measure of the uncertainty in the hazard estimates can be determined. From this, the range of values the hazard might take on can be specified.

The basic steps in the EPRI/SOG Methodology to estimate seismic hazard are:

1. Identify seismic sources that contribute to the hazard at a site.

2. Determine the seismicity parameters (i.e., activity rates, b-values, and maximum magnitude) for each seismic source.

3. Select ground motion attenuation models to describe the level of shaking as a function of earthquake magnitude and distance.

4. Calculate the seismic hazard at a site considering the hazard for each seismic source and alternative model parameters (e.g., source combinations, ground motion attenuation models, estimates of maximum magnitudes, etc.).

Figure 3-1 shows the steps in the hazard analysis.

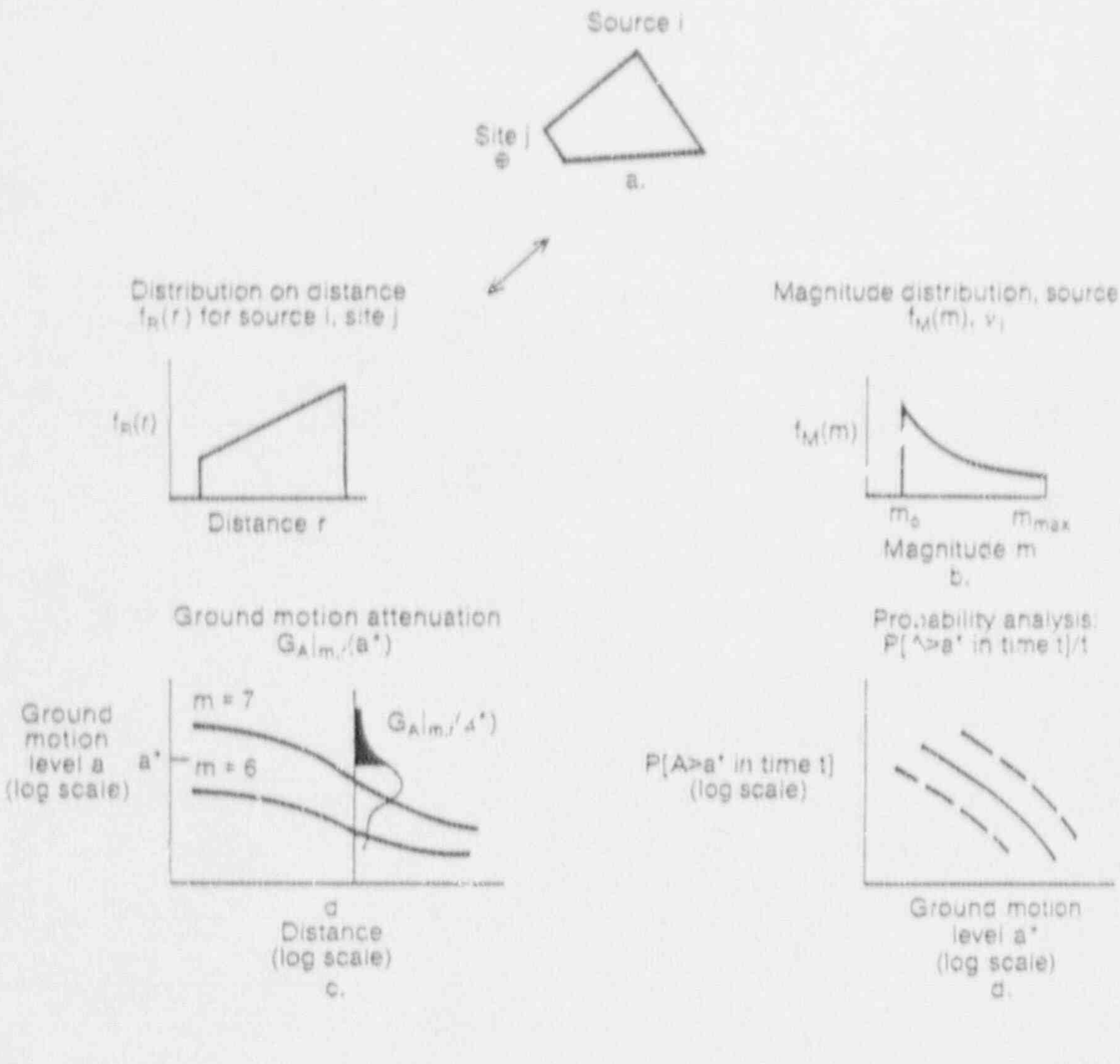

Figure 3-1. Steps in a seismic hazard evaluation (2).

3.2 Seismic Source and Seismicity Data

To estimate the seismic hazard at sites in the EUS, the seismic source and seismicity data developed by six Earth Science Teams as part of the EPRI/SOG research project is used. The data includes seismic source geometries, seismicity parameters, and estimates of the maximum earthquake magnitude for each source. As part of their assessment each team specifies the possible combinations of seismic sources that may be simultaneously active in a region (2). The Earth Science Team interpretations of scientific data on seismicity and tectonic processes in the EUS is reported in References 9 through 14.

3.3 Ground Motion Attenuation Models

The ALWR SH is evaluated for peak ground acceleration. The ground motion attenuation models used in the EPRI/SOG seismic hazard project are discussed in Section 4. The general form of the model to estimate ground shakin is given by,

$$P(Y > y|m,r) = g(m,r) * \epsilon \quad (3\text{-}1)$$

where Y is the ground motion measure, m is the earthquake magnitude, r is the hypocentral distance, g(m,r) describes the variation of the median level of ground motion with m and r, and ϵ is a random variable which is lognormally distributed that has a median of 1 and logarithmic standard deviation, σ_y. The distribution of ϵ quantifies the randomness in ground motion.

As part of this study the seismic hazard is calculated for PGA. In addition, a selected number of calculations are performed for spectral acceleration at 2.5 hz. The calculations at 2.5 hz are used to compare the spectral values predicted in the EPRI/SOG project with those derived in this study based on the ground motion model described in Section 4 in which alternative estimates of the variability on ground motion and truncation on ground motion are considered.

The comparison of these results is discussed further in Section 5.

3.4 Hazard Analysis Results

The seismic hazard estimates obtained using the input for the six Earth Science Teams are aggregated by assigning a weight to the results generated for each team's data. As part of the hazard computations the probability distribution on the frequency of exceedance is derived. The hazard results are typically presented in terms of fractile hazard curves as shown in Figure 3-2. The expected value (mean) of the frequency of exceeding ground motion levels can be computed from the complete distribution. The ALWR SH is defined as a mean seismic hazard curve.

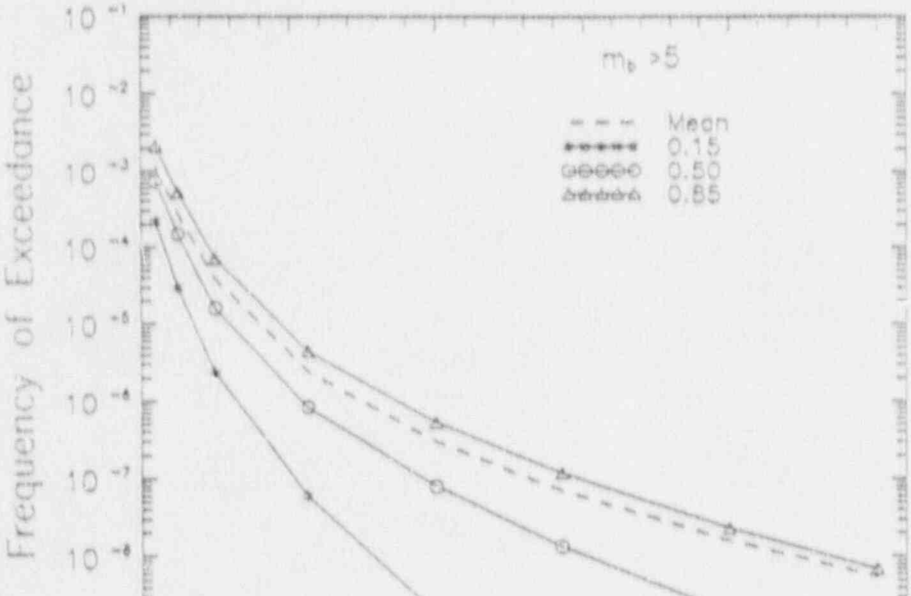

Figure 3-2. Sample seismic hazard results.

4.0 GROUND MOTION ATTENUATION FOR THE EASTERN U.S.

4.1 Introduction

As input to the seismic hazard assessment, ground motion attenuation models must be specified that estimate the level of motion as a function of earthquake magnitude and distance (see Fig. 3-1). In this study the ground motion models developed as part of the EPRI/SOG seismic hazard project are used. However, their use in the evaluation of the ALWR SH is modified to reflect an alternative measure of the variability of ground motion and to account for possible limits on the level of shaking that can occur.

Given the design requirements of the ALWR, it is anticipated that the plant will have a high seismic capacity. Based on the evaluation of the ALWR core damage fragility developed in Section 6, the median capacity of the plant is expected to be greater than 1.0g PGA. As a result, for purposes of calculating the seismic risk of core damage, seismic hazard information must be provided for high-ground motion levels (greater than 1.0g PGA). Given the anticipated importance of these ground motion levels to the frequency of core damage, consideration is given to the models that determine the likelihood that high levels of shaking can occur and to the possibility that limits of ground motion may exist.

In order that the ALWR SH will be applicable to the majority of possible site (soil) conditions that exist in the EUS, adjustment factors that were developed as part of the EPRI/SOG seismic hazard project are used. The adjustment factors provide the basis to convert seismic hazard results developed for rock sites, to the motion that would occur at the surface of a soil deposit.

In Section 4.2 the probabilistic ground motion model that is used in the seismic hazard analysis is described. The EPRI/SOG ground motion attenuation models that are used in this study are also given. In Section 4.3 the results of a literature review on the variability of ground motion are presented.

Section 4.4 considers the development of limits on strong-ground motion. In Section 4.5 the EPRI/SOG soil factors are presented.

4.2 Ground Motion Model

As part of the probabilistic seismic hazard analysis, ground motion at a site is modeled as a function of earthquake magnitude and distance to the site. Predictions of earthquake ground motion are made using an attenuation model of the form,

$$\ln(y) = g(m,r) + \epsilon \qquad (4\text{-}1)$$

where,

- y - ground motion measure (e.g., peak ground acceleration)
- m - earthquake magnitude (e.g., m_b)
- r - distance from the earthquake source to the site
- $g(m,r)$ - function that defines the mean log ground motion level as a function of earthquake magnitude and distance
- ϵ - normally distributed random variable with a mean of 0 and standard deviation, σ_y

From eq. 4-1 the probability that specified levels of ground motion are exceeded for an earthquake of a given magnitude and distance can be determined. Figure 4-1 illustrates the features of the ground motion model in eq. 4-1.

In the probabilistic estimation of ground motion, there are three parameters that must be determined. These are:

- mean attenuation function, $g(m,r)$,
- variability on ground motion, and
- limits on ground motion amplitudes.

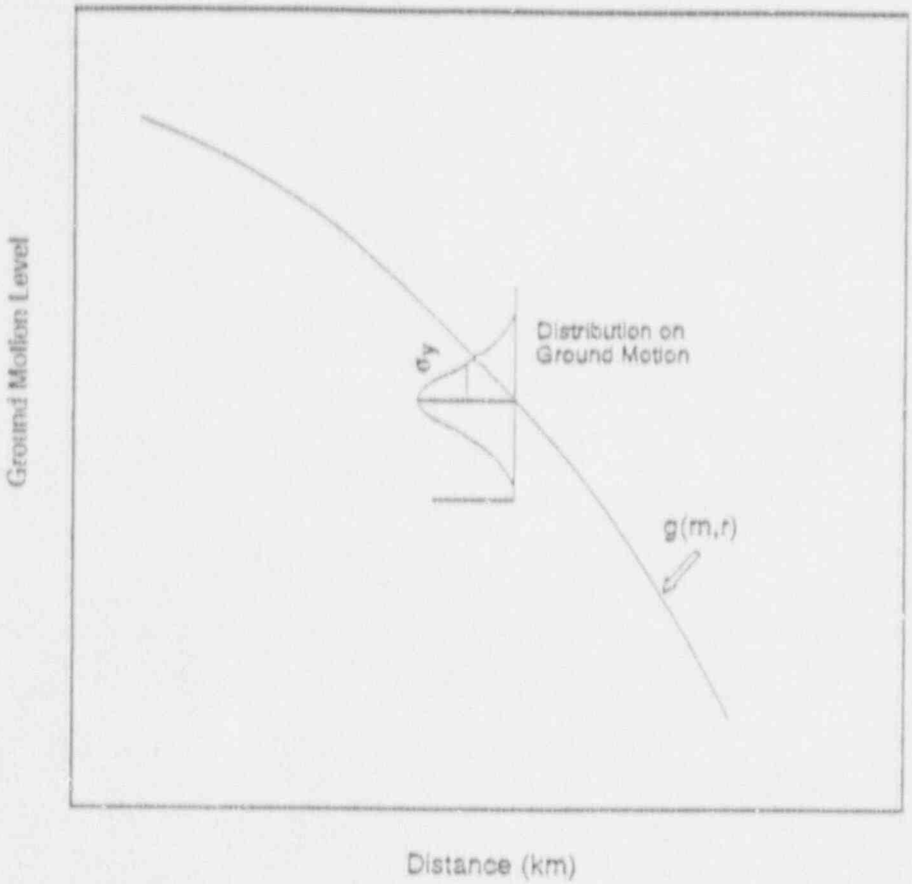

Figure 4-1 Illustration of the features of the ground motion attenuation model.

According to the attenuation model in eq. 4-1, the distribution on ground motion amplitudes is unbounded (i.e., the lognormal distribution on ϵ is unbounded). Therefore, theoretically some probability of exceedance can be assigned to any level of motion. The notion of specifying a limit on ground motion is an attempt to truncate the distribution on ϵ.

In the EPRI/SOG seismic hazard project a set of three attenuation models are used to estimate ground motion in the EUS. Three models are specified to account for the uncertainty in ground motion estimation in the EUS. Table 4-1 lists the parameters of each PGA attenuation model and the probability weights that were assigned as part of the uncertainty analysis. Figure 4-2 shows the PGA models for earthquakes of magnitude 7.0.

Table 4-1

Parameters of the EPRI/SOG PGA Attenuation Models

$$\ln(PGA^1) = a + b\, m_b + c \ln(R) + d\, R$$

Model	Weight	a	b	c	d
McGuire et al. (6)	0.50	2.55	1.00	-1.00	-0.0045
Boore & Atkinson (15)	0.25	A complicated functional form is used by these authors, see Figure 4-2 for a comparison with the other models and Reference 5.			
Nuttli (16)[2]	0.25	-3.55	1.15	-0.83	-0.0028

1 PGA is defined in units of cm/sec^2

2 For given m_b and R, ln(PGA) is the smaller of $a + b\, m_b + c \ln(R) + d\, R$ and $-8.3 + 2.3\, m_b - 0.83 \ln(R) - 0.0012\, R$

Depending on the particular application for which the results of the seismic hazard analysis may be applied, the issue of whether or not limits on ground motion should be modeled in the hazard analysis can be addressed. This topic is discussed in Section 4.4. In the next section the variability on ground motion is discussed.

4.3 Ground Motion Variability

The variability on ground motion as modeled by the lognormal distribution (see eq. 4-1) is generally estimated from empirical studies that provide an estimate of the logarithmic standard deviation of the residuals about the mean, g(m,r). As pointed out by Bernreuter et al. (17), the estimate of σ_y as obtained from statistical regression analyses of strong motion data is a measure the lack-of-fit of the model to the data (e.g., standard error of estimation). The lack-of-fit is attributed to the inability of the model to

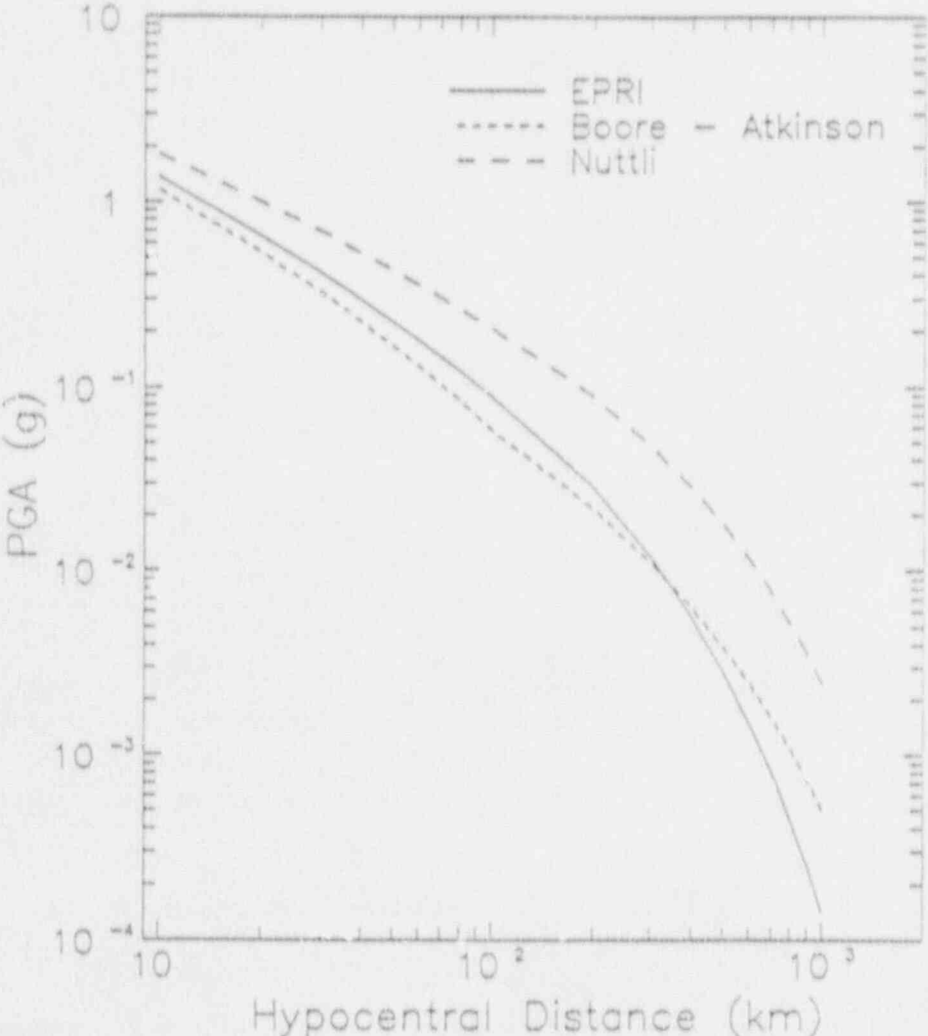

Figure 4-2 EPRI/SOG peak ground acceleration attenuation models (5).

explain the data. In practice the standard error of the residuals is taken as the estimate of the logarithmic standard deviation of ground motion. The estimate of σ_y is a function of the model being used and the strong motion dataset.

Estimating the variability of ground motion for earthquakes in the EUS is limited by a lack of strong motion data. As a result, efforts at developing attenuation models for the EUS have focussed on estimating g(m,r). Relatively few direct estimates of σ_y for ground motion in the EUS are available. For the most part, experts who must specify the variability on ground motion in the EUS rely on experience from statistical studies of western U.S. attenuation.

As discussed in the Introduction, it is anticipated that high-ground motion levels (i.e., greater than 1.0g) will be important contributors to the ALWR seismic risk. Therefore as part of the development of the ALWR seismic hazard, consideration is given to the variability on ground motion which is an important parameter in determining the likelihood of high ground motion levels. The larger the value of σ_y, the lognormal distribution becomes broader and thus a higher likelihood is assigned to ground motion levels greater than the mean value (i.e., g(m,r)).

In recent studies on ground motion attenuation, evaluations have demonstrated that the variation of ground motion residuals changes with earthquake magnitude (18-20). Generally, the ground motion associated with smaller earthquakes exhibits greater variation than the motion associated with larger events. Figure 4-3 illustrates the results of a number of studies that have estimated σ_y as a function of earthquake magnitude. The results in Figure 4-3 are based on ground motion studies of western U.S. ground motion and data recorded by the SMART Array in Taiwan.

In the ALWR SH evaluation the relationship developed as part of the Diablo Canyon (DC) seismic hazard evaluation (19) is used. This relationship is generally consistent with the other models and it is the most recent attempt to estimate σ_y as a function of magnitude. Since the DC estimate of σ_y is based on moment magnitude, a relationship between m_b and **M** must be used to express σ_y as a function of m_b. Using the m_b-**M** relationship developed as part of the EPRI/SOG seismic hazard project, this result is,

$$\sigma_y = 0.102 + 0.391\, m_b - 0.048\, m_b^2 \qquad 5.0 < m_b \le 6.58 \qquad (4\text{-}2)$$

$$\sigma_y = 0.36 \qquad m_b > 6.58$$

Figure 4-4 shows σ_y as a function of m_b.

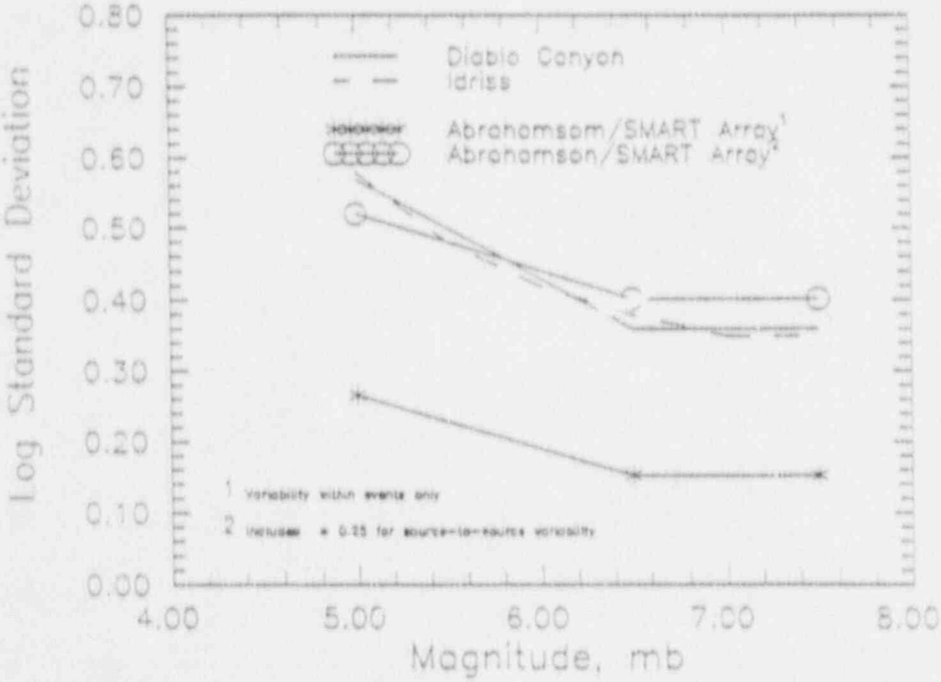

Figure 4-3 Illustration of estimates of the variability of ground motion as a function of moment magnitude.

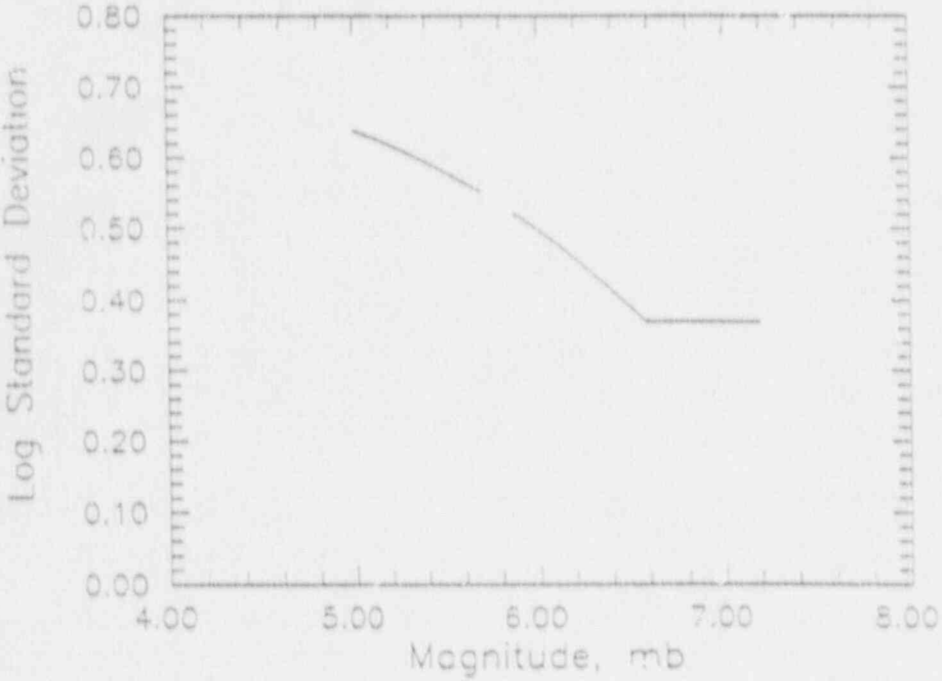

Figure 4-4 Variability of ground motion as a function of m_b used to estimate the seismic hazard in the EUS.

4.4 Truncating Strong Ground Motion

4.4.1 Background

Section 4.1 described the attenuation model used in seismic hazard analysis in terms of a functional model that defines the mean logarithmic amplitude of ground motion and a lognormal distribution that defines the random variation. Theoretically, the lognormal distribution is unbounded such that large amplitudes are predicted with some probability of exceedance. From time to time engineers and seismologists have considered whether there is a physical limit on the amplitude of motion that can be generated by earthquakes and transmitted by surficial-geologic materials. Realistically, physical limits on ground motion amplitudes exist as determined by the mechanical properties of the crustal materials at the fault where seismic waves are generated and the ability of surficial deposits to transmit seismic waves.

The problem of assessing limits on ground motion is difficult. It can, however, have important implications, depending on the applications of the seismic hazard results. For example, there are cases in seismic PRAs where limits on ground motion have had an important impact on the results. Efforts to develop physical arguments as to the limits on PGA levels that can occur have been suggested in the literature and met with limited acceptance. As more strong motion data has been retrieved in recent years, the number of recordings above 1.0g PGA has led to continued reappraisal of this issue.

In the next subsection methods that can be used to truncate or limit PGA that are estimated in the seismic hazard analysis are discussed. In Section 4.4.3 the results of a literature survey are presented. First, the results of a search of the world-wide strong motion database that identified strong motion recordings greater than 1.0g are presented. Next, the findings of a survey of the literature that identified various proposals to specify limits on ground motion are described. Finally, studies that report the distribution of ground motion residuals are summarized.

4.4.2 Methods to Truncate Ground Motion Amplitudes

Various alternatives are available to incorporate limits on ground motion amplitudes in a probabilistic seismic hazard analysis. The options include:

1. Define an absolute limit on the level of ground motion that cannot be exceeded that is independent of earthquake magnitude and distance.

2. The maximum ground motion is defined as a function of earthquake magnitude and distance. In this case the maximum value is specified in terms of the number of standard deviations above the median (or mean log) ground motion level (e.g., g(m,r)). Alternatively, the maximum value could be defined in terms of absolute limits (similar to the approach above) for specified magnitude and distance ranges. However, this approach is typically not used.

3. As a third approach, the limiting level on ground motion can be defined as a combination of the first two approaches. In this case the limit on ground motion is defined as the minimum of an absolute limit or a fixed number of standard deviations above the mean. This approach defines an envelope of the first two methods.

Figure 4-5 illustrates each of these approaches. Note, the first truncation approach defines a limit that is independent of magnitude and distance, whereas the second approach establishes a limiting curve that parallels the median estimate of ground motion. The third truncation procedure defines an envelope of the first two approaches. These truncation methods are similar to those used in the LLNL SHCP (3).

The procedure to truncate the ground motions that can occur is straightforward, whichever approach is taken. By incorporating a truncation level in the analysis, the probability of exceedance is defined as,

$$P(Y>y) = 0 \qquad Y \geq y_{max}$$

$$P(Y>Y) = \phi'(u) \qquad Y < y_{max}$$

where $\phi'(u)$ is the normalized complementary cumulative normal distribution

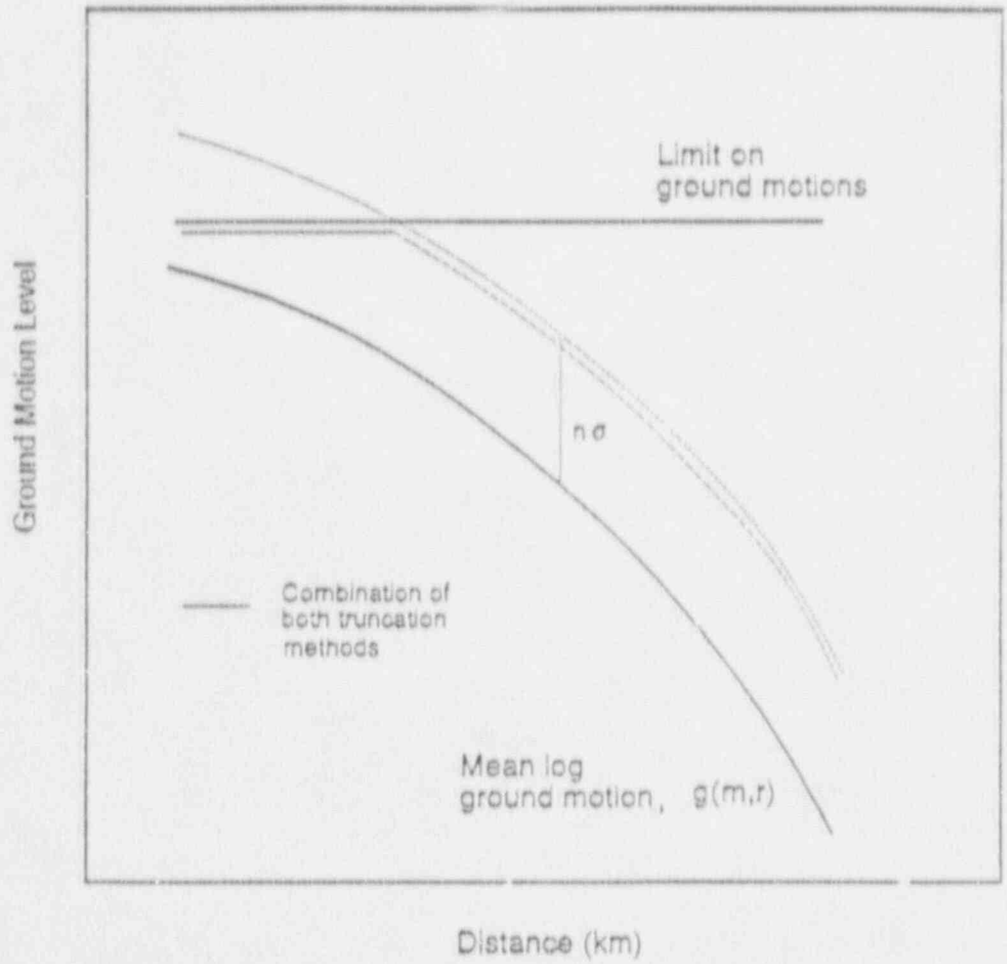

Figure 4-5 Illustration of methods for truncating ground motion.

function (CCDF) and y_{max} is a truncation level specified by one of the methods described above. The distribution is normalized so that the total area under the normal density function is one. The term u is the standard normal variate.

4.4.3 Results of the Literature Survey

A literature survey was conducted to gather information concerning limits on ground motion. As part of this survey three areas were considered:

- maximum recorded PGA motions,
- estimation of ground motion limits by theoretical arguments or expert assessments, and the

- limit of the extremes of ground motion residuals derived in empirical studies.

The first two topics provide input on possible absolute limits on ground motion, whereas the third topic supplies information on the possible limit of observed ground motions in terms of the number of standard deviations above mean predictions.

Strong-Motion Data

As a starting point to consider limits on PGA, the world-wide database of strong motion recordings was surveyed (21). The SMCAT database published by NOAA was sorted to identify recordings in the free-field, in the basement of buildings, or at dam abutments that recorded motions of 1.0g or greater. A total of 9 such recordings with at least one component of motion having a PGA of 1.0g or greater were identified. It should be noted that the data in the SMCAT contains corrected PGA information. Due to the effects of the numerical processing of the digital strong-motion data, the processed peak motions are often lower in amplitude than the original, uncorrected data. As a result, it is possible that other recordings exist whose uncorrected motion might exceed 1.0g. Table 4-2 lists the recordings that were identified. For each record the PGA for all three components of motion are listed. In addition, each site is categorized in terms of the surficial-geologic material (e.g., rock, soft soil (alluvium), stiff soil, shallow-soil deposits (less than 10 meters in depth to bedrock)).

The data in Table 4-2 suggest that ground motions of 1.0g are possible, and fairly-common place. With the relatively large disbursement of strong-motion instruments in the last 10-15 years throughout California and the U.S. in general, it is reasonable to anticipate that the database of recordings of large amplitude (> 1.0g) ground motions, near moderate to large magnitude earthquakes will grow. Furthermore, it is worth noting that median predictions for ground motions in the EUS exceed 1.0g for large-magnitude earthquakes (see Fig. 4-2). In addition, given the inherent variability in ground motion, attenuation models readily predict motions greater than 1.0g.

Table 4-2

Partial List of PGA Recordings that Exceed 1.0g

No.	Station Name	Earthquake	Date/Time	MMI	Magnitude M_L	Magnitude m_b	Magnitude M_S	Distance Epicentral (KM)	Soil Conditions	PGA (cm/sec^2) Longitudinal	PGA (cm/sec^2) Transverse	PGA (cm/sec^2) Vertical
1	Long Valley Dam (abutment)	Mammoth Lakes Aftershock, CA	05/27/80 14:50	6	6.2			14	Rock	1003.52		
2	Site #1	Nahanni Aftershock, Canada	12/23/85 5:16	9		6.4	6.9	6	Rock	1080.46	1319.08	2322.38
3	Pacoima Dam (abutment)	San Fernando, CA	02/09/71 14:00	11	6.4		6.6	7	Rock	1054.95	1148.06	
4	Pleasant Valley Pump Plant	Coalinga Aftershock	07/22/83 2:39	6	6.0			17		1071.78	1083.27	
5	Coyote Lake Dam San Martin (abutment)	Morgan Hill, CA	04/24/84 21:15	7	6.2		6.1	25	Franciscan Formation	882.90	1265.49	392.40
6	Karakyr Point	Gazli, USSR	05/17/76 2:58	10	6.4		7.0	10	Sandstone and Clay	647.46	686.70	1330.64
7	Mammoth Lake, H.S. Gym. Center	Mammoth Lakes, CA	05/25/80 16:33	7	6.15			11	Glacial (~ 75m)	958.73	1376.76	
8	Array 6, Huston Road, El Centro	Imperial Valley, CA	10/15/79 23:16	9			6.5	27	Alluvium	706.32	441.45	1562.70
9	91004	Cerro Prieto, CA	02/06/87	8	5.4			11		850.53	1125.21	

The survey of strong-motion data recordings greater than 1.0g PGA does not provide specific input to the assessment of limits on PGA. Rather, the multiple observations of peak motions above 1.0g establishes a general confirmation of attenuation models that predict motions of this magnitude and certainly define a lower-bound on possible limits of PGA.

<u>Specifying Limits on Peak Ground Acceleration</u>

Two different sources of input are available concerning the specification of absolute limits on ground motion. In both cases however, the available data is limited, due to the fact that the subject has not attracted a great deal of study. The two sources of information include theoretical studies that consider the maximum acceleration that could be generated by the stress release at the fault and expert assessments on ground motion limits. The following subsections discuss these topics.

<u>Theoretical Limits on Ground Motion</u> - As part of a study of earthquake source spectra and ground motion, Brune estimated the maximum PGA that could be generated by the stress release at a fault. Based on the elastic properties of rock at the fault zone, Brune estimated a maximum PGA of 2.0g (<u>22</u>).

In a more recent study, McGarr studied the ground motion generated by mine-blasts (<u>23</u>). In this data he observed motions that exceeded 1.0g. Based on theoretical arguments McGarr estimated a maximum PGA of 2.5g in rock.

Hanks and Johnson (<u>24</u>) postulate possible limits on ground motions derived from a theoretical-source spectrum model and limits on crustal shear strength. Based on shear strengths ranging from 2,000 to 5,000 bars, limiting PGA values range from 0.75g to 1.80g.

Each of the above referenced studies has provided estimates of maximum peak acceleration in rock. The survey of the literature suggests less focus has been given to the assessment of limiting ground motions on soil deposits. This is a much more difficult task since surficial soils are likely to behave in a nonlinear way during high ground motions. As a result making predictions of theoretical limits on ground motion is much more difficult.

A paper by Ambrasseys (25) did suggest possible limits on ground motion that might be transmitted by soils. However, these limits have not been widely accepted. In addition, the number of large-amplitude recordings on soil sites suggests they may not be applicable.

Practically speaking, it is reasonable to suggest that surficial soils are limited in terms of the amplitude of seismic waves that they can transmit. However, there does not exist, even for rock sites, a consensus assessment of the maximum motions that can occur (see the next subsection). As a result any detailed consideration of limiting ground motions at soil sites must be performed on a site-specific basis, based on an evaluation of individual site soil properties.

Expert Assessments

As part of the LLNL seismic hazard project to estimate the hazard in the EUS, a panel of ground motion experts were asked to consider the assessment of possible limits on ground motion that would be estimated in the seismic hazard calculations. The experts were allowed to select among the three truncation procedures described above. They also had the option to specify that no truncation at all be used. The results of the LLNL survey are listed in Table 4-3. Three of the experts preferred not to define a limit on PGA, although one of these experts did indicate he felt there was a limit.

The data in Table 4-3 suggest that subjective (expert) assessments are divided. Combined with theoretical studies, they suggest that a maximum PGA may be 2.0g or higher.

Distribution of Ground Motion Data

In this section, possible limits on ground motion are considered by reviewing the distribution of ground motion residuals as obtained in empirical attenuation studies. A literature survey was performed to identify studies that documented the distribution of the residuals of ground motion data about

Table 4-3

LLNL Ground Motion Expert Assessment of Limits On Peak Ground Acceleration (3)

Expert	Truncation Level
1	None
2	2.5g or 2.5 standard deviations
3	None
4	None
5	4 standard deviations

best-fit curves. The distribution of residuals provides information on the shape of the distribution, as well as a measure of the extremes. Figure 4-6 shows one example of a histogram of the residuals for the data studied by Campbell (26). The observed limit of the distribution of ground motion residuals provides input to consider a truncation scheme based on the number of standard deviations above the mean (see Fig. 4-5).

In addition to published studies, an evaluation of the database of strong-motion recordings in the EUS was made (6). Using the three EPRI/SOG attenuation models, the residuals about each model were estimated. Table 4-4 summarizes information on the limit of observed ground-motion residuals. The data in the table suggest that the distribution of ground motion residuals is defined up to approximately three standard deviations. This observation suggests that the randomness in ground motion is defined over a fairly wide range about the mean.

Table 4-4

Summary of the Maximum Ground Motion Residual Observed in Empirical Studies

Author	Database	Number of Data	Parameter $(A_{max}/\bar{A})$	Maximum[1] Residual
Atkinson (27)	EUS	30	$\bar{A}$	0.62
Campbell (26)	WUS, Worldwide	229	$\bar{A}$	2.60 3.00
Joyner and Boore (28)	WUS, Worldwide	182	A_{max}	3.50
Abrahamson (18)	Taiwan, SMART Array	732	A_{max}	3.22
		366	$\bar{A}$	3.19
Campbell (29)	EUS (M < 5.0)	225	$\bar{A}$	3.15
			$\bar{A}$	1.6
Toro-McGuire (6)	EUS (6) and 1988 Saugenay Earthquake Data; Hypocentral Distance < 100 km	23	$\bar{A}$	1.41
Toro-McGuire (6)	EUS (6); Hypocentral Distance < 100 km	15	$\bar{A}$	1.29
Boore-Atkinson (15)	EUS (6) and 1988 Saugenay Earthquake Data; Hypocentral Distance < 100 km	23	$\bar{A}$	1.55

Table 4-4 (continued)

Summary of the Maximum Ground Motion Residual Observed in Empirical Studies

Author	Database	Number of Data	Parameter ($A_{max}/\bar{A}$)	Maximum Residual[1]
Boore-Atkinson (15)	EUS (6); Hypocentral Distance < 100 km	15	$\bar{A}$	1.11
Nuttli (16)	EUS (6) and 1988 Saugenay Earthquake Data; Hypocentral Distance < 100 km	23	$\bar{A}$	1.66
Nuttli (16)	EUS (6); Hypocentral Distance < 100 km	15	$\bar{A}$	1.63

[1] The residuals for the Toro-McGuire, Boore-Atkinson and Nuttli attenuation models have been corrected for any bias in the model predictions (i.e., residuals have zero mean).

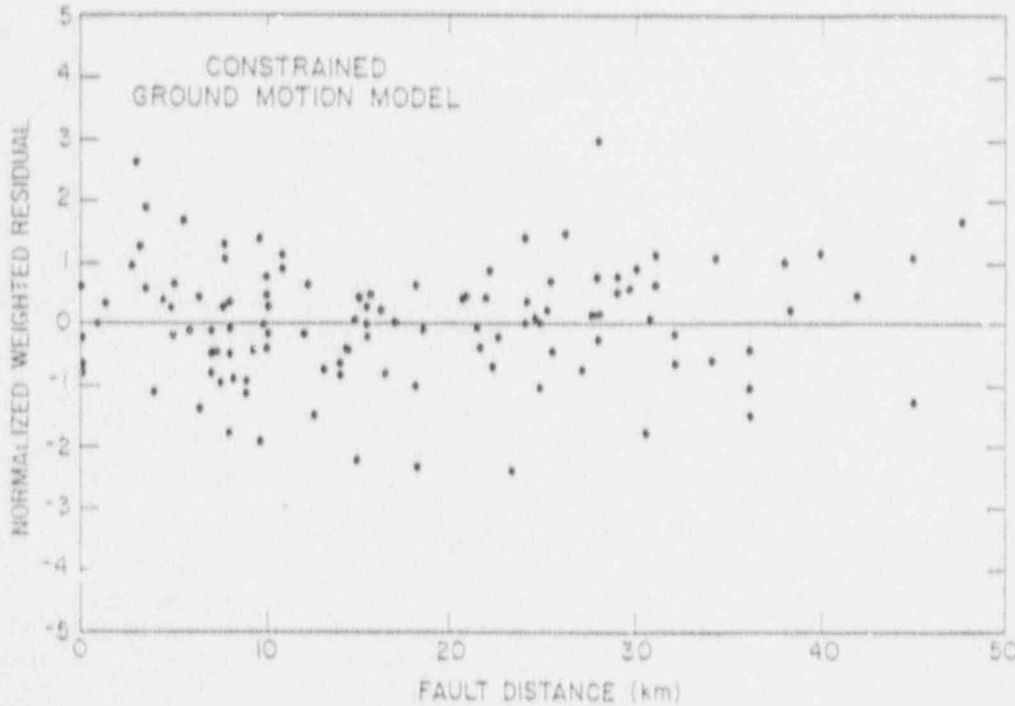

Figure 4-6 Histogram of the residuals of ground motion (reproduced from Campbell (26).

4.4.4 Recommended Truncation Level For PGA

The results of the study described above suggests there does not exist a single method or consensus expert assessment to establish a limit on PGA amplitudes that can occur at rock or soil sites. The results of the LLNL study demonstrate that experts are divided in terms of whether a limit should be used in the seismic hazard analysis, and if so how the truncation should be applied.

For purposes of the ALWR seismic hazard calculations, the following limits on ground motion will be used:

- maximum PGA - 2.5g, and a
- maximum of 3.0 standard deviations above the mean.

Both levels will be used in the seismic hazard calculations such that the lower of the two limits will apply at a given magnitude and distance. This corresponds to the third procedure described above.

4.5 Soil Adjustment Factors

In the EPRI/SOG methodology ground motion attenuation functions are used that estimate the motion for rock-sites (see Section 4.2). To determine the ground shaking at soil sites, soil factors were developed to adjust the rock motion to the corresponding motion on soil. The analysis involved the evaluation of the nonlinear response of a soil column to earthquake ground motion. For each soil-site category that was considered, the soil response was evaluated for a range of earthquake magnitudes and input (rock) ground motion levels. The final soil factors that were developed are defined for each site category as a function of the amplitude of the rock input motion to the motion at the top of the soil column.

In the EPRI/SOG project six site categories were considered. They are rock and five soil categories. The soil categories are defined in terms of the depth of the soil to bedrock. Other parameters that were used to define each soil profile (i.e., shear-wave velocity profile) are described in Reference 6. Table 4-5 lists the EPRI/SOG soil categories. The first soil category is a special case that corresponds to shallow soils, less than 30 ft. to rock. Soil deposits that are 30 ft. in thickness or less will be removed as part of the foundation preparation for the ALWR. For this reason site category S1 is not considered in this evaluation. Figure 4-7 shows the adjustment factor for peak ground acceleration for each soil category.

In this analysis the regional and site-specific hazard calculations are performed for rock site conditions. Using the procedure described in Reference 6 the soil factors in Figure 4-7 are used to determine the seismic hazard for each soil category.

Table 4-5

EPRI/SOG Site Categories

Category	Depth (ft)
1	10 - 30
2	30 - 80
3	80 - 180
4	180 - 400
5	> 400

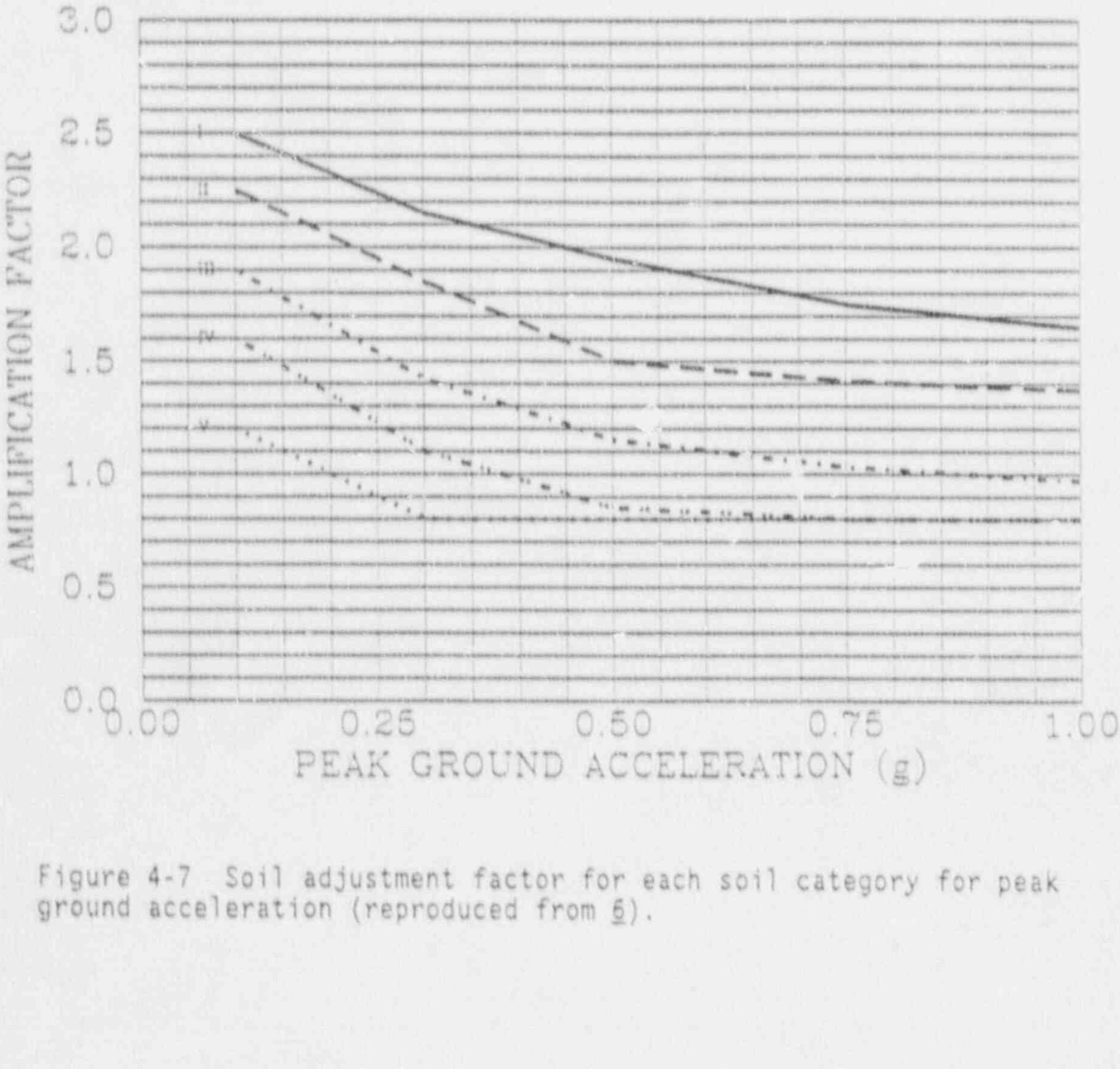

Figure 4-7 Soil adjustment factor for each soil category for peak ground acceleration (reproduced from 6).

5.0 SEISMIC HAZARD EVALUATIONS

5.1 Overview

This section presents the results of the seismic hazard calculations for the EUS and the development of the ALWR SH response spectrum shape. The hazard calculations and the response spectrum are developed for each site category described in Section 4. Two sets of hazard calculations are performed. The first are the regional calculations that are performed for a grid of sites throughout the EUS. The second set consists of site-specific hazard analyses that are performed using the EPRI/SOG seismic hazard methodology and data at a selected number of sites.

As described in Section 4 the EPRI/SOG ground motion models are defined for rock site conditions. By adjusting the hazard curves using the appropriate soil factors, the hazard for each site category is determined. In this section the regional hazard results and the site-specific calculations are compared to demonstrate the accuracy of the regional evaluation. Since the same soil factors are used to convert the site-specific and regional-hazard results, the same consistency observed for the rock sites will exist for the soil site results as well. For simplicity only the site-specific hazard results for all soil categories are shown. Plots showing the comparison of the site-specific and regional-hazard results for all soil categories are not presented. However, the seismic risk calculations performed in Section 7 will be performed for all site conditions using the site-specific and the regional hazard results.

Section 5.2 describes the method and data used to perform the regional seismic hazard calculations. Based on a review of the regional seismic hazard analysis, sites that are located in or near areas of high seismicity are selected. In Section 5.3 the site-specific hazard calculations are described. Section 5.4 shows the comparison of the regional and site-specific hazard calculations. Section 5.5 presents the mean seismic hazard curves for each soil category based on the site-specific hazard calculations. In Section 5.6 the development of the ALWR SH response-spectrum shape for each site category is described.

5.2 Regional Seismic Hazard Calculations

In order to estimate the seismic hazard throughout the EUS the regional-hazard analysis described in Section 2 is performed. Figure 5-1 shows the geometry of the seismic source that is used. The input to the analysis consists of the seismicity parameters for the each cell in the seismic source, an estimate of the maximum magnitude and a ground motion attenuation model.

To estimate the seismicity parameters for the seismic source in Figure 5-1, the EQHAZARD code EQPARAM is used. EQPARAM calculates the seismicity parameters, a- and b-values, for each one-degree cell in the source. As input to EQPARAM, the user can specify the degree of spatial variation (smoothing) of the seismicity parameters (2, 4). When no smoothing is used, the pattern of historic earthquake occurrences defines the variation of the seismicity parameters from cell-to-cell. As smoothing on the a- and b-values is considered, the estimate of each parameter in a cell departs from the historic pattern, toward a smoother spatial variation. In the limit, if a high degree of smoothing is used, the seismicity is modeled as homogeneous, resulting in constant a- and b-values throughout the source. To account for the uncertainty in the evaluation of seismicity parameters, a range of smoothing values is used.

Due to the uncertainty in each part of the hazard analysis, alternative values for each parameter must be considered (2). For example, multiple ground motion attenuation models are used (see Section 4), different seismicity options (e.g., smoothing on a- and b-values) are considered and alternative values of maximum magnitude are defined. For each parameter, a probability weight is assigned to the alternative values that are considered. This defines a probability distribution that quantifies the uncertainty in the

Figure 5-1 Seismic source considered in the regional hazard calculations.

possible parameter. The EQHAZARD code, EQHAZ, is used to calculate the seismic hazard at each site in the grid for all possible combinations of the parameter values used in the analysis.

By considering the combinations of seismicity options, attenuation models and maximum magnitudes, a suite of hazard curves is determined for a site. These hazard curves and their corresponding probability weights are used to compute the mean seismic hazard. Program EQHAZ was modified to compute the mean seismic hazard curve for all possible combinations of the analysis parameters and to systematically calculate the seismic hazard at all sites in a grid. In the following subsections the alternative values for each parameter used in the regional hazard analysis is described.

5.2.1 Seismicity Options

In this application three smoothing options are used. These options represent low, moderate and high smoothing on the seismicity parameters, a- and b-values (30). Table 5-1 shows the values of the smoothing parameters. Equal weight is assigned to the three smoothing options. As part of the analysis the incompleteness of the earthquake catalog was considered using the probability of detection values estimated in the EPRI/SOG seismic hazard project (2)

5.2.2 Maximum-Magnitude

To perform the regional-seismic hazard calculations a discrete-probability distribution on magnitude is used. The values of m_{max} represent a reasonable sample of the magnitude estimates that have been defined by the Earth Science Teams for the EUS. Because the EUS is modelled by a single seismic source it is not possible to define a distribution on maximum magnitude that is sensitive to local tectonics and the potential for large magnitude earthquakes. In some cases, m_{max} may be underestimated (e.g., the

Table 5-1

Alternative Smoothing Options Used in the Regional Seismic Hazard Evaluation

Option	Probability Weight	Degree of Smoothing	PENA[1]	PENB[1]
1	0.33	Low	5	20
2	0.34	Moderate	10	50
3	0.33	High	20	50

[1]Input parameters to EQPARAM

New Madrid seismic zone) whereas in other cases it may be overstated (e.g., in the gulf coast states). In general, it is believed that a single probability distribution on m_{max} can be defined that provides a reasonable estimate of the seismic hazard at the majority of locations. Since the regional-seismic hazard calculations serve as a surrogate measure of the hazard, they need only capture the relative variation of the hazard with geographic position, the absolute accuracy of the analysis is not required. However, as demonstrated later the regional-seismic hazard results do provide a realistic and accurate estimate of the seismic hazard in the EUS with a single maximum-magnitude distribution that is spatially invariant. Recall that site-specific hazard calculations will be used to calibrate the regional-hazard results. Table 5-2 shows the maximum-magnitude distribution that is used in the analysis.

5.2.3 Ground-Motion Attenuation Models

Section 4 described the ground motion attenuation models that are used in the seismic hazard analysis. The same models are used in the regional and site-specific hazard calculations.

Table 5-2

Maximum Magnitude Distribution Used in the Regional-Seismic Hazard Evaluation

Maximum Magnitude	Probability
6.0	0.20
6.5	0.60
7.2	0.20

5.2.4 Lower-Bound Magnitude

A lower-bound magnitude (LBM) of 5.0 is used. This is consistent with the LBM used in the EPRI/SOG seismic hazard project.

5.3 Site-Specific Seismic Hazard Calculations

Site-specific seismic hazard calculations are performed using the methodology and data developed in the EPRI/SOG seismic hazard project. The input from the six Earth Science Teams is used to define the seismic sources that are active in a region, the seismicity parameters and the maximum-magnitude distribution for each source. The team inputs are specified in their individual project reports (9-14). An aggregate estimate of the hazard at a site is obtained by assigning equal weight to the results for each team. From the composite distribution on seismic hazard the mean frequency of exceedance is derived.

Based on a review of the regional-hazard calculations, areas of high seismic hazard were identified. In each area, locations were selected where site-specific calculations are performed. The sites considered include locations of existing nuclear power plants as well as other sites located in or near high-seismic regions. The sites considered are listed in Table 5-3 and are shown in Figure 5-2. Figures 5-3 and 5-4 show the sites selected in the New Madrid and Charleston seismic zones.

5.4 Seismic Hazard Results

In this section the results of the regional and site-specific hazard calculations are reported for rock site conditions. Results of the site-specific hazard calculation for soil sites are given in Section 5.6.

5.4.1 Regional Hazard Calculations

The regional-hazard analysis is performed for a grid with a 1/4° x 1/4° spacing. In all, the seismic hazard is evaluated at 12,837 sites. At each site in the grid 27 hazard calculations are performed corresponding to the combination of alternative parameter values; 3 seismicity options x 3 attenuation models x 3 maximum magnitude values. In all, 346,599 (12,837 x 27) hazard calculations are performed.

5.4.2 Site-Specific Hazard Results

For each site listed in Table 5-3, data were generated for input to the EQHAZARD codes EQHAZ and EQPOST. The EPRI/SOG data files were used to generate the input for each site. Figures 5-5 to 5-10 show the mean hazard curves for each site in the regions listed in Table 5-3.

5.4.3 Comparison of the Regional- and Site-Specific Hazard Calculations

A measure of the accuracy of the regional-hazard calculations can be made by a comparison with the EPRI/SOG results. Figures 5-11 to 5-39 show a comparison for each site of the mean seismic-hazard curves produced by the two methods. Based on these comparisons the following observations are made:

Table 5-3[1]

Location of Site-Specific Seismic Hazard Calculations

Region	Sites[1]
New England	Seabrook
	Pilgrim
	Maine Yankee
	Millstone
	New England
Charleston, South Carolina	Summer
	Vogtle
	Charleston - 1
	Charleston - 2
	Charleston - 3
	Charleston - 4
New Madrid	Arkansas (ANO)
	New Madrid - 1
	New Madrid - 2
	New Madrid - 3
	New Madrid - 4
Virginia	Surry
	North Anna
	Virginia (VA) - 1
	Virginia (VA) - 2
Piedmont	Catawba
	Oconee
	Sequoyah
	Watts Bar
Other	Limerick
	Clinton
	Davis Besse
	Wolf Creek
	Anna, Ohio

[1] See Figures 5-2, 5-3 and 5-4 for site locations

Figure 5-2 Location of sites where site-specific seismic hazard calculations were performed.

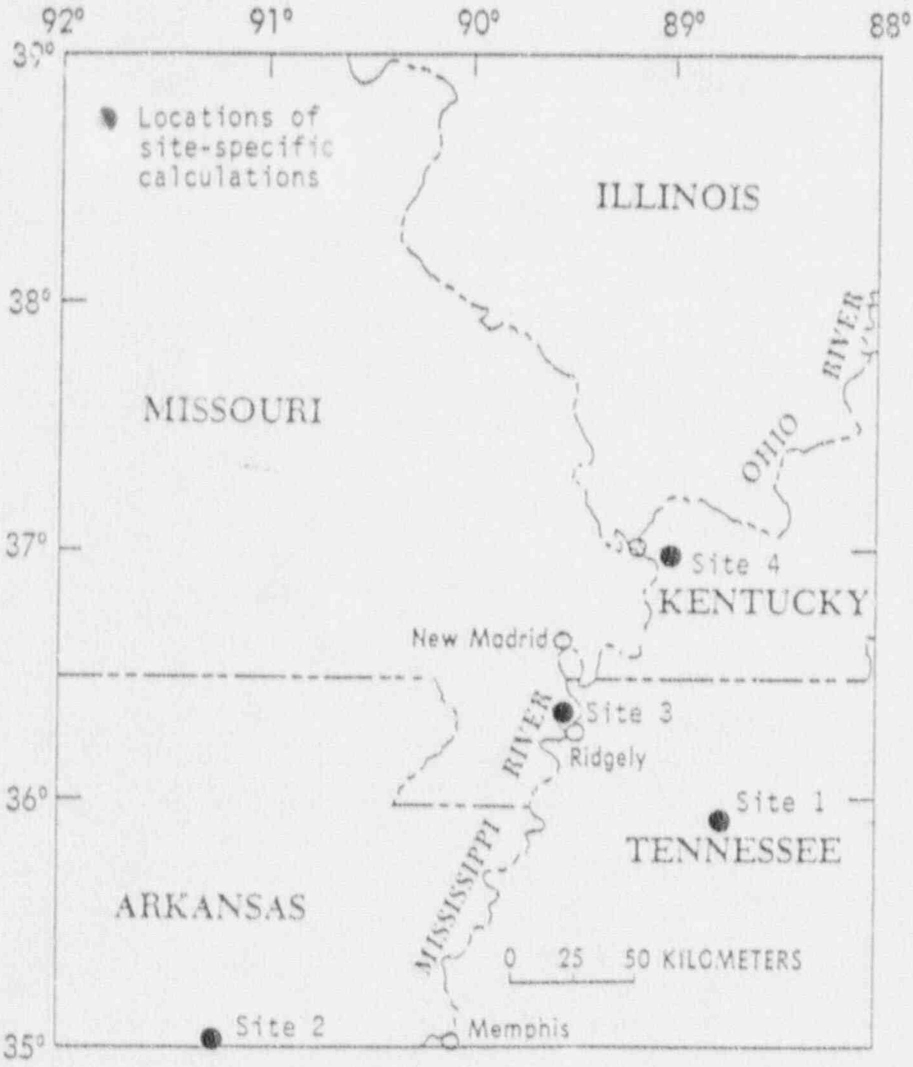

Figure 5-3 Locatio of the sites in the New Madrid area considered in the site-specific hazard calculations.

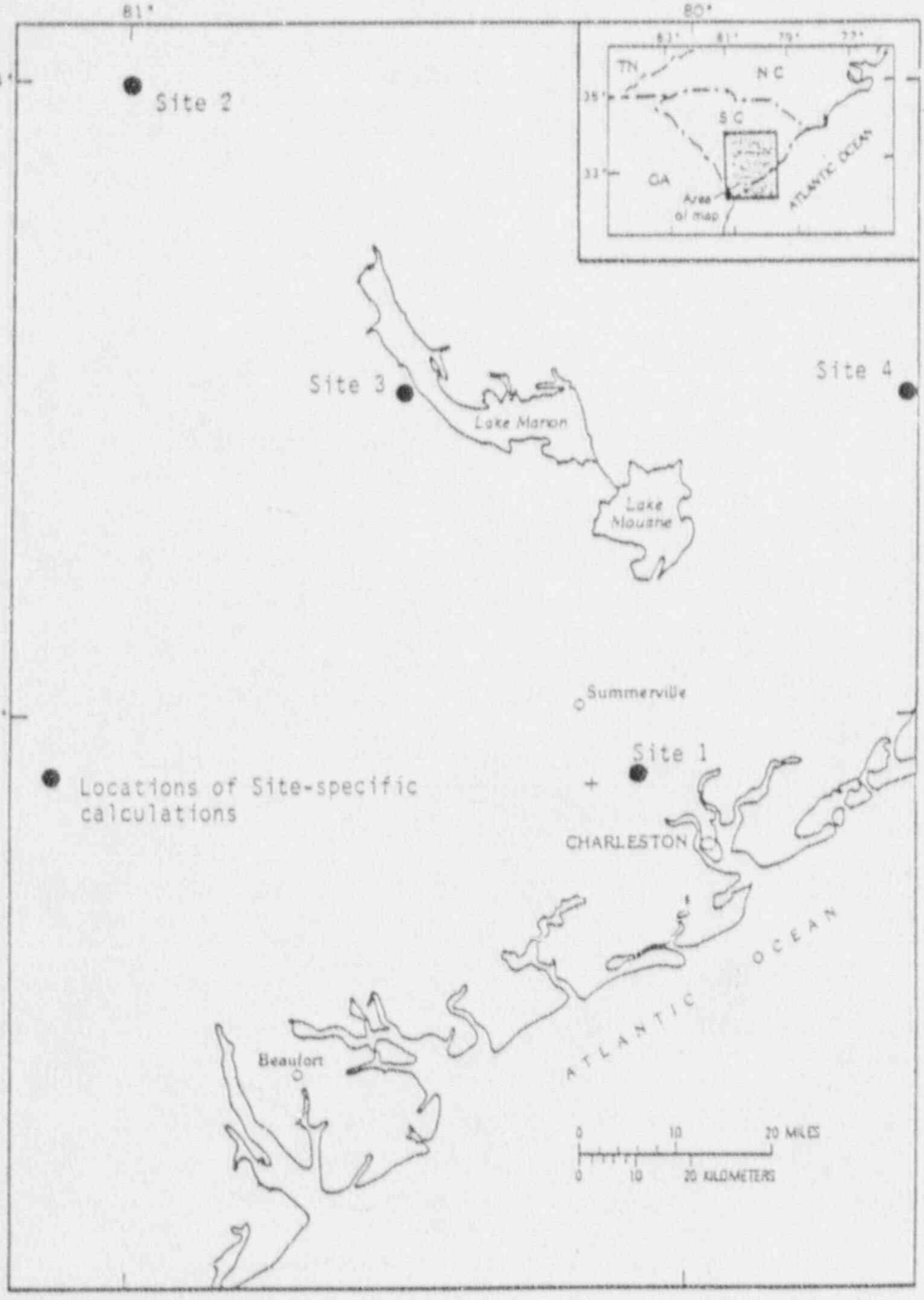

Figure 5-4 Location of the sites in the Charleston area considered in the site-specific hazard calculations.

- The regional-hazard results compare favorably with the site-specific calculations even for accelerations beyond 1.0g. A comparison of the regional and site-specific hazard results at 1.40g (the median capacity of the ALWR on rock sites, see Section 6), produces the following,

Factor[1]	Number of Sites
1-3	19
3-5	5
5-10	2
>10	3

[1]Ratio of the regional to site-specific hazard at 1.4g. In the majority of cases (24 sites) the regional-hazard results are within a few percent or higher than the site-specific results. Where differences are greater than about a factor 5, the regional results underestimate the hazard. (One exception is the Clinton site, where the regional hazard results overestimate the hazard.)

- Large differences (greater than a factor of 5) exist where the maximum-magnitude distribution used in the regional hazard calculations differs from that assumed by the Earth Science Teams (e.g., New Madrid, Charleston, etc.). At these locations the seismic hazard is underestimated.

- In cases where the regional-hazard results do not compare well with the site-specific calculations, there is good agreement at the low ground acceleration levels, indicating that the overall rate of earthquake occurrences between the two calculations are consistent.

The second of these observations was tested in an earlier part of this study (31). By revising the maximum-magnitude distribution such that it would be generally consistent with the m_{max} values used by the Earth Science Teams for the New Madrid seismic zone. This distribution is given in Table 5-4. Figure 5-40 shows a comparison of the New Madrid site-specific seismic hazard results and the revised regional hazard calculation for site 3 (see Fig. 5-3). The comparison in this case is much better. (These earlier calculations were

Table 5-4

Revised Maximum-Magnitude Distribution for the New Madrid Region

Maximum Magnitude	Probability
6.8	0.20
7.0	0.60
7.2	0.20

the same as those reported here with the exception that the variability of ground motion was constant and no truncation was considered).

The general agreement between the regional- and site-specific hazard calculations suggest that the regional results provide a reasonable basis to identify areas of high-seismic hazard. In most regions the regional calculations provide an accurate or conservative estimate of the EPRI/SOG hazard results. When calibrated with the site-specific hazard analysis, the regional results should provide a realistic measure of the ALWR seismic risk calculated in Section 7.

5.5 Soil-Site Hazard Results

Using the procedure described in Section 4, the regional- and site-specific hazard results were modified to produce the mean hazard curves for the four soil categories. For simplicity, the results of the site-specific hazard calculations only are displayed here. For each soil category, the hazard curves in each region are plotted as they were for the rock-site results (see Figs. 5-5 to 5-10). The results for each soil-site category are given in Figures 5-41 to 5-64.

5.6 ALWR SH Response Spectra

In this section the ALWR SH response spectra for each site category are given. As described in Section 2, the results of the EPRI/SOG seismic hazard calculations are used (5). However, as discussed in Section 4 the EPRI/SOG hazard calculations were performed using a constant variability on ground motion and no truncation. As a result the ground-response spectra that were developed as part of the EPRI/SOG seismic hazard project do not strictly correspond to the PGA hazard curves estimated in this project.

In Section 5.6.1 the development of ALWR SH response spectra are presented. In Section 5.6.2 a comparison is made between the response-spectrum shape estimated in the EPRI/SOG analysis and that obtained here. Any difference in the spectral shape is attributed to differences in ground motion variability and truncation. The results of this evaluation are used in the development of the ALWR core-damage fragility curve (see Section 6).

5.6.1 Response Spectrum Results

As part of the EPRI/SOG project the seismic hazard was estimated at 57 nuclear power plant sites in the EUS (5). For purposes of defining a response-spectrum shape for the ALWR SH that represents the ground motion in the EUS the results of the EPRI/SOG project are used. For each of the 57 sites the seismic hazard was estimated for 6 ground motion measures that correspond to ordinates of a response spectrum. Using the seismic-hazard curve at a site for each spectral ordinate, uniform-hazard response spectra were developed. The UHS is defined such that each ordinate of the response spectrum has the same annual frequency of being exceeded.

The UHS at each of the 57 sites comprise a data base that is used to estimate an average response-spectrum shape for the EUS. Starting with the hazard results for rock-site conditions, the mean UHS corresponding to a frequency of 10^{-6} per year is determined. The 10^{-6} spectrum is used since it corresponds approximately to the ground motion levels that will be the primary contributors to seismic risk for the ALWR (see Sections 2 and 7). The average of the 57 response-spectra is determined and normalized to 1.0g PGA. The normalized response spectrum shape is the ALWR SH spectrum for rock sites.

By estimating the seismic hazard at each of the 57 sites for each site category and repeating this process, the ALWR SH response spectrum for each site category is determined. Figure 5-65 shows the average (over the 57 sites) 10^{-6} UHS for each site category (rock, S2, S3, S4, S5). The spectra are normalized to 1.0g for use in the seismic fragility analysis. The normalized spectra are shown in Figure 5-66 and tabulated in Table 5-5.

Table 5-5

ALWR Response Spectrum Values for Each Site Category

Frequency (hz)	EPRI Soil Category				
	Rock	S2	S3	S4	S5
1.0	0.504	0.332	0.516	0.951	1.078
2.5	1.097	1.055	1.896	1.991	1.702
5.0	1.532	2.192	2.268	2.307	1.801
10.0	1.668	2.159	2.014	1.961	1.755
25.0	1.862	1.804	1.563	1.736	1.838
50.0*	1.000	1.000	1.000	1.000	1.000

* Assumed frequency at which response spectrum returns to PGA.

5.6.2 Comparison of EPRI/SOG and Current Hazard Results

In this study seismic hazard results were computed using a variability on ground motion that varied with earthquake magnitude and a truncation on ground motion (see Section 4). The response spectra developed in the previous subsection are based on the EPRI/SOG seismic hazard results which used a constant variability and no truncation. Ideally, the uniform hazard spectra would be developed by repeating the 57 site-hazard calculations using the variability and truncation parameters in this study.

Since the seismic hazard analysis for the ALWR was performed for PGA only, a direct assessment of the response spectra based on the parameters used in this analysis (i.e., ground motion variability and truncation) was not possible. To determine whether a difference in the response spectra from the two studies does exist, a limited number of seismic hazard calculations were performed for spectral acceleration (S_a) at 2.5 hz using the EPRI/SOG attenuation models and the variability and truncation parameters used in this analysis. The 2.5 hz frequency was chosen since studies of ground motion indicate that the spectral amplitude for frequencies near 2.5 hz are important contributors to earthquake damage (32).

To test whether the two sets of hazard calculations (EPRI/SOG and this study) produce response-spectrum shapes that are different, the ratio between the spectral acceleration at 2.5 hz and PGA was computed. This ratio was computed for the mean 10^{-6} uniform-hazard spectrum for 17 sites. By comparing this ratio for the two sets of results, a measure of the consistency of the two hazard calculations is obtained. This evaluation was performed for each site category.

The conclusion is that the spectral ratio (S_a/PGA) derived from the EPRI/SOG results are generally higher by about 15%. This difference is consistent for all site conditions, with the exception of site category S2, where the difference is about 24%. This suggests that the ALWR SH response-spectrum shape is slightly conservative (by about 15% in most cases) in the mid-frequency range, 2-10 hz. This observation is used in Section 6 as part of the development of the ALWR core-damage fragility curve.

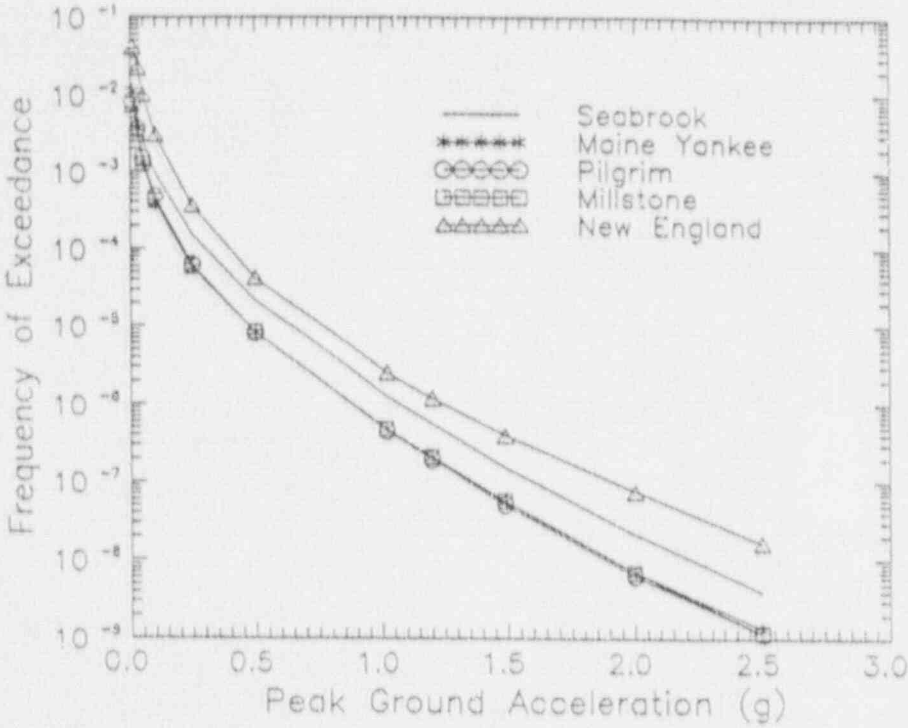

Figure 5-5 Mean seismic hazard curves for sites in the New England area.

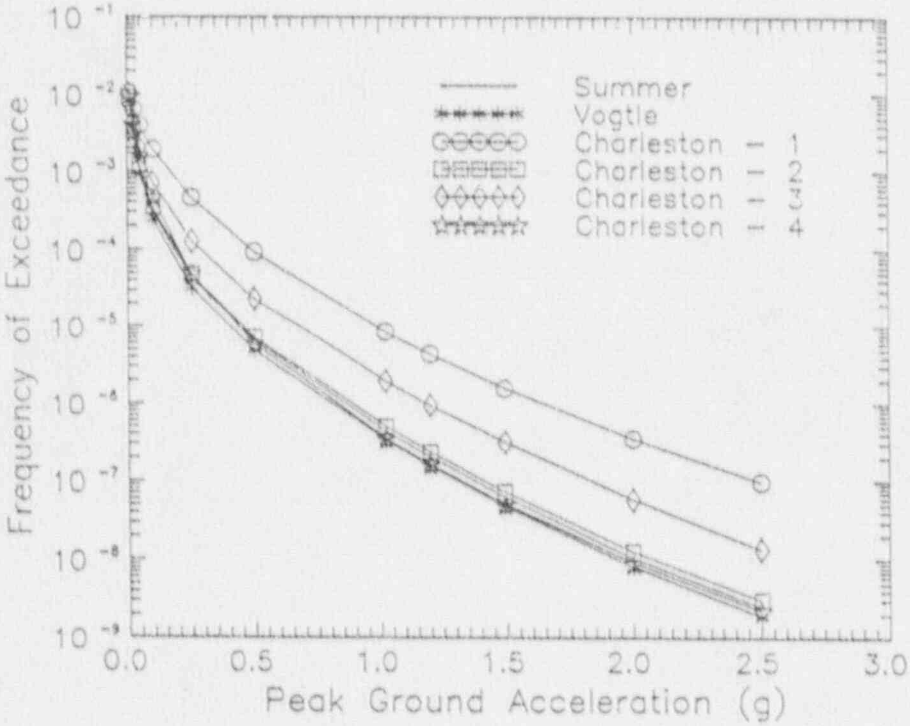

Figure 5-6 Mean seismic hazard curves for the sites in the Charleston area.

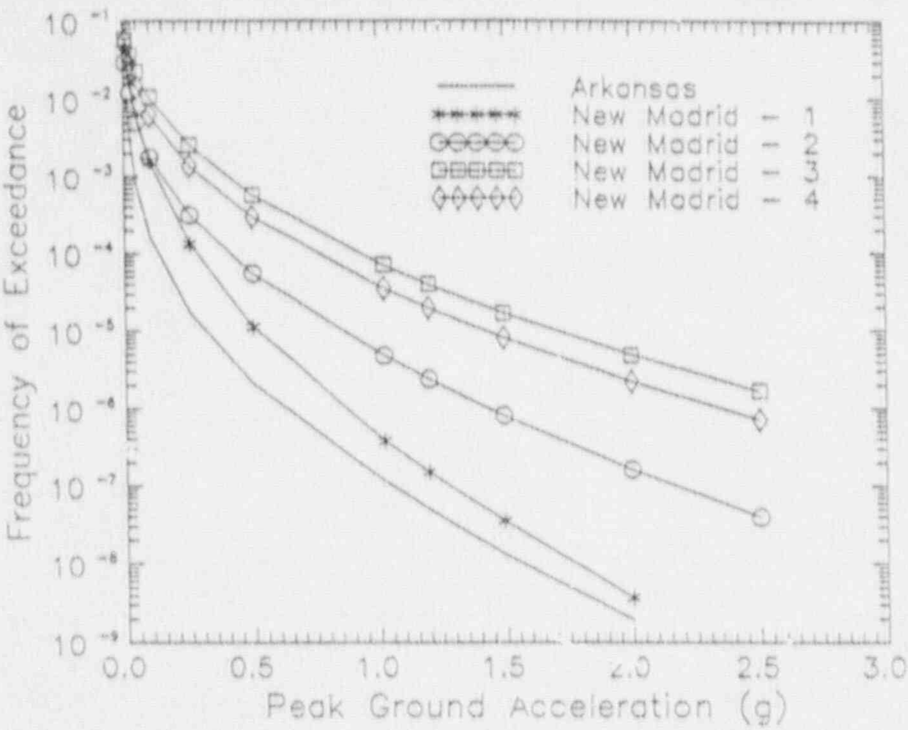

Figure 5-7 Mean seismic hazard curves for the sites in the New Madrid area.

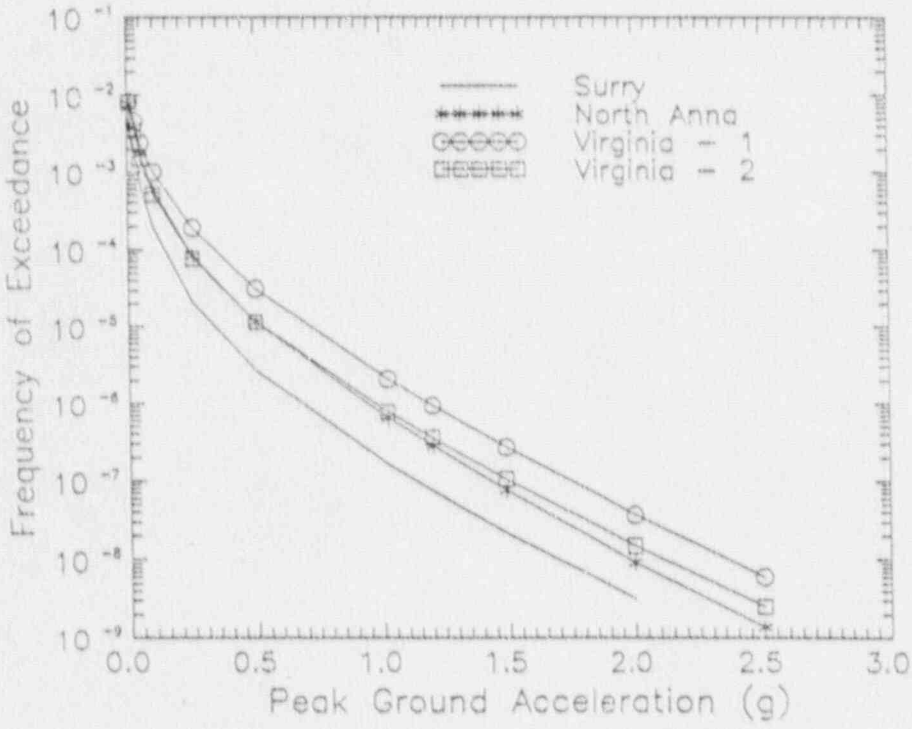

Figure 5-8 Mean seismic hazard curves for the sites in the Virginia area.

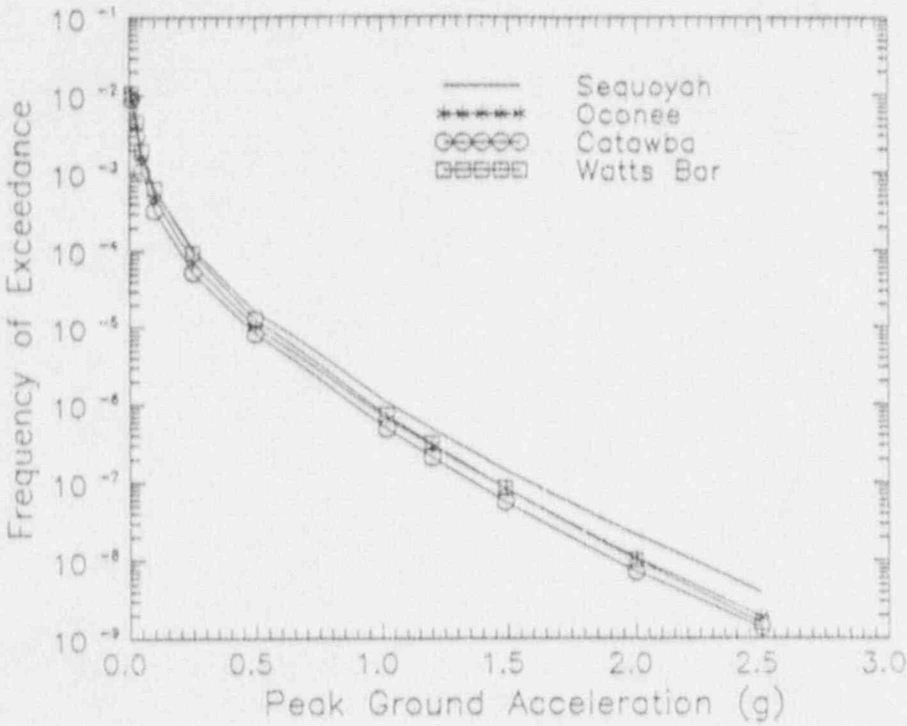

Figure 5-9 Mean seismic hazard curves for the sites in the Piedmont area.

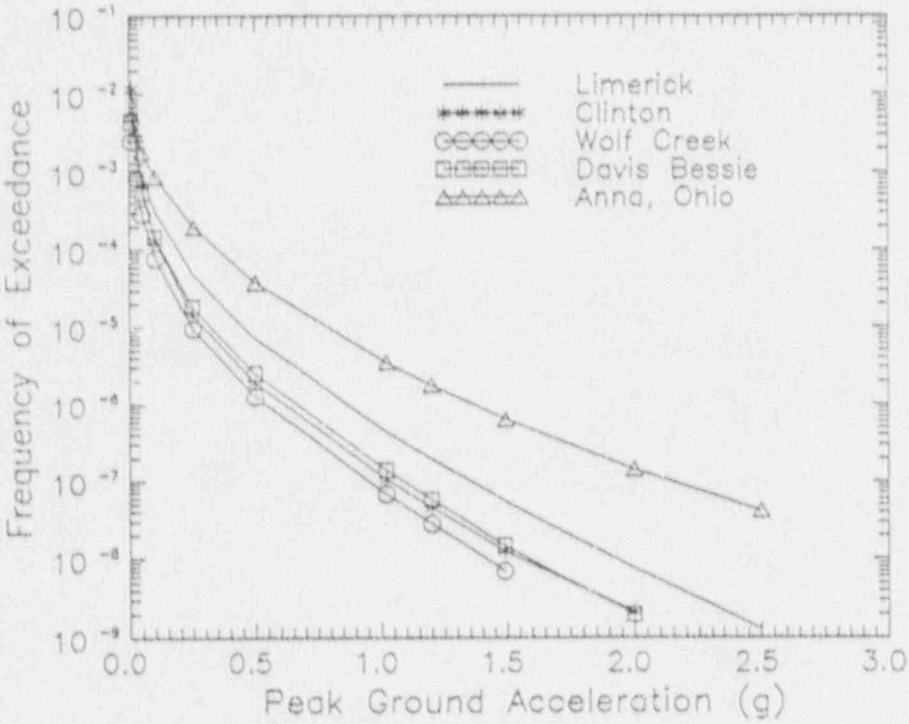

Figure 5-10 Mean seismic hazard curves for the other sites considered.

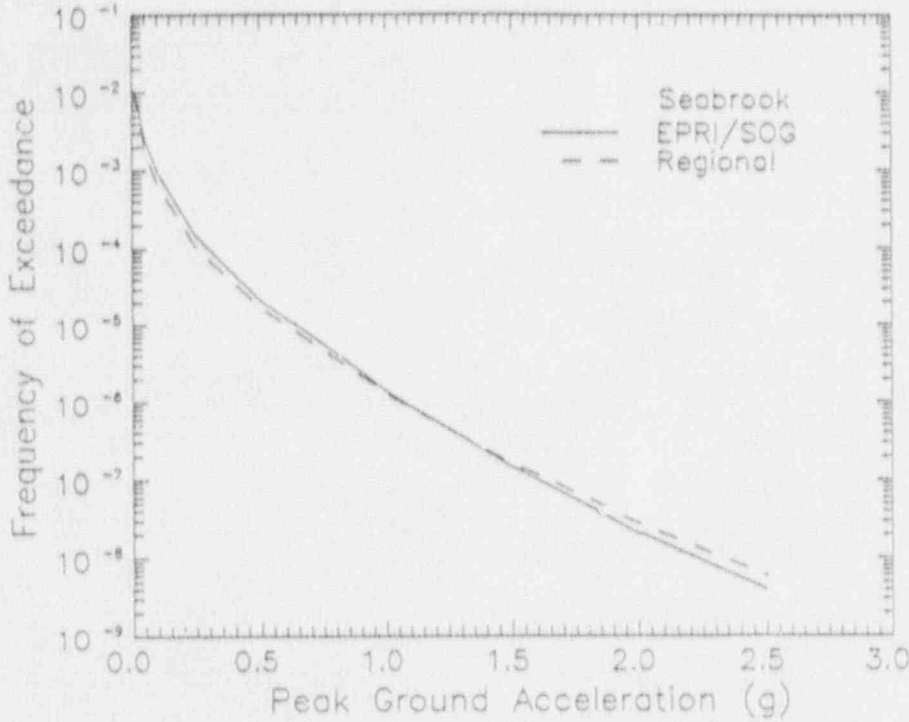

Figure 5-11 Comparison of the regional and site-specific mean seismic hazard curves for Seabrook.

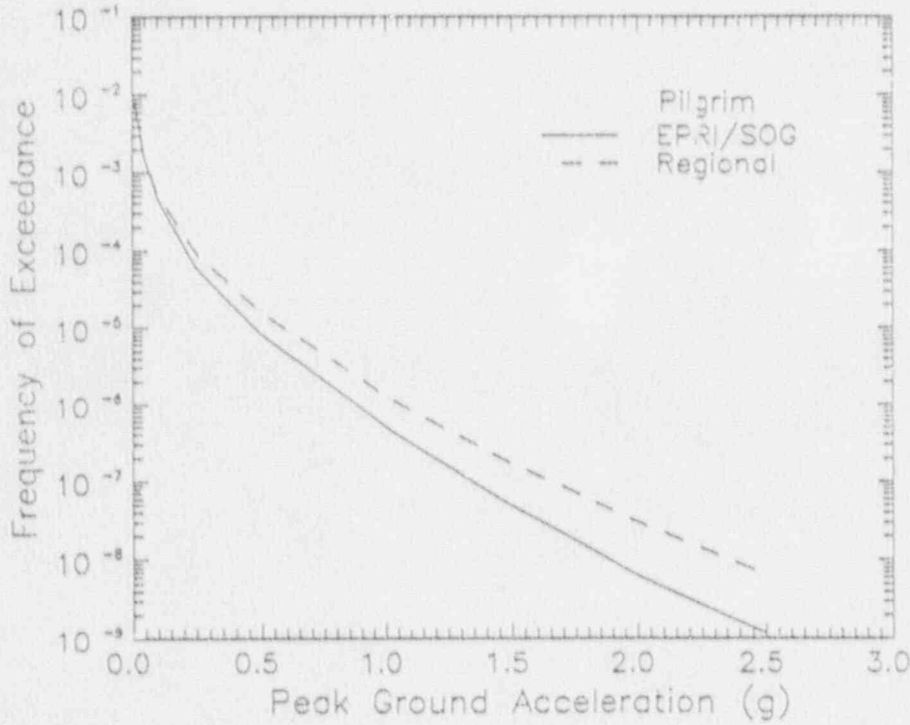

Figure 5-12 Comparison of the regional and site-specific mean seismic hazard curves for Pilgrim.

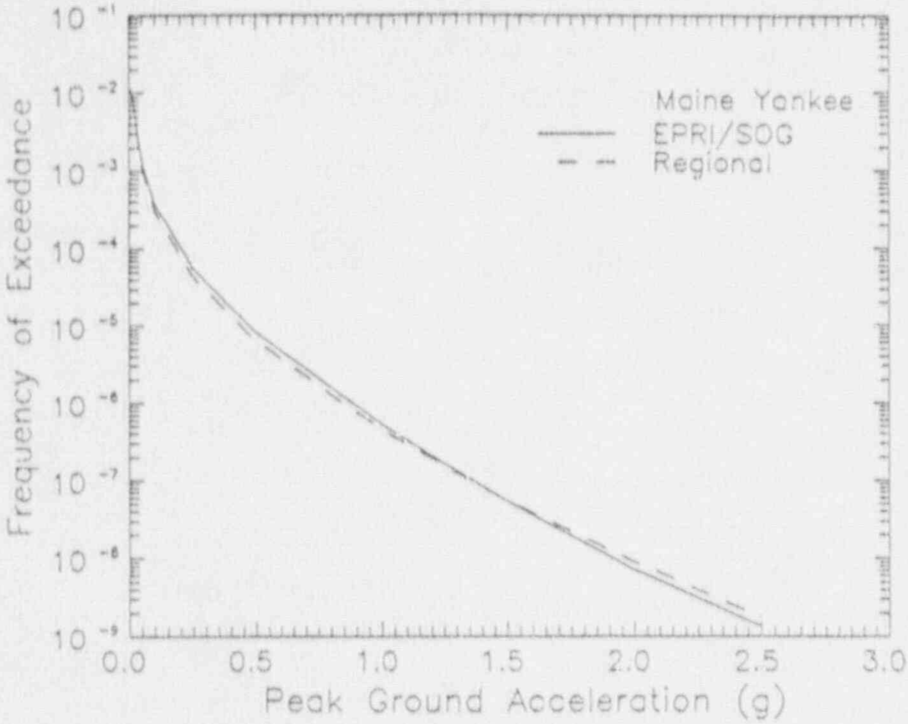

Figure 5-13 Comparison of the regional and site-specific mean seismic hazard curves for Maine Yankee.

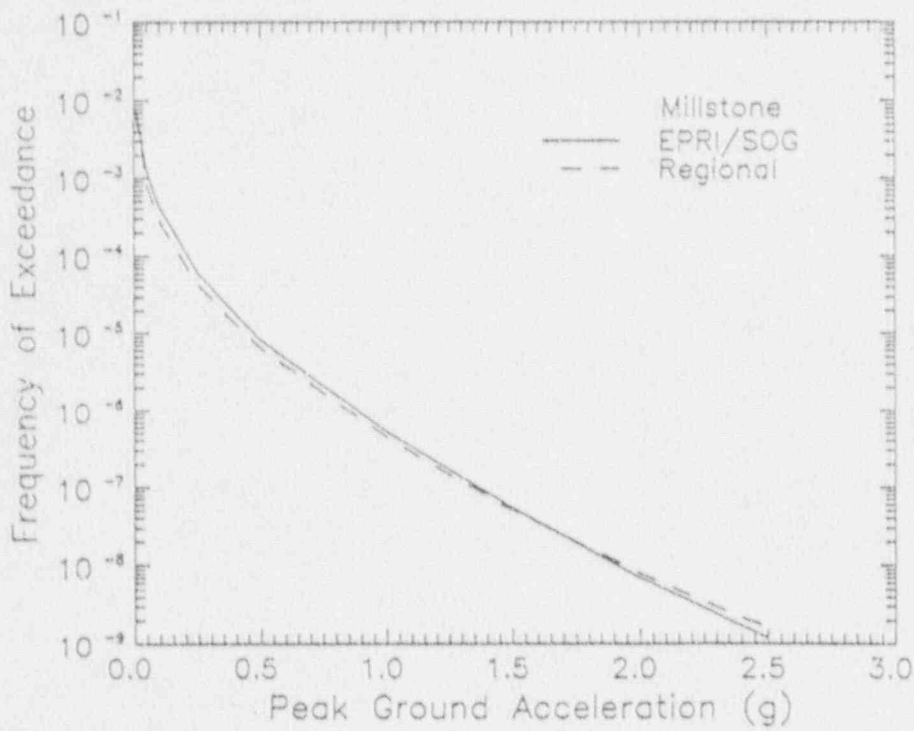

Figure 5-14 Comparison of the regional and site-specific mean seismic hazard curves for Millstone.

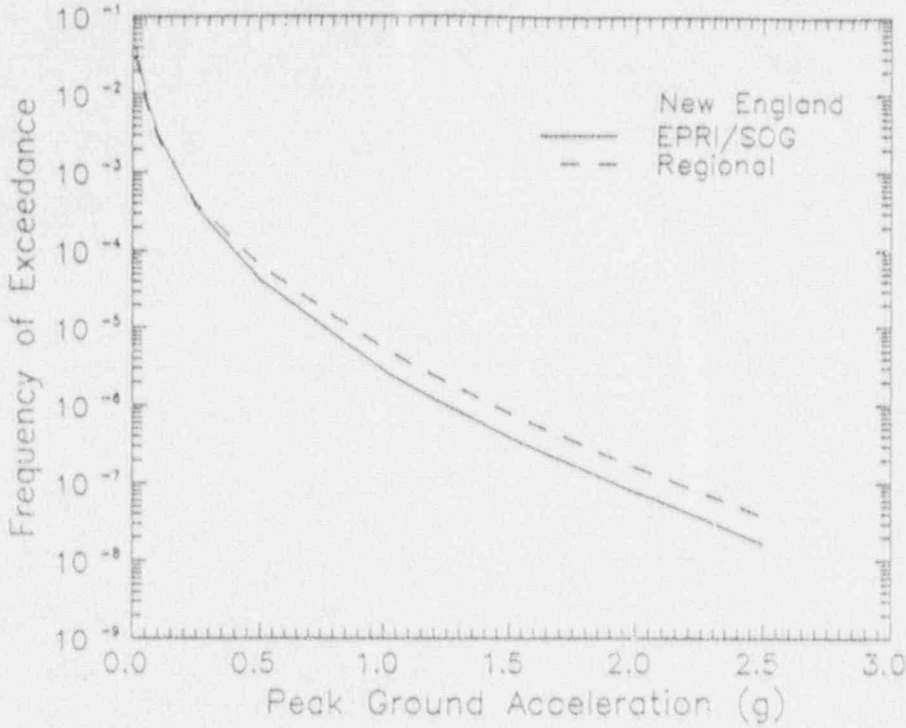

Figure 5-15 Comparison of the regional and site-specific mean seismic hazard curves for the New England site.

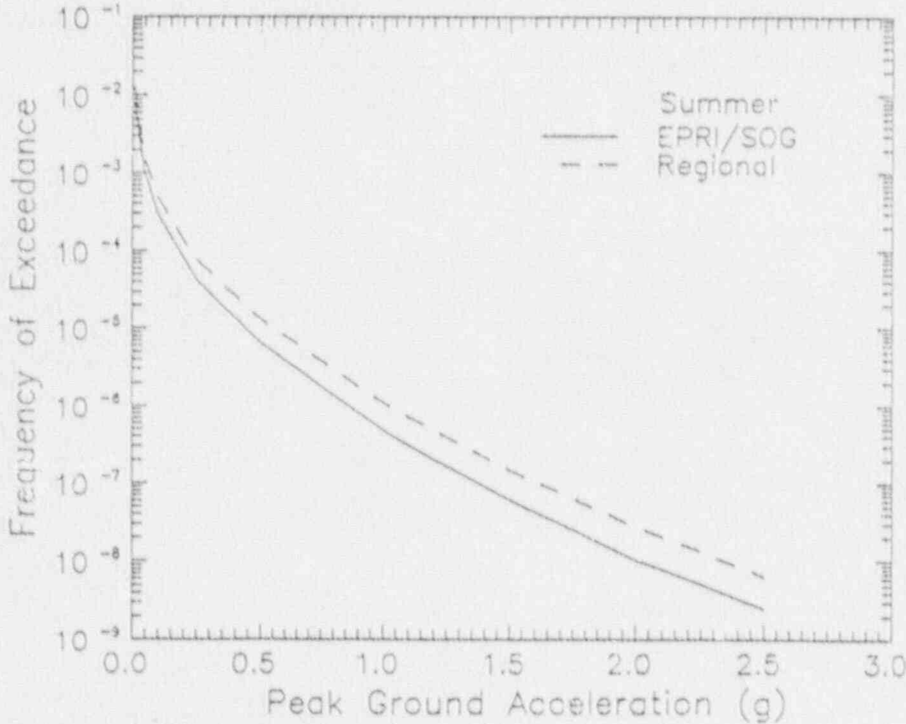

Figure 5-16 Comparison of the regional and site-specific mean seismic hazard curves for Summer.

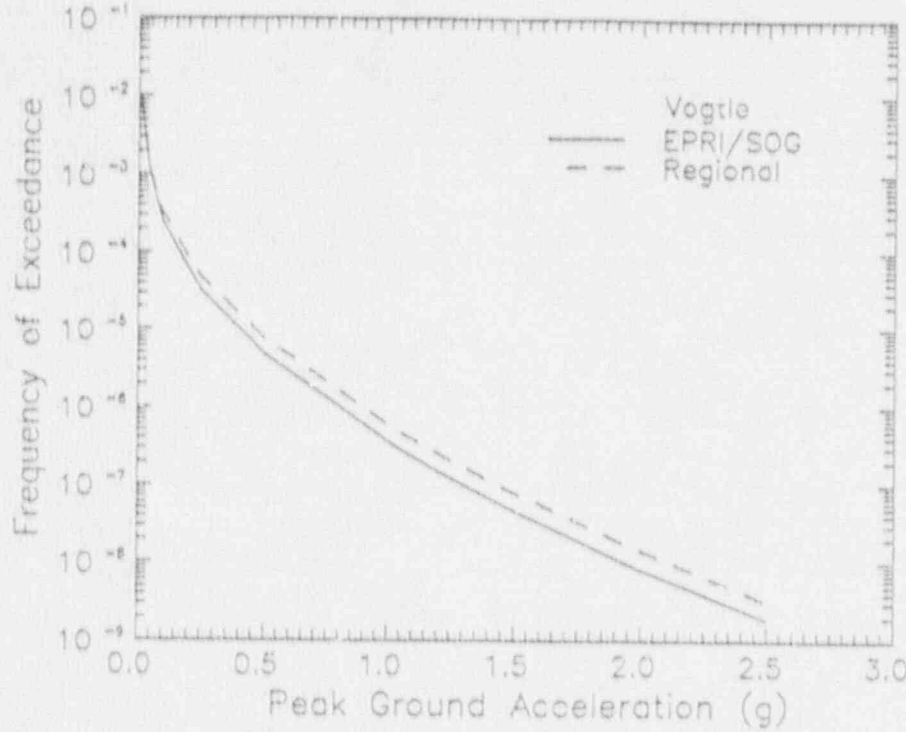

Figure 5-17 Comparison of the regional and site-specific mean seismic hazard curves for Vogtle.

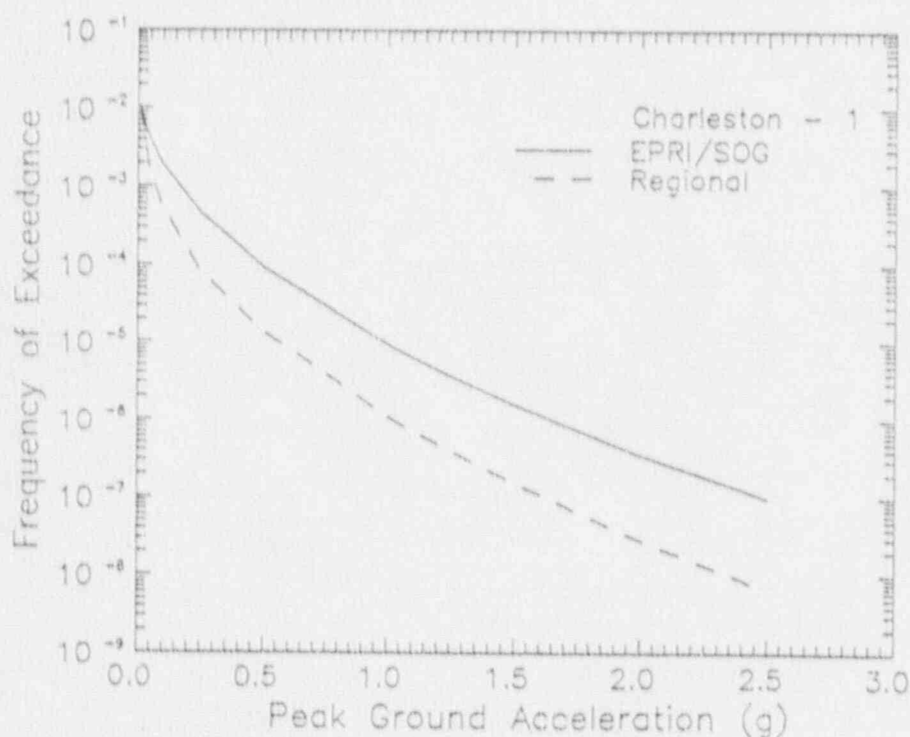

Figure 5-18 Comparison of the regional and site-specific mean seismic hazard curves for Charleston-1.

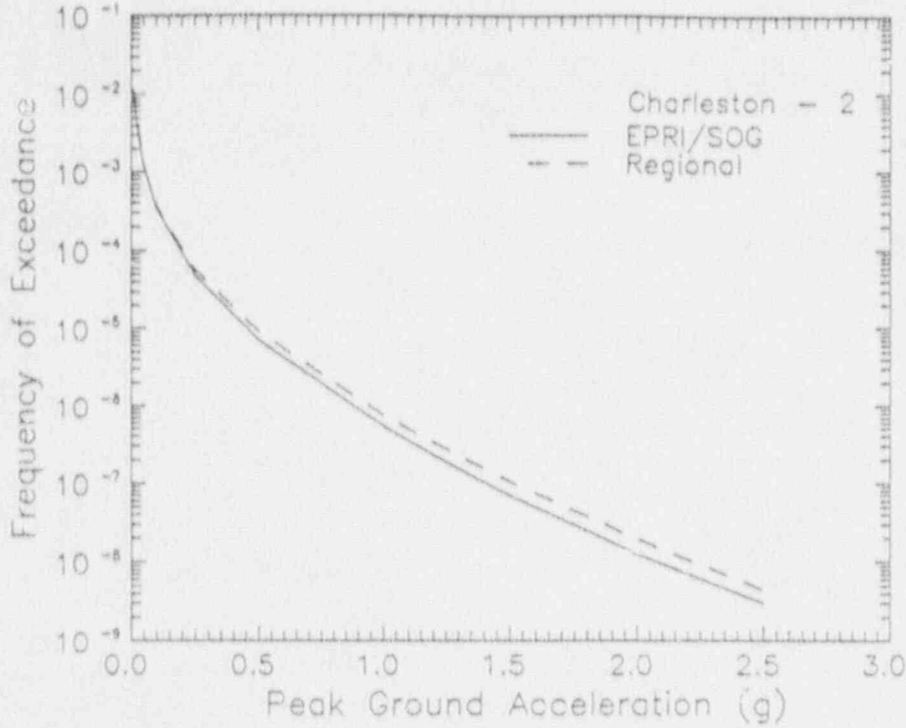

Figure 5-19 Comparison of the regional and site-specific mean seismic hazard curves for Charleston-2.

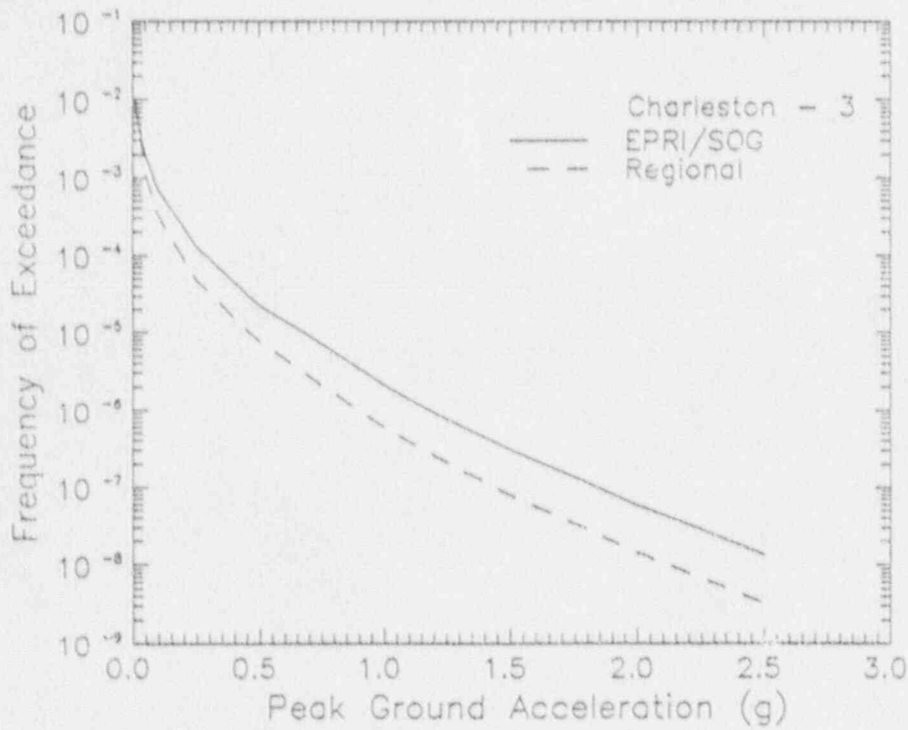

Figure 5-20 Comparison of the regional and site-specific mean seismic hazard curves for Charleston-3.

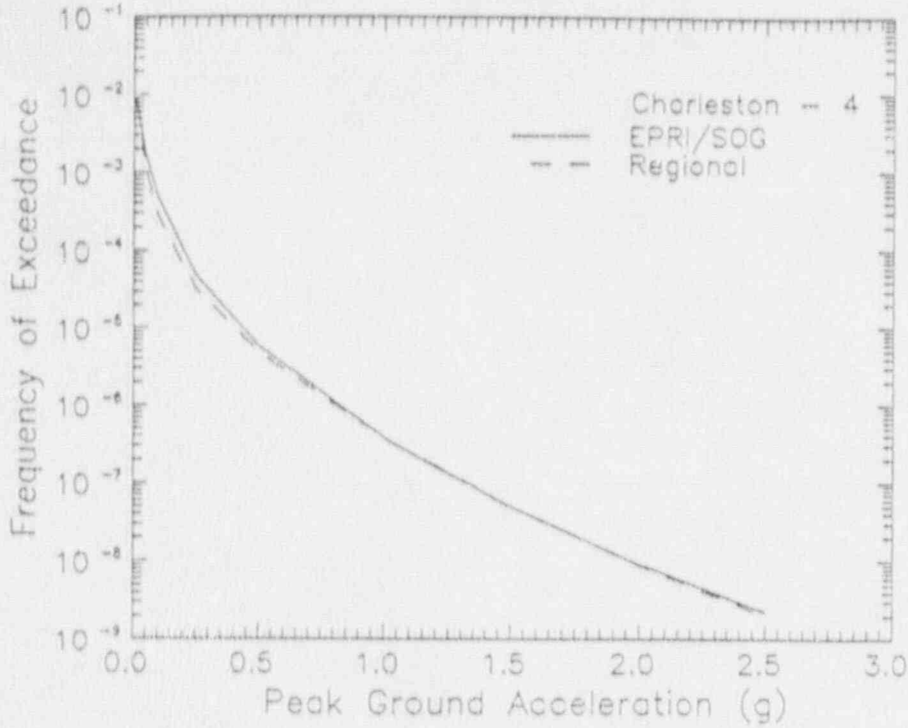

Figure 5-21 Comparison of the regional and site-specific mean seismic hazard curves for Charleston-4.

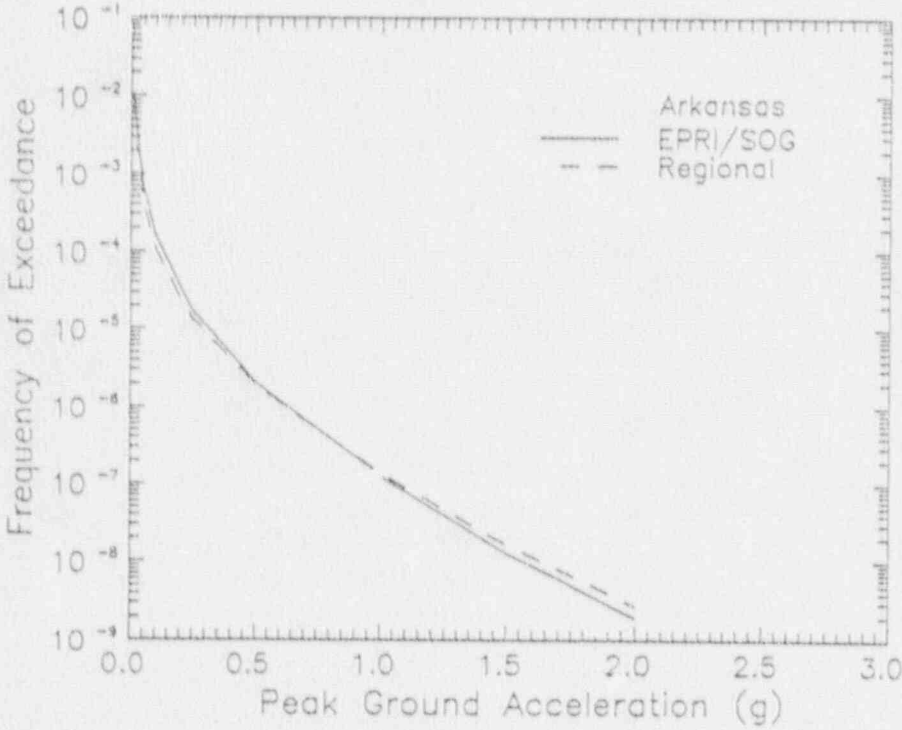

Figure 5-22 Comparison of the regional and site-specific mean seismic hazard curves for ANO.

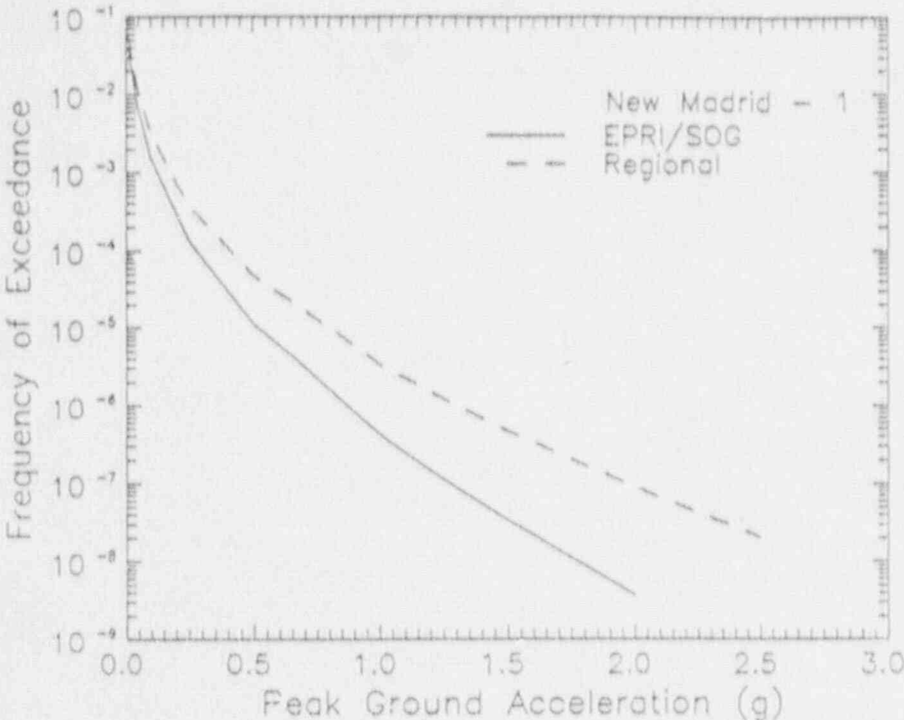

Figure 5-23 Comparison of the regional and site-specific mean seismic hazard curves for New Madrid-1.

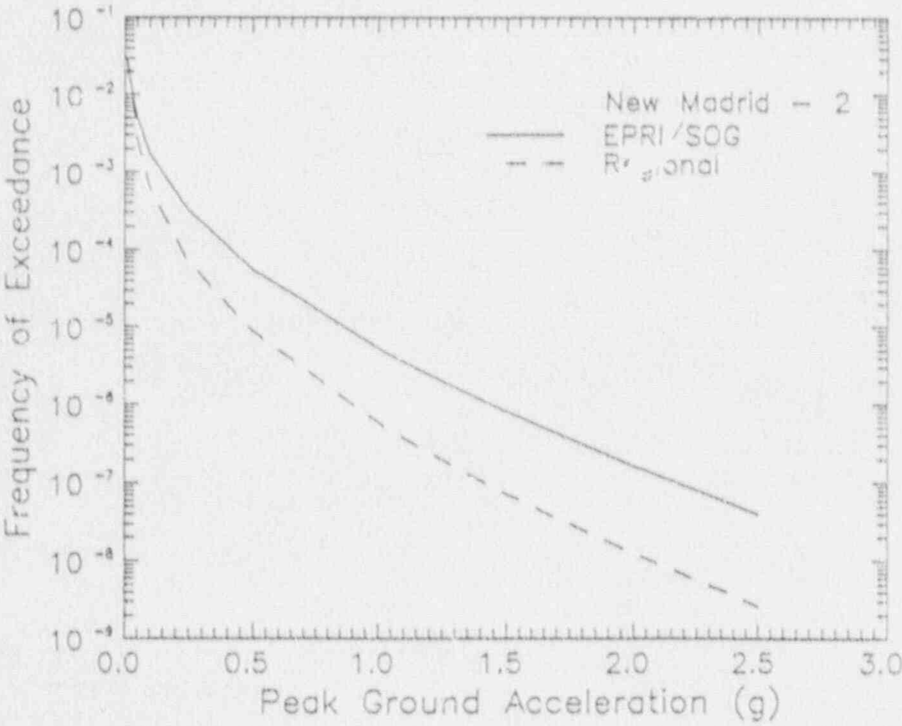

Figure 5-24 Comparison of the regional and site-specific mean seismic hazard curves for New Madrid-2.

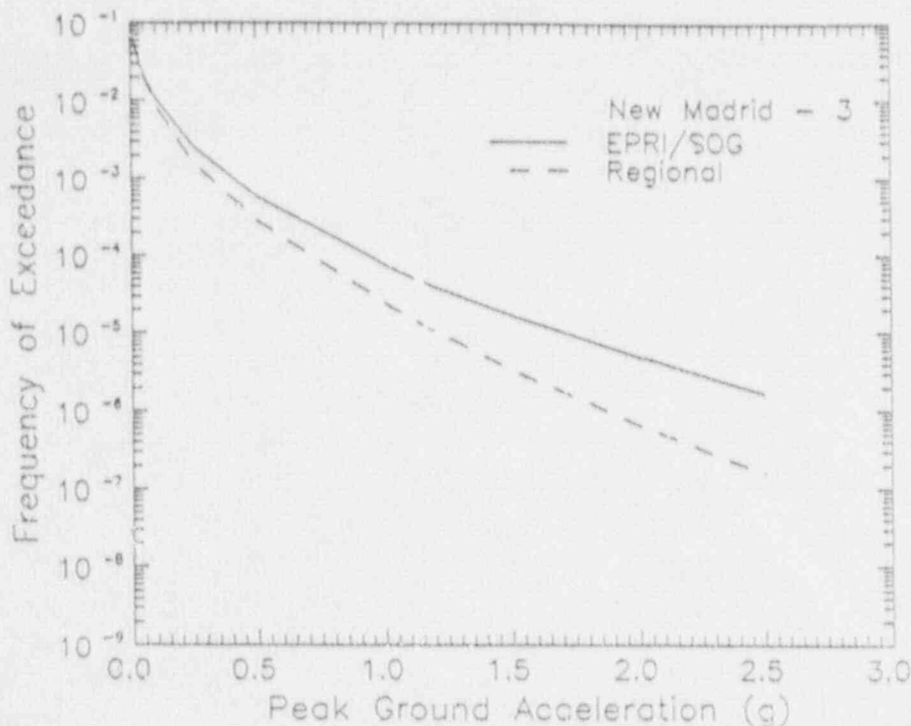

Figure 5-25 Comparison of the regional and site-specific mean seismic hazard curves for New Madrid-3.

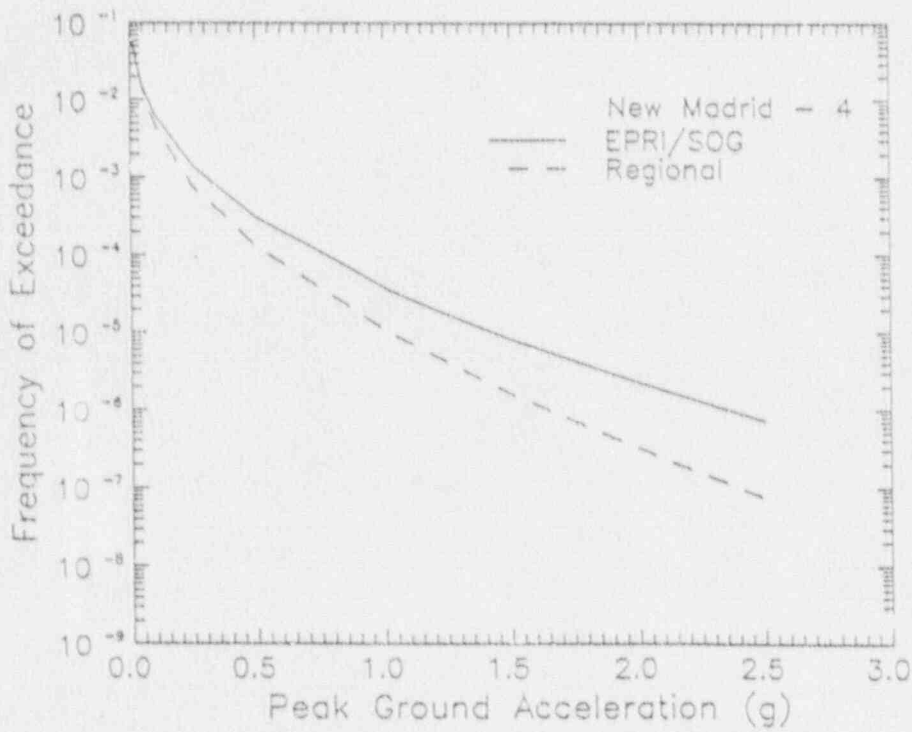

Figure 5-26 Comparison of the regional and site-specific mean seismic hazard curves for New Madrid-4.

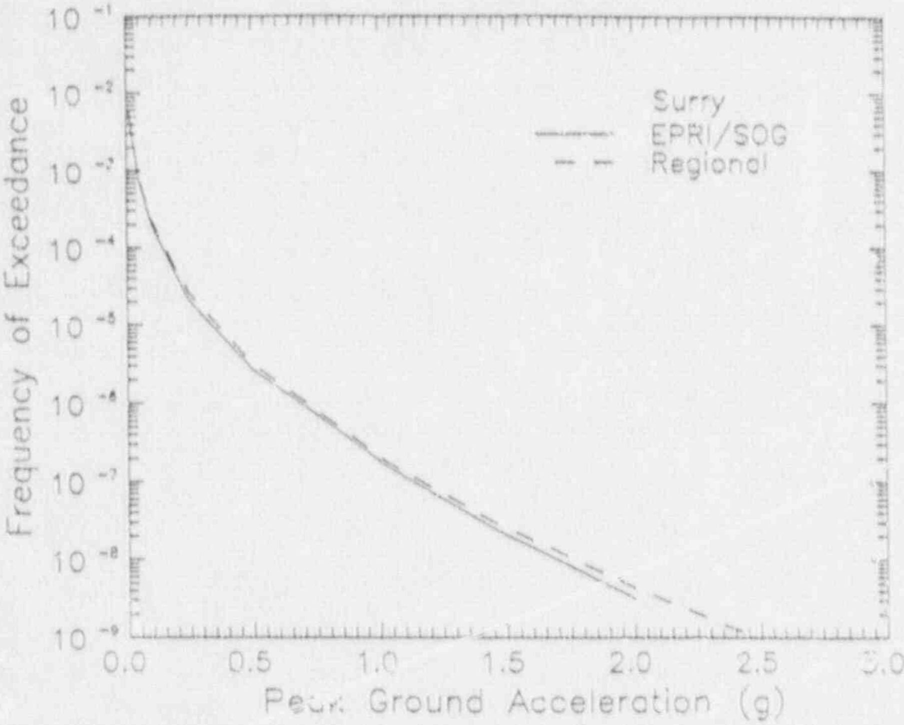

Figure 5-27 Comparison of the regional and site-specific mean seismic hazard curves for Surrey.

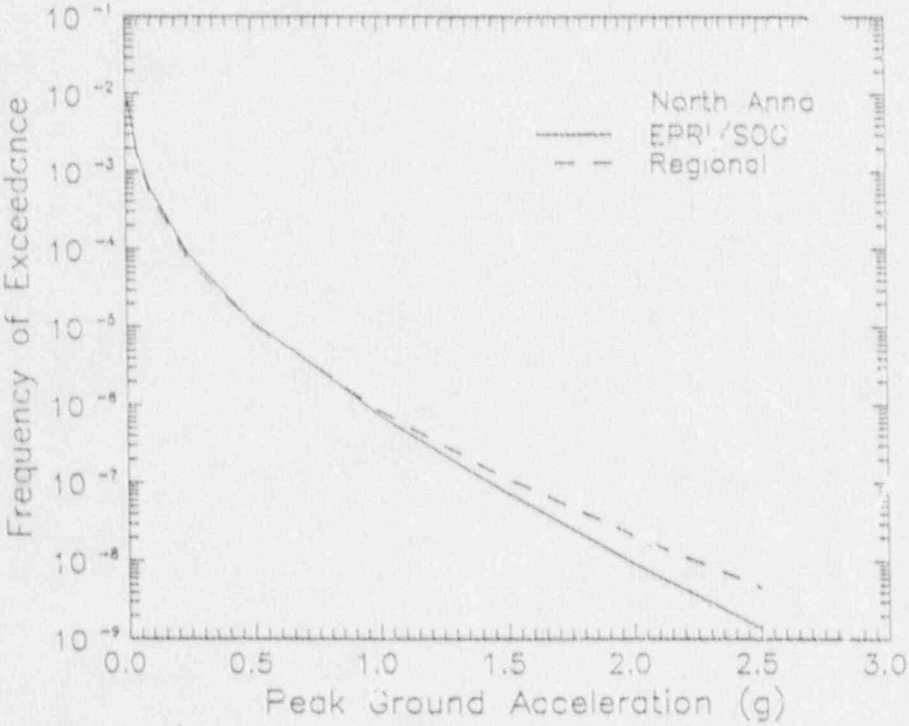

Figure 5-28 Comparison of the regional and site-specific mean seismic hazard curves for North Anna.

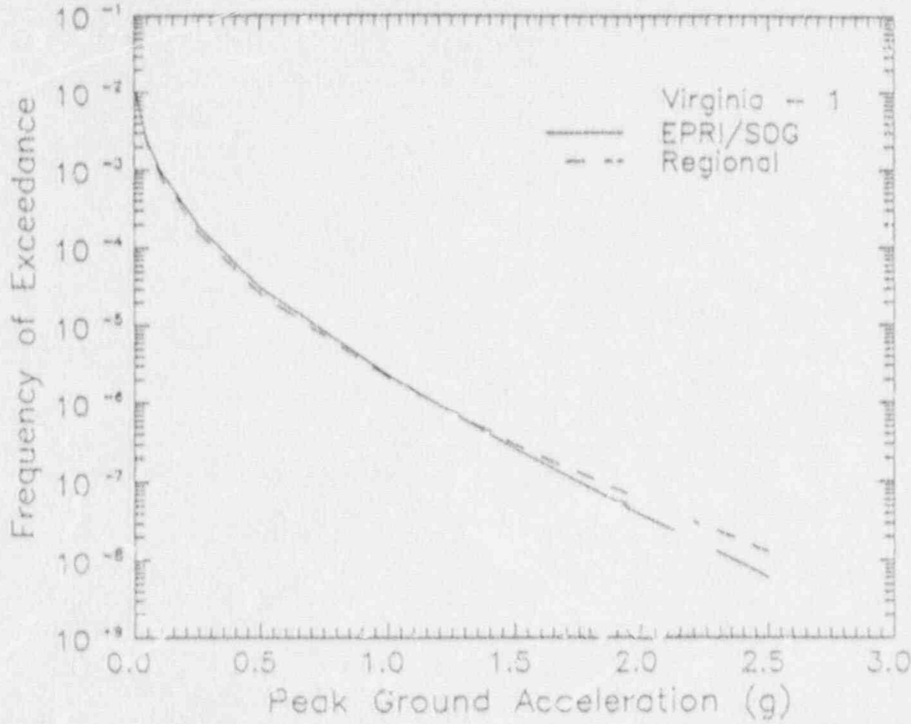

Figure 5-29 Comparison of the regional and site-specific mean seismic hazard curves for VA-1.

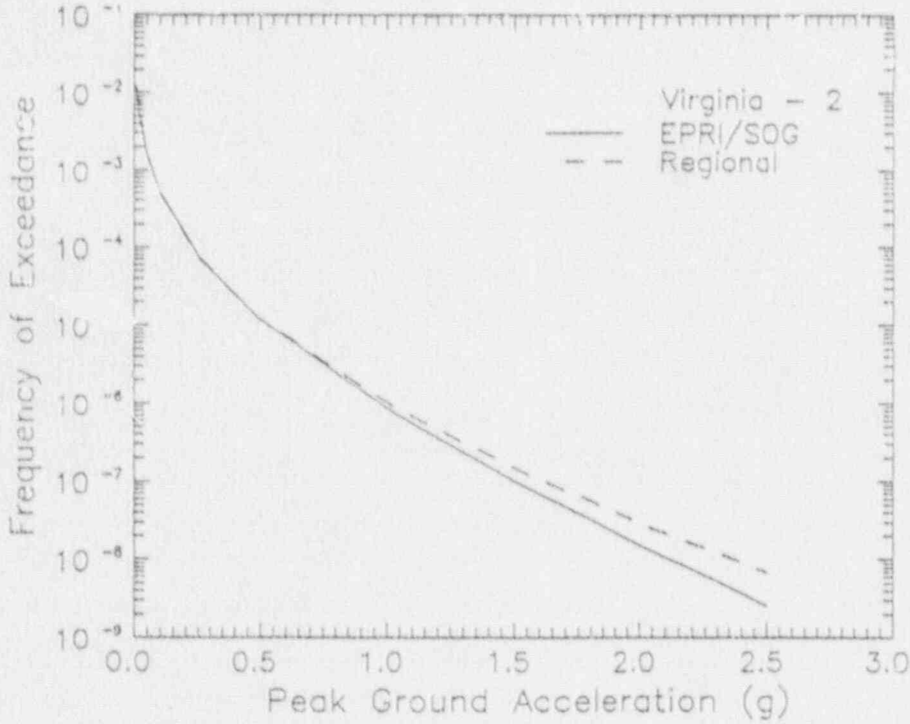

Figure 5-30 Comparison of the regional and site-specific mean seismic hazard curves for VA-2.

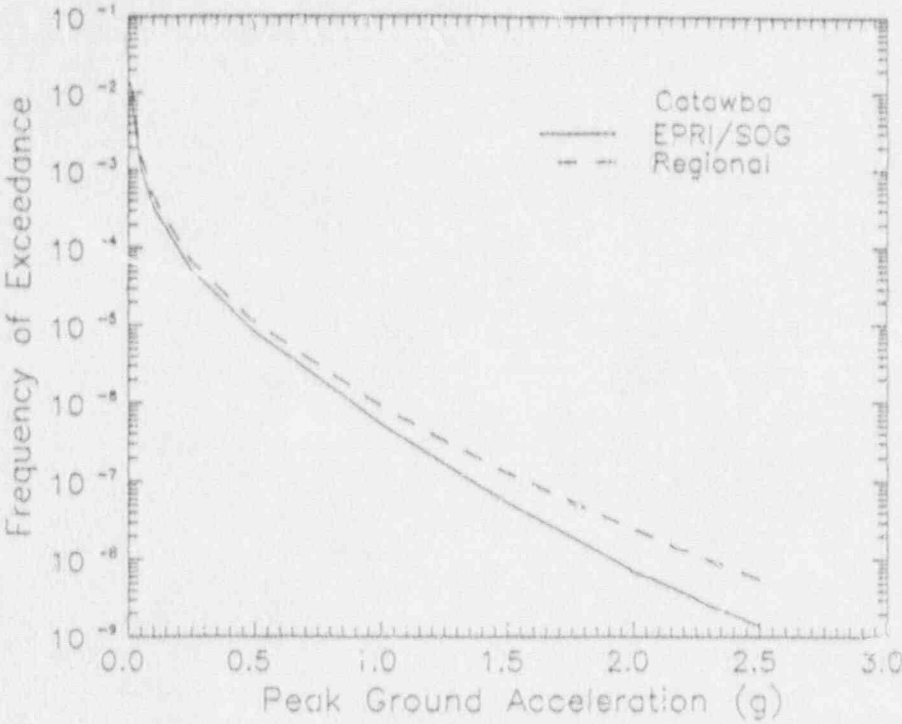

Figure 5-31 Comparison of the regional and site-specific mean seismic hazard curves for Catawba.

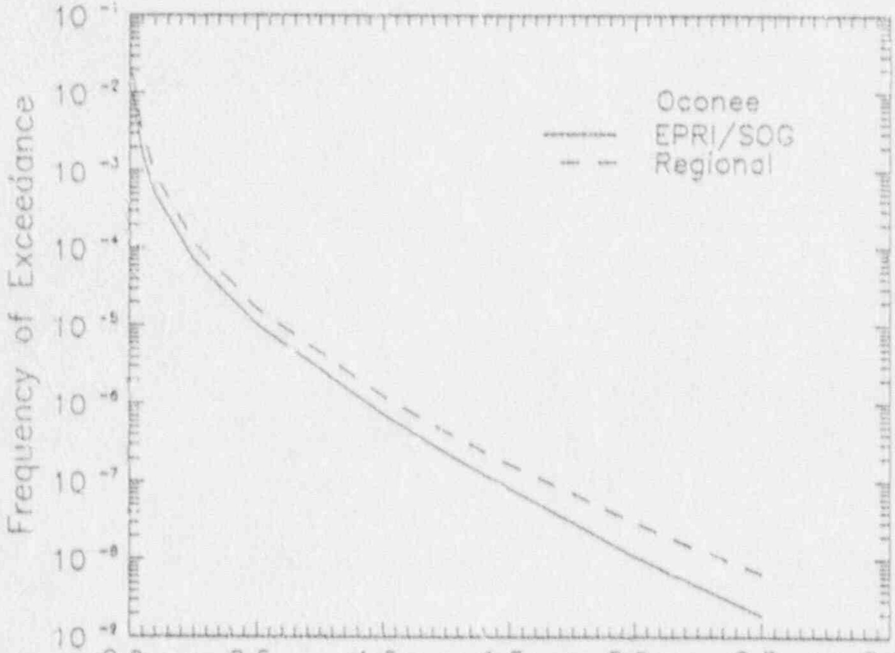

Figure 5-32 Comparison of the regional and site-specific mean seismic hazard curves for Oconee.

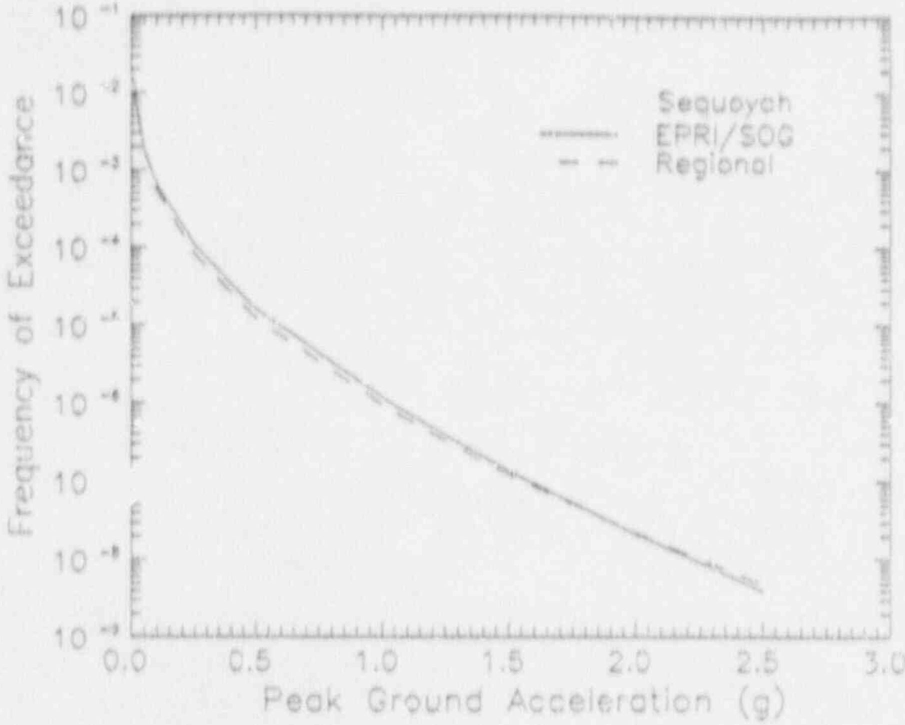

Figure 5-33 Comparison of the regional and site-specific mean seismic hazard curves for Sequoyah.

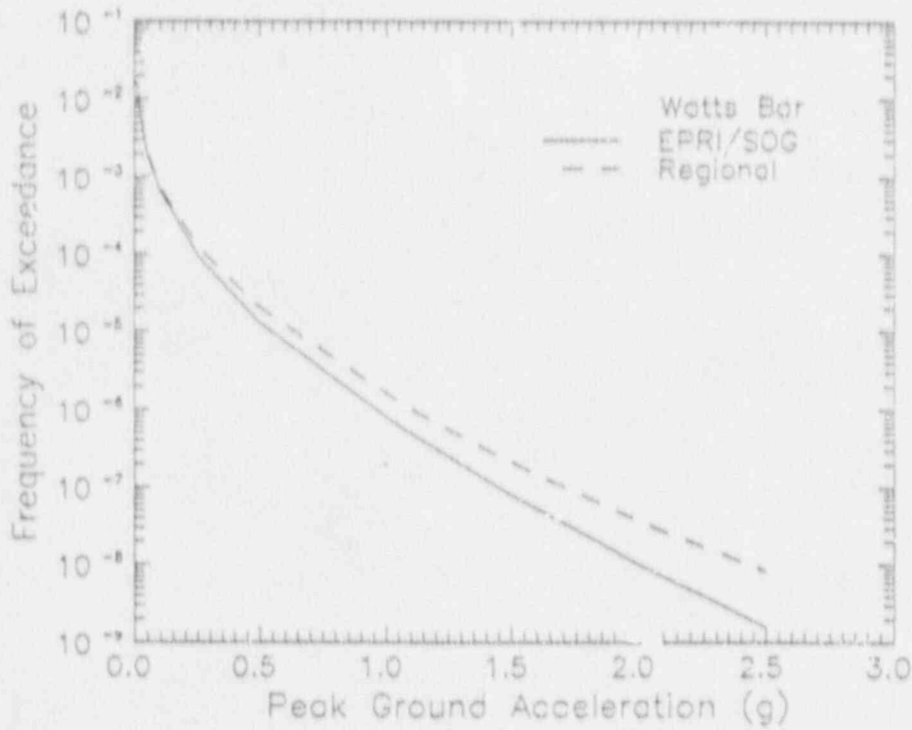

Figure 5-34 Comparison of the regional and site-specific mean seismic hazard curves for Watts Bar.

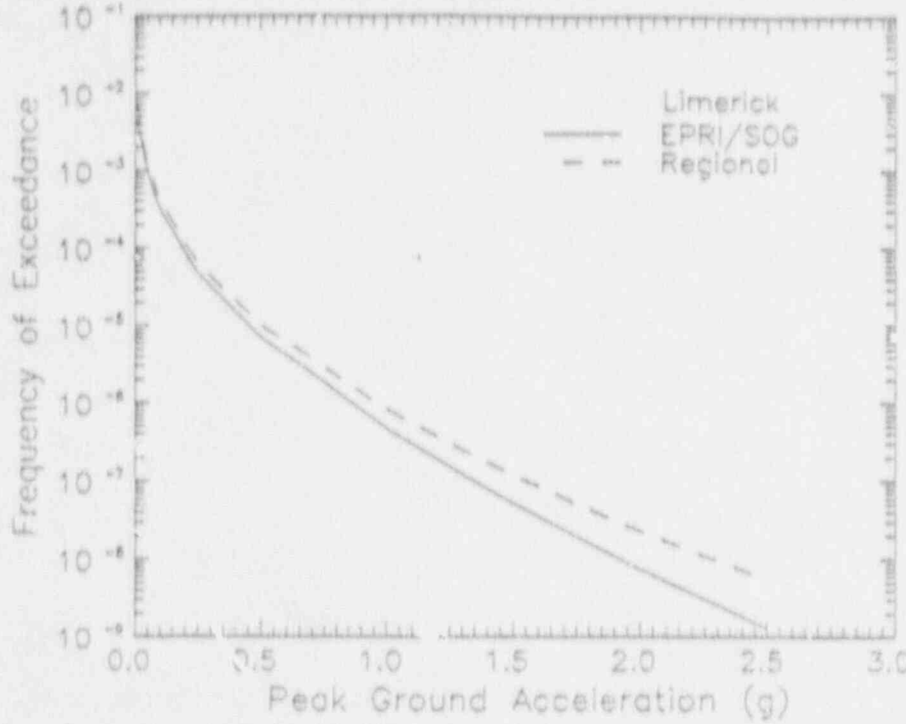

Figure 5-35 Comparison of the regional and site-specific mean seismic hazard curves for Limerick.

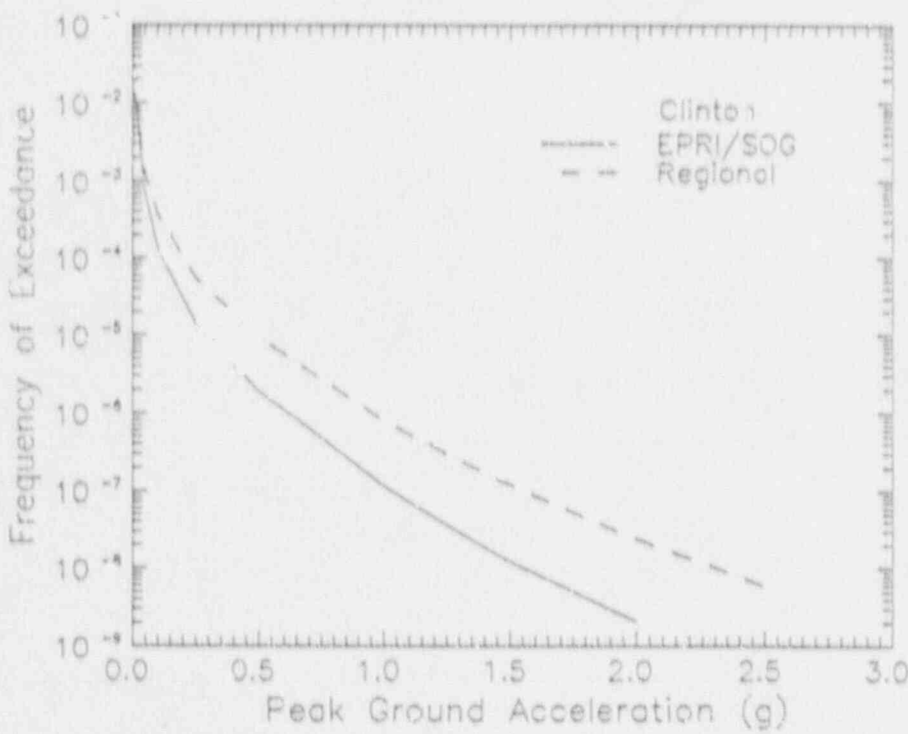

Figure 5-36 Comparison of the regional and site-specific mean seismic hazard curves for Clinton.

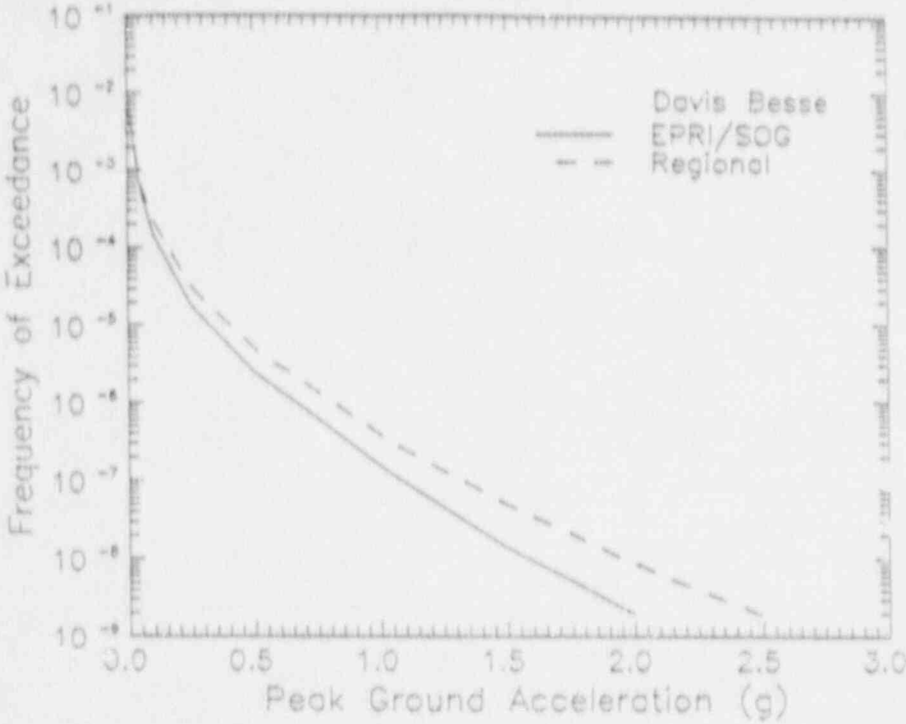

Figure 5-37 Comparison of the regional and site-specific mean seismic hazard curves for Davis Besse.

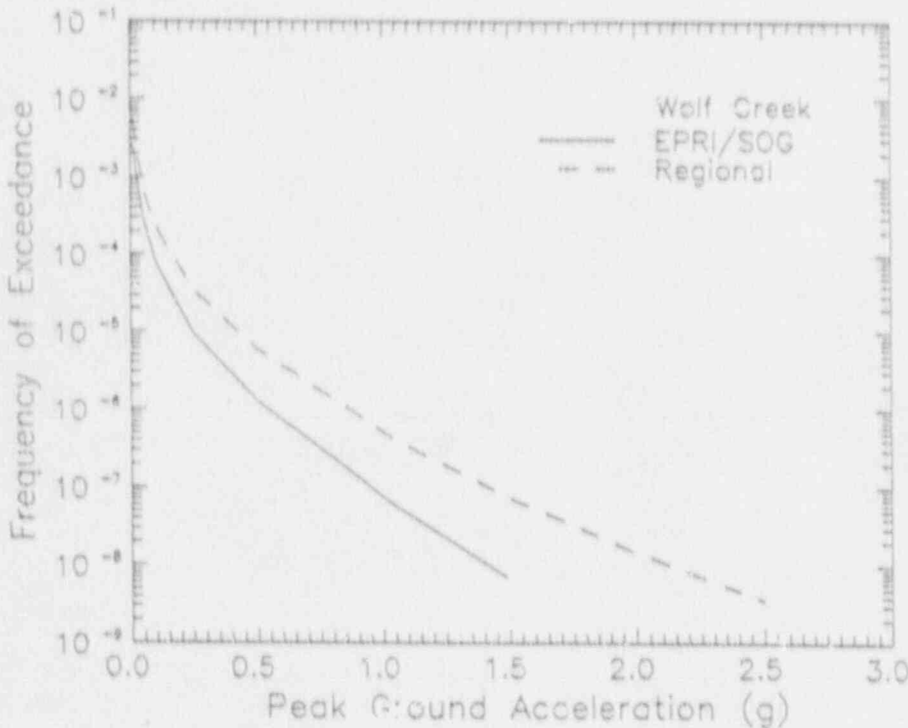

Figure 5-38 Comparison of the regional and site-specific mean seismic hazard curves for Wolf Creek.

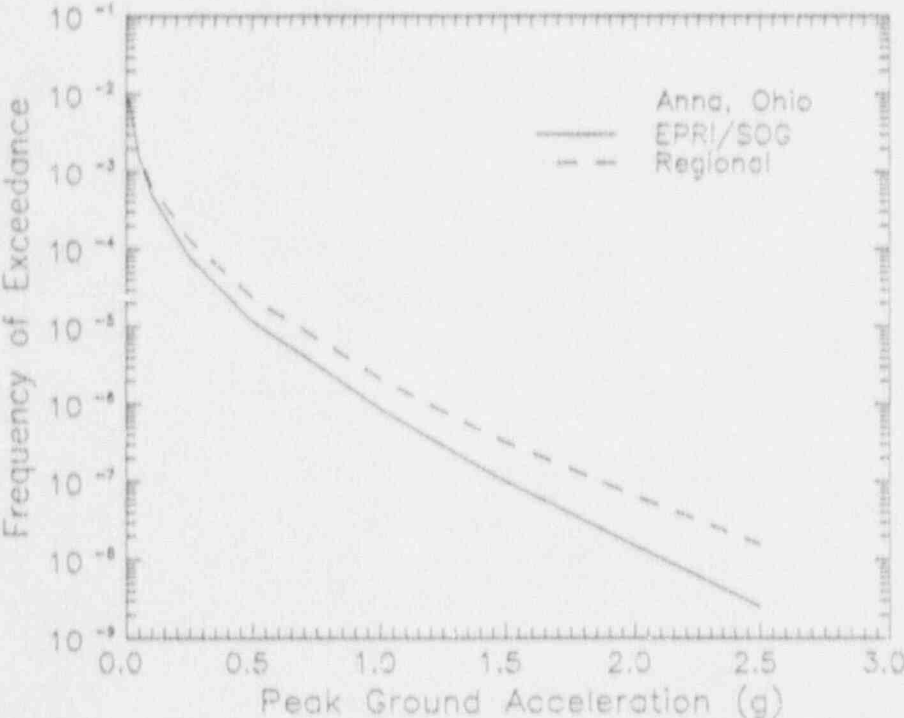

Figure 5-39 Comparison of the regional and site-specific mean seismic hazard curves for Anna, Ohio.

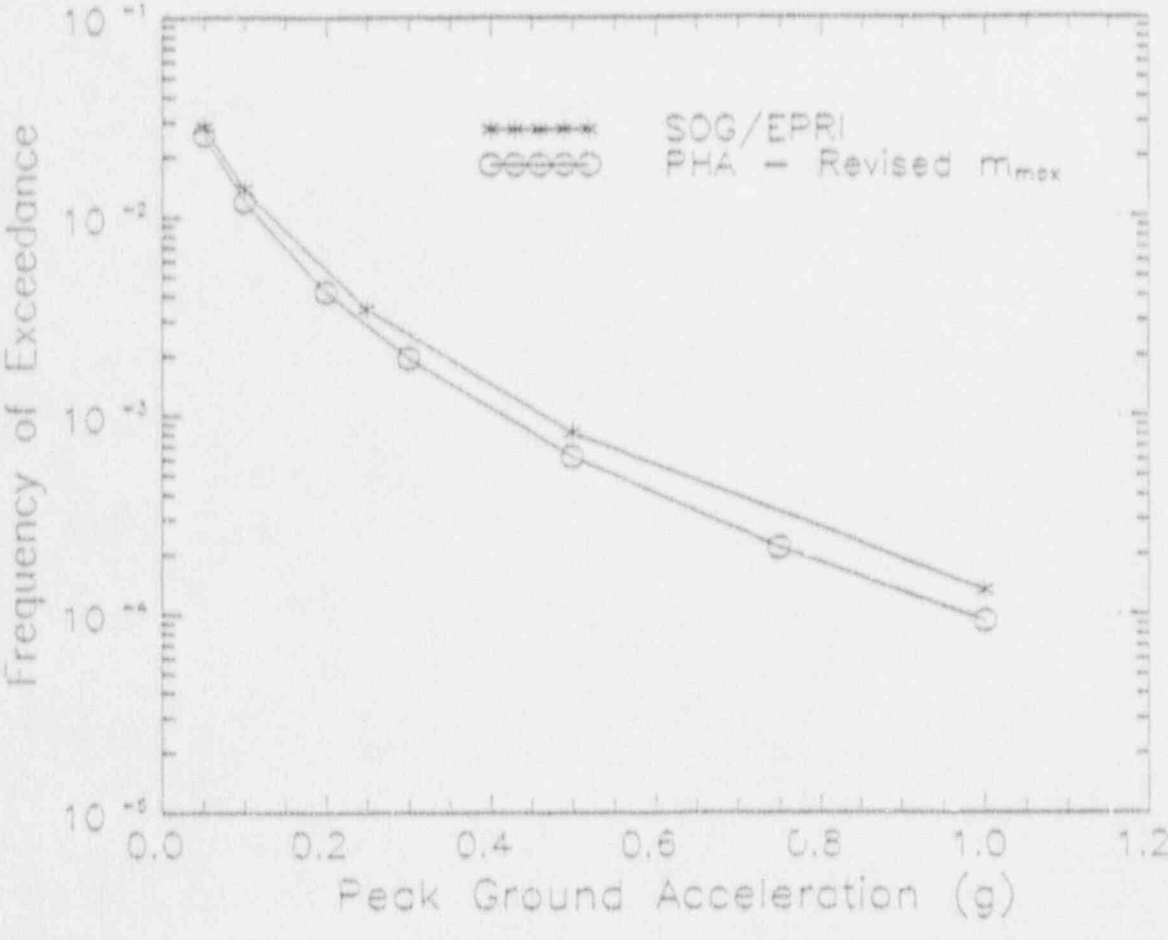

Figure 5-40 Comparison of the regional seismic hazard results using the revised maximum-magnitude distribution for the New Madrid area (see Table 5-4) and the site-specific calculations for New Madrid-3.

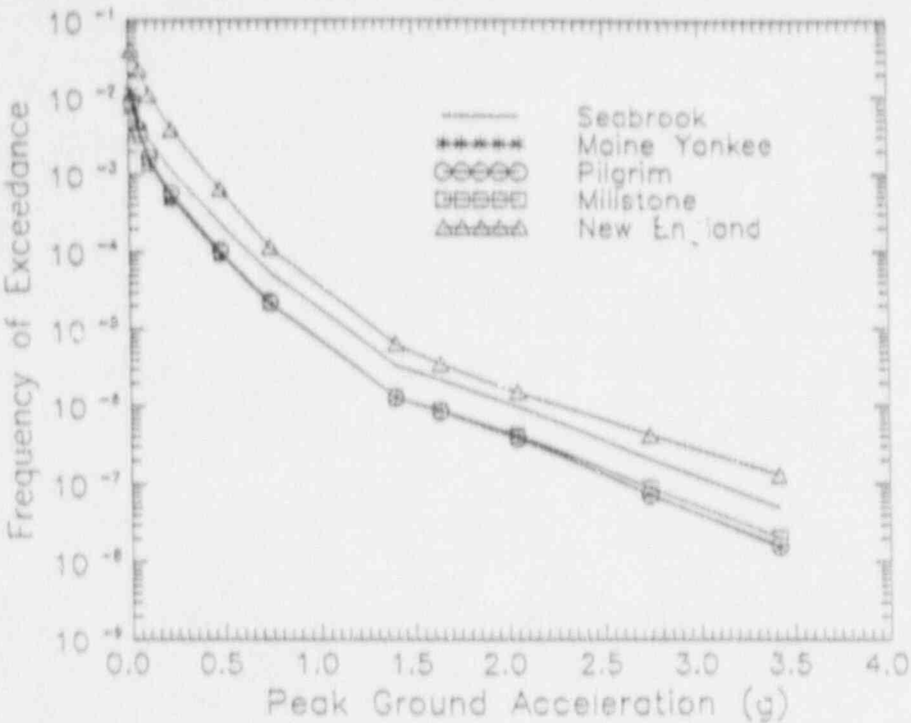

Figure 5-41 Mean site-specific seismic hazard curves for site category S2 for sites in the New England area.

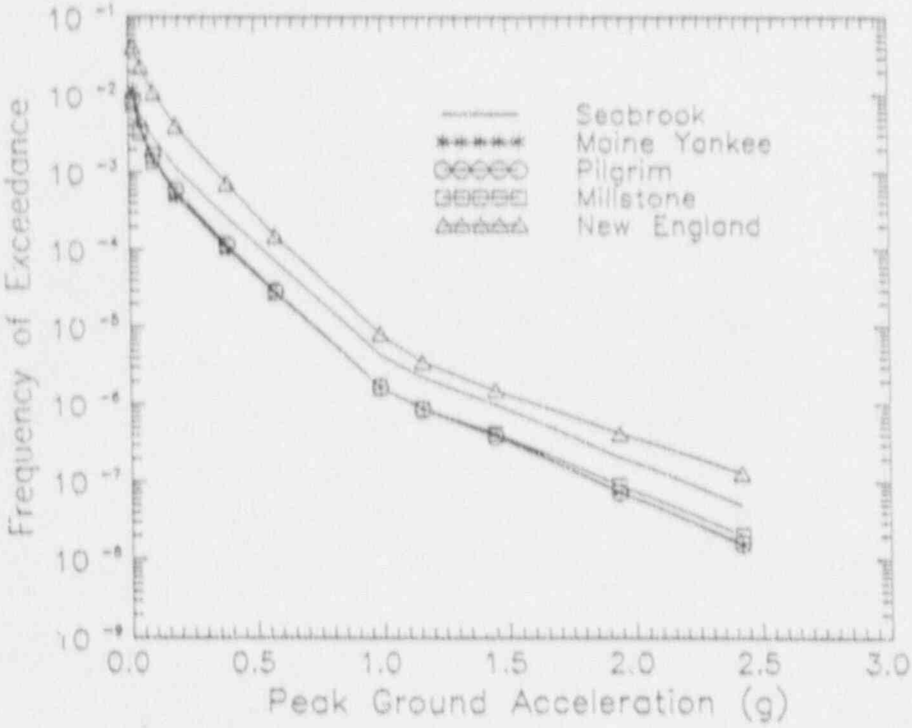

Figure 5-42 Mean site-specific seismic hazard curves for site category S3 for sites in the New England area.

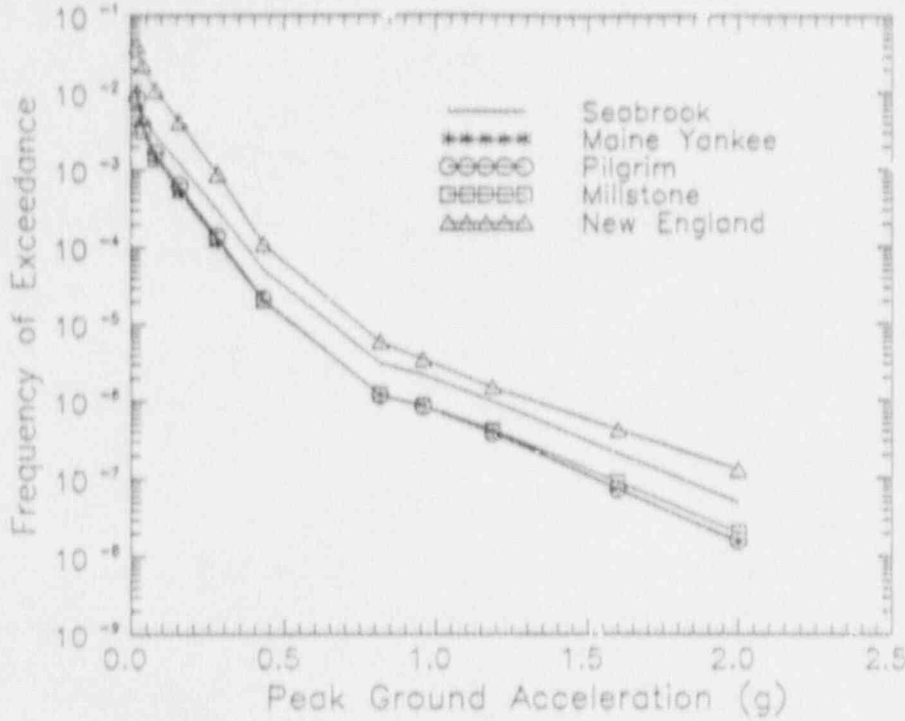

Figure 5-43 Mean site-specific seismic hazard curves for site category S4 for sites in the New England area.

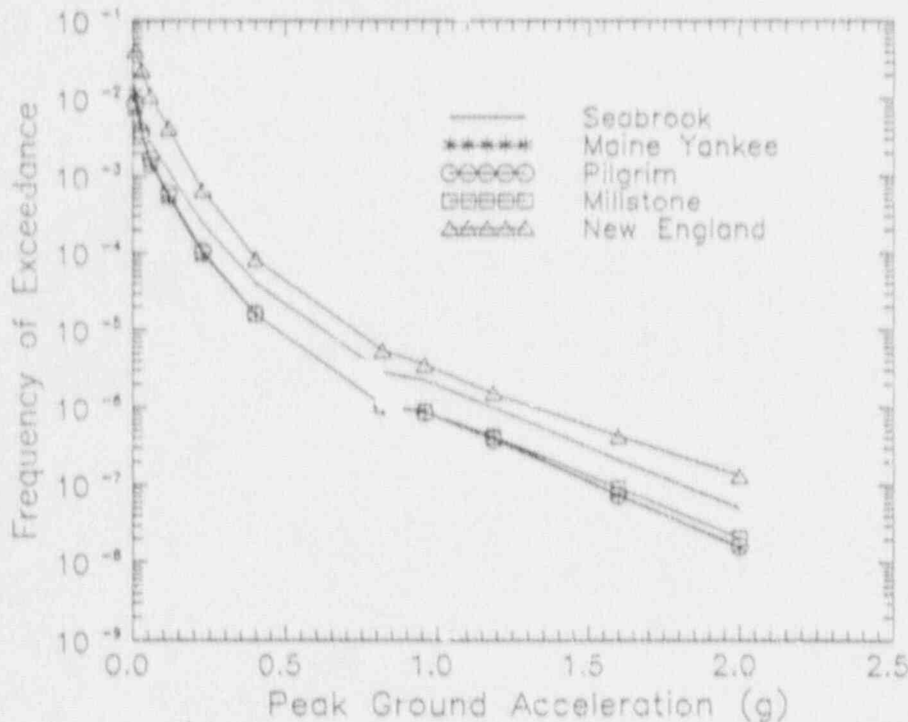

Figure 5-44 Mean site-specific seismic hazard curves for site category S5 for sites in the New England area.

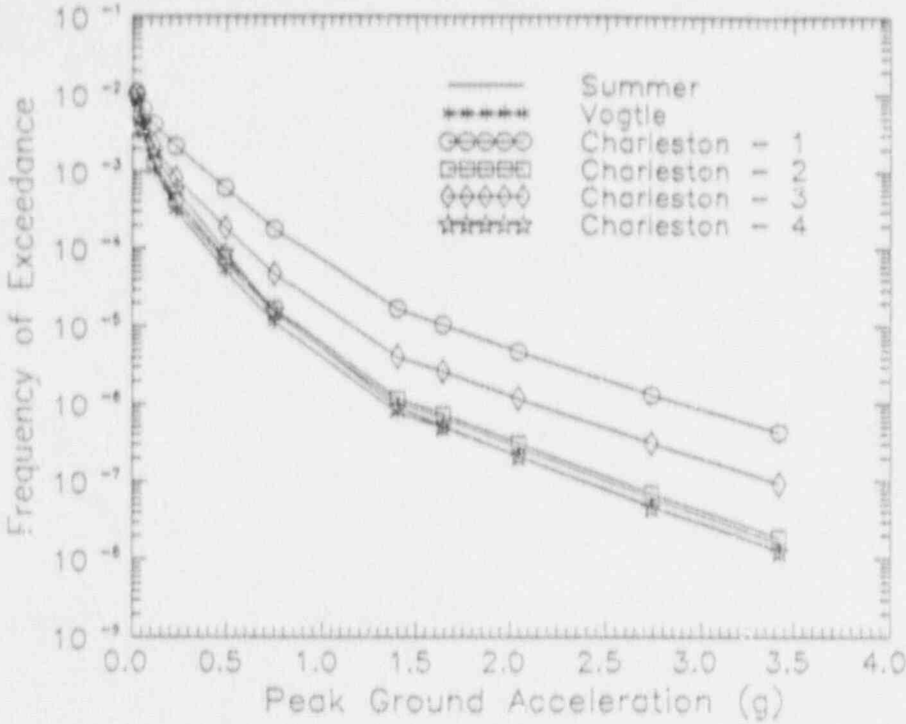

Figure 5-45 Mean site-specific seismic hazard curves for site category S2 for sites in the Charleston area.

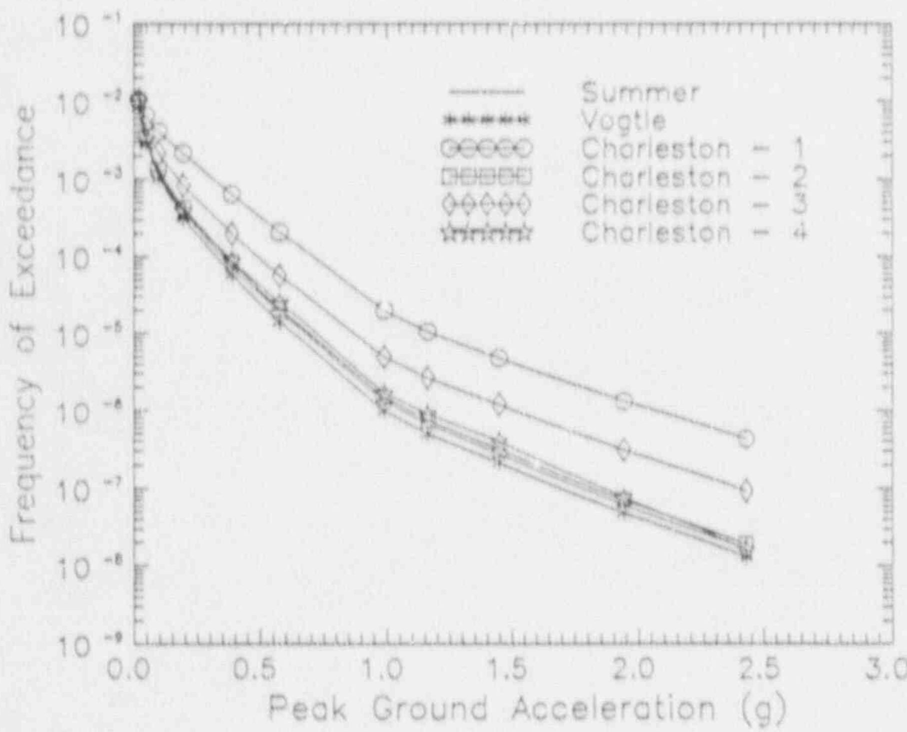

Figure 5-46 Mean site-specific seismic hazard curves for site category S3 for sites in the Charleston area.

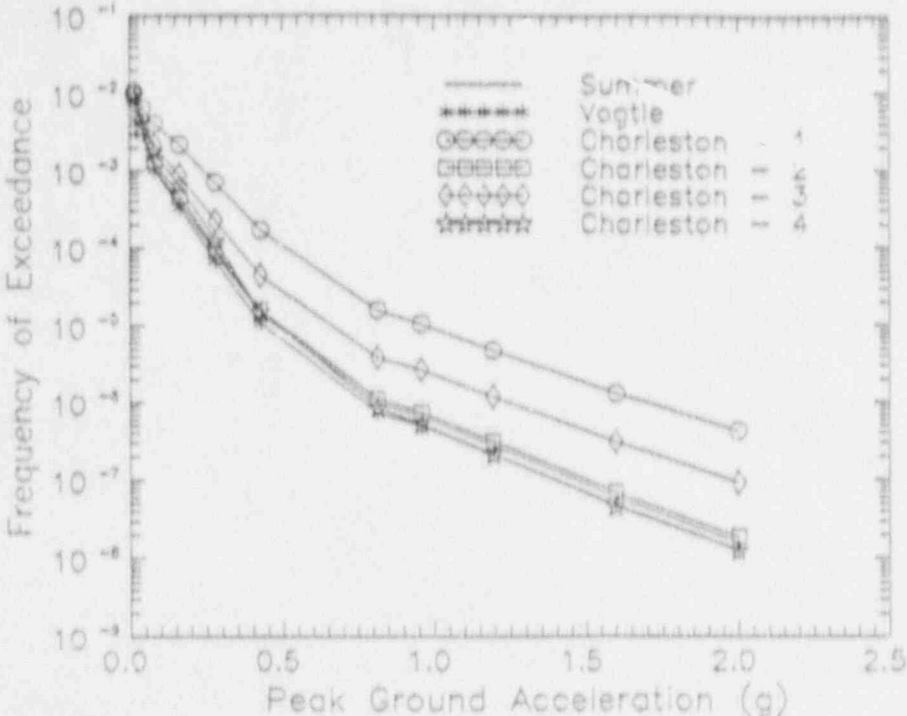

Figure 5-47 Mean site-specific seismic hazard curves for site category S4 for sites in the Charleston area.

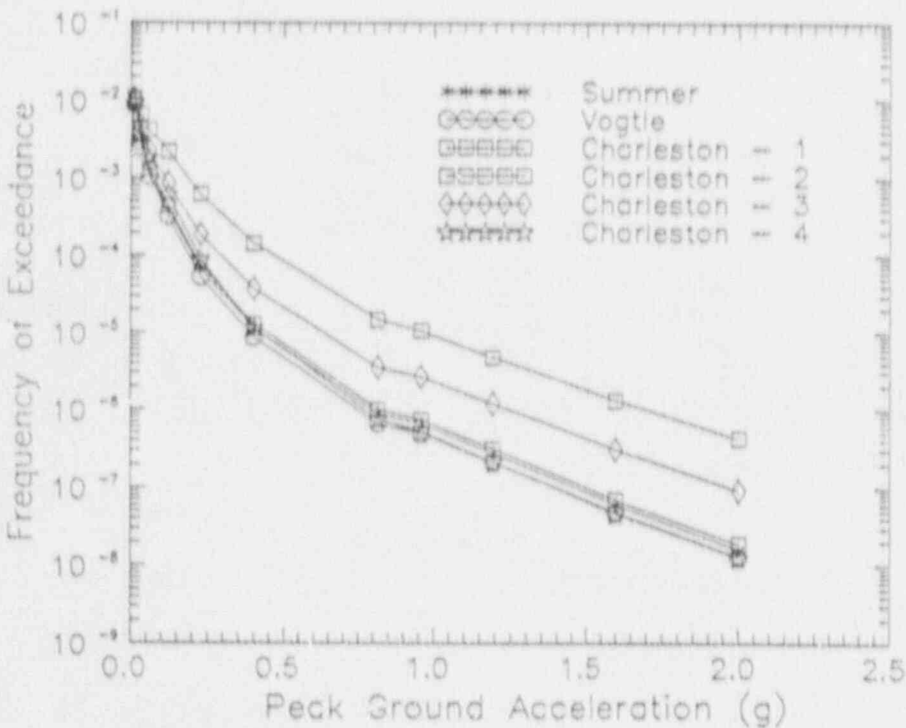

Figure 5-48 Mean site-specific seismic hazard curves for site category S5 for sites in the Charleston area.

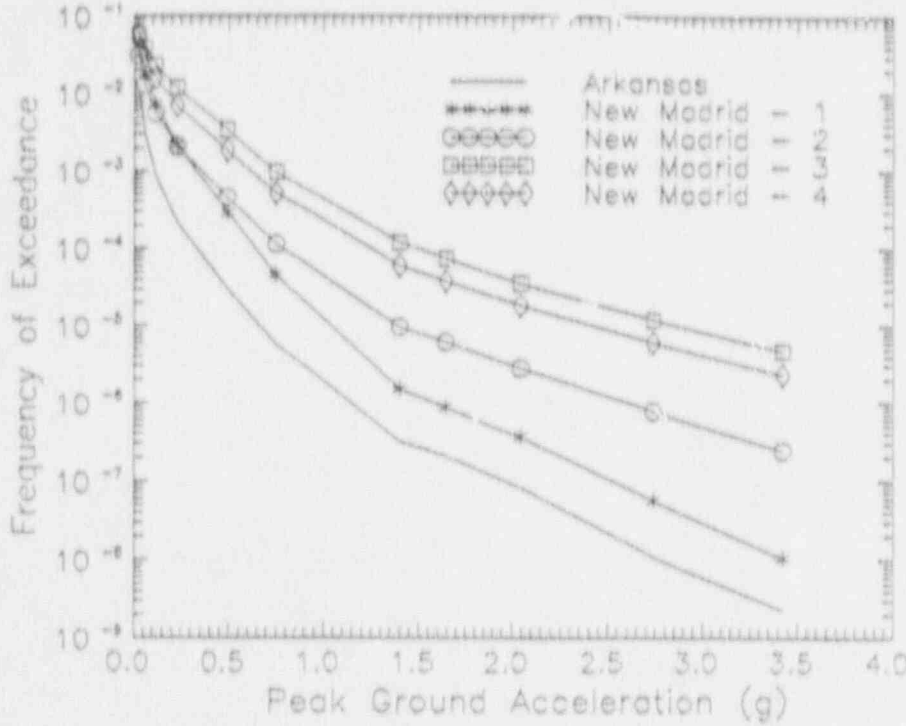

Figure 5-49 Mean site-specific seismic hazard curves for site category S2 for sites in the New Madrid area.

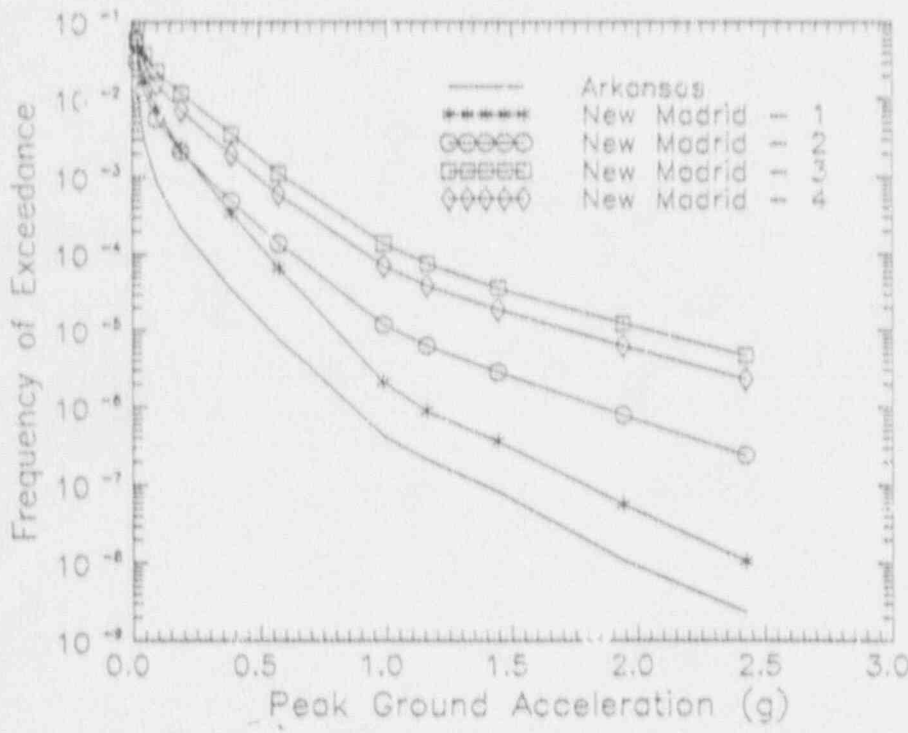

Figure 5-50 Mean site-specific seismic hazard curves for site category S3 for sites in the New Madrid area.

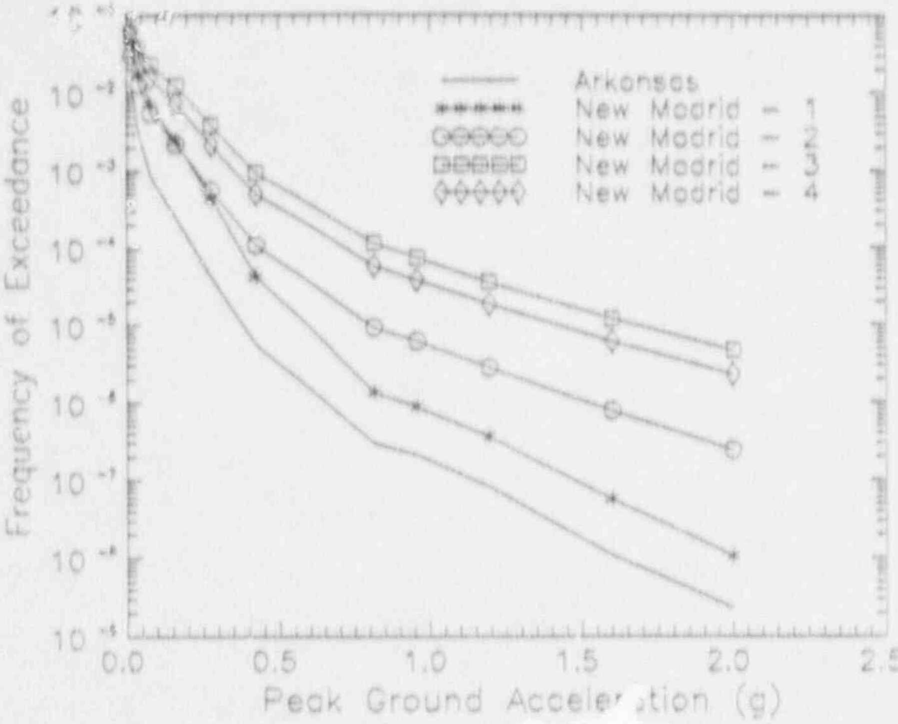

Figure 5-51 Mean site-specific seismic h[illegible] for site category S4 for sites in the New Madrid a[illegible]

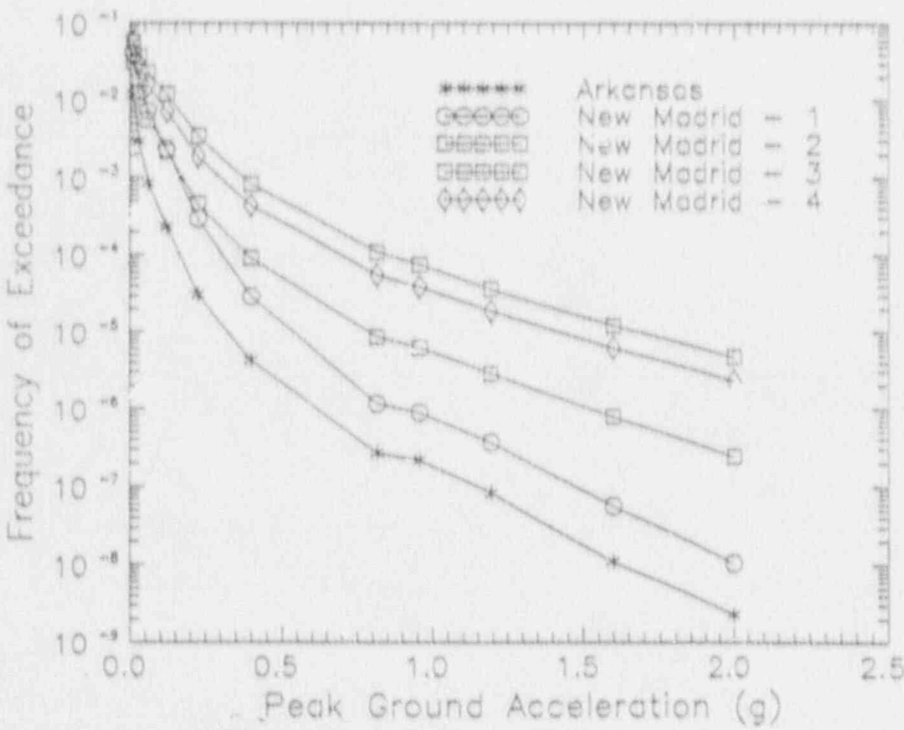

Figure 5-52 Mean site-specific seismic hazard curves for site category S5 for sites in the New Madrid area.

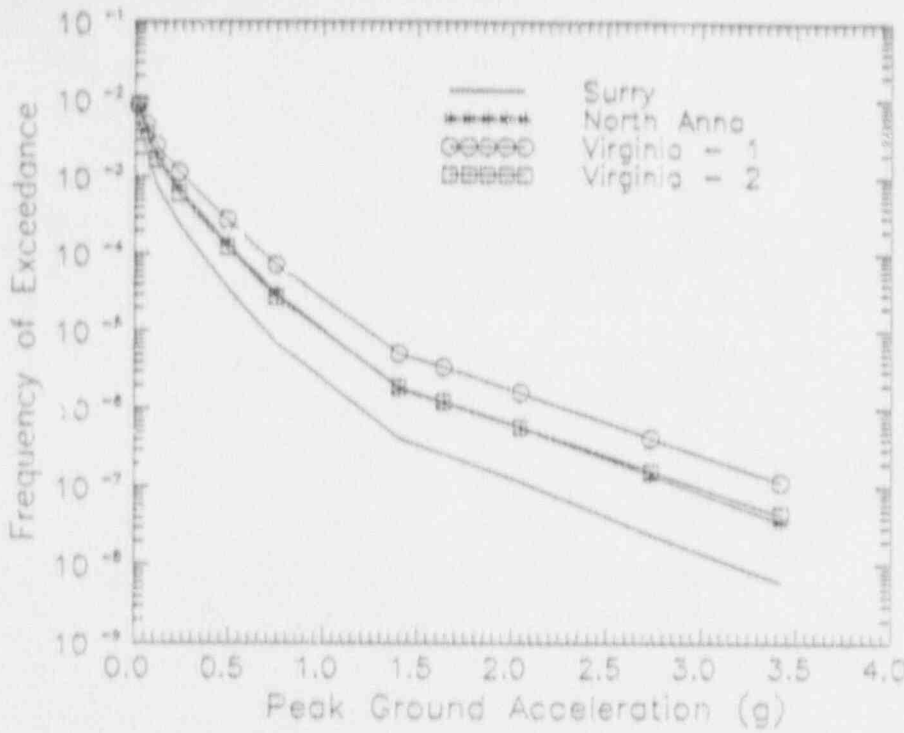

Figure 5-53 Mean site-specific seismic hazard curves for site category S2 for sites in the Virginia area.

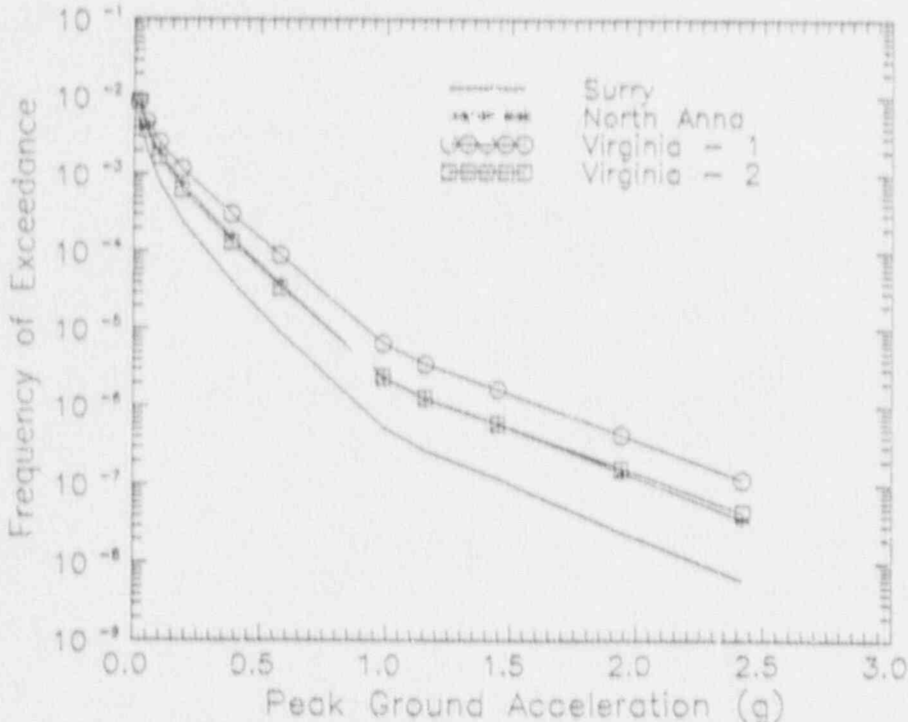

Figure 5-54 Mean site-specific seismic hazard curves for site category S3 for sites in the Virginia area.

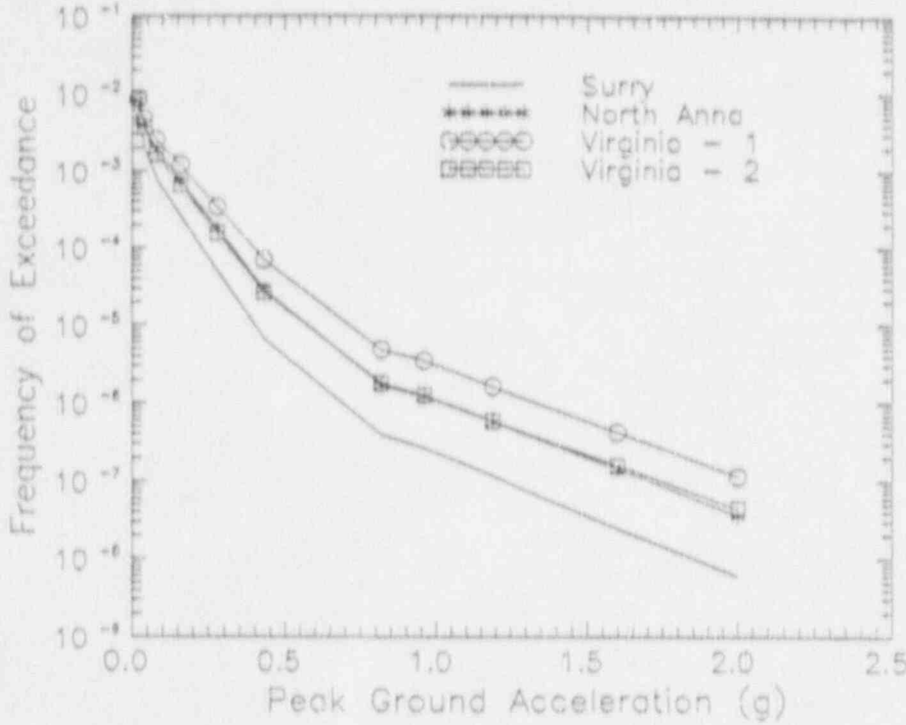

Figure 5-55 Mean site-specific seismic hazard curves for site category S4 for sites in the Virginia area.

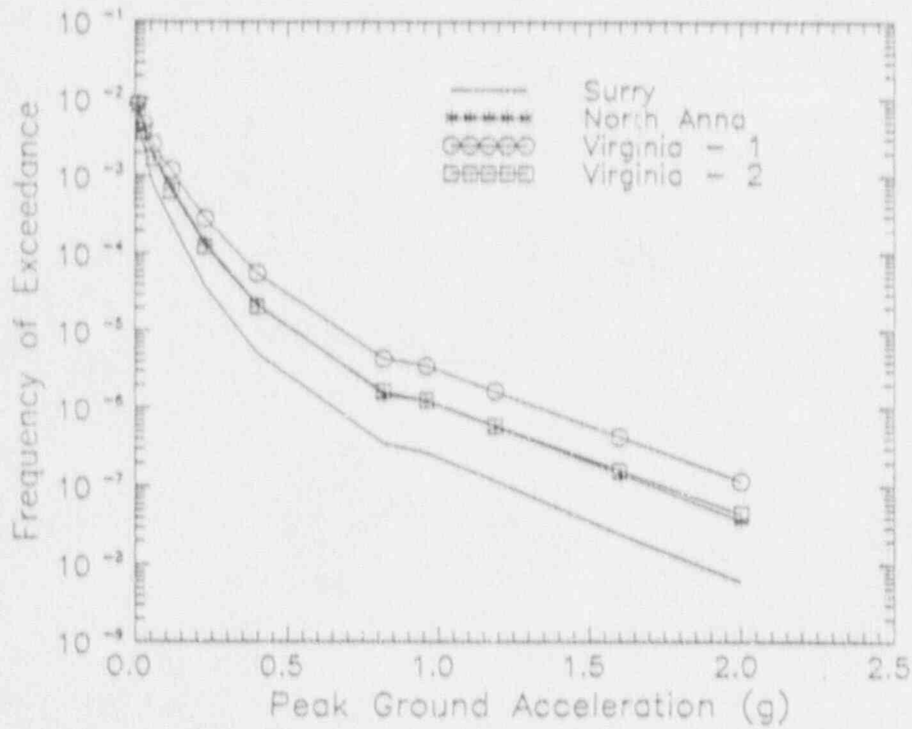

Figure 5-56 Mean site-specific seismic hazard curves for site category S5 for sites in the Virginia area.

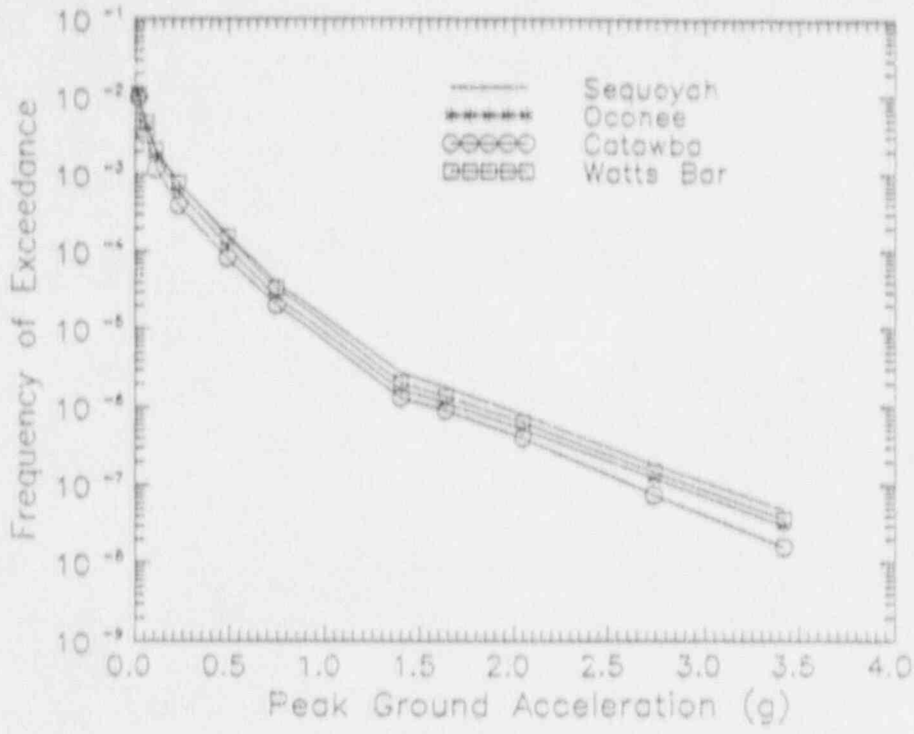

Figure 5-57 Mean site-specific seismic hazard curves for site category S2 for sites in the Piedmont area.

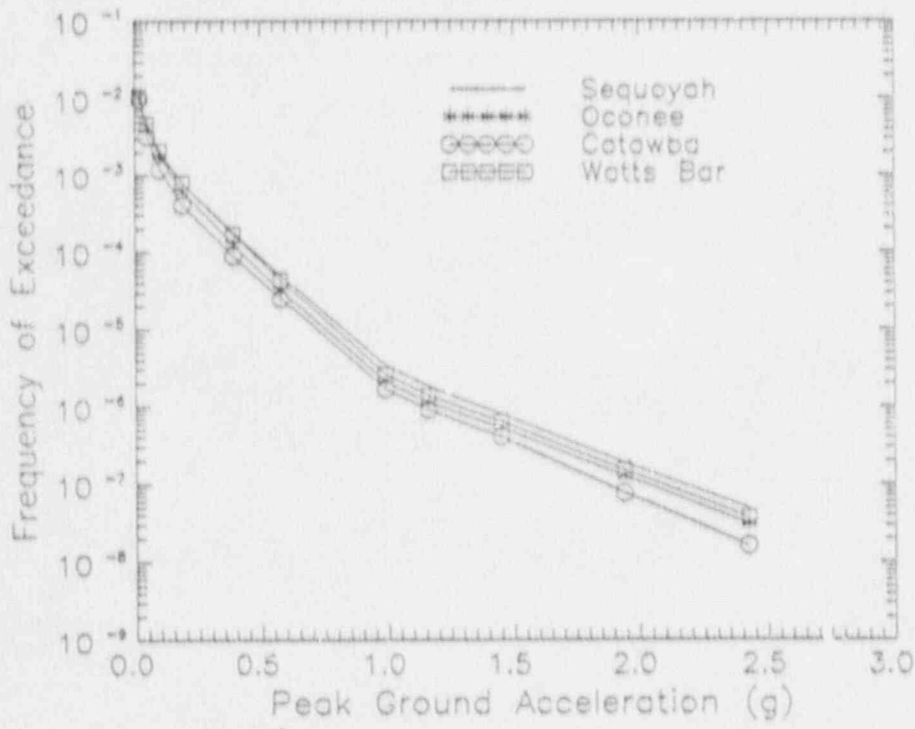

Figure 5-58 Mean site-specific seismic hazard curves for site category S3 for sites in the Piedmont area.

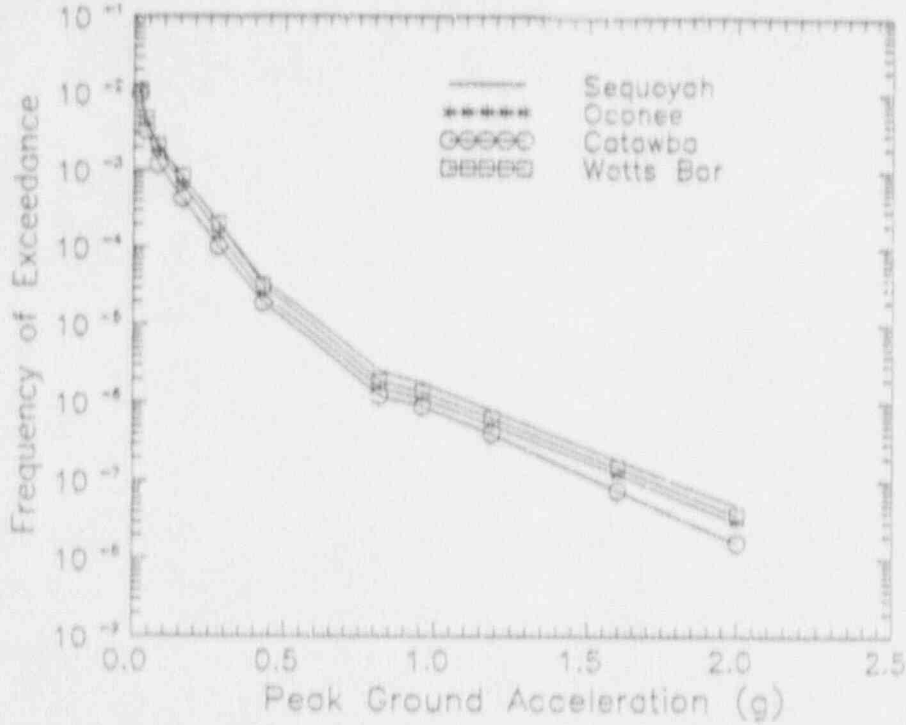

Figure 5-59 Mean site-specific seismic hazard curves for site category S4 for sites in the Piedmont area.

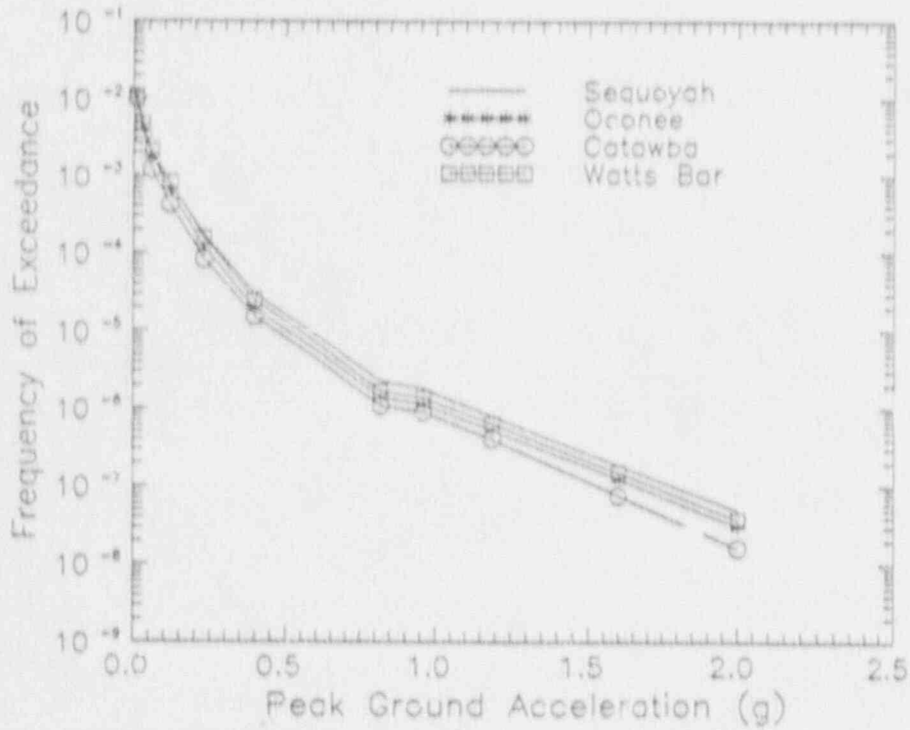

Figure 5-60 Mean site-specific seismic hazard curves for site category S5 for sites in the Piedmont area.

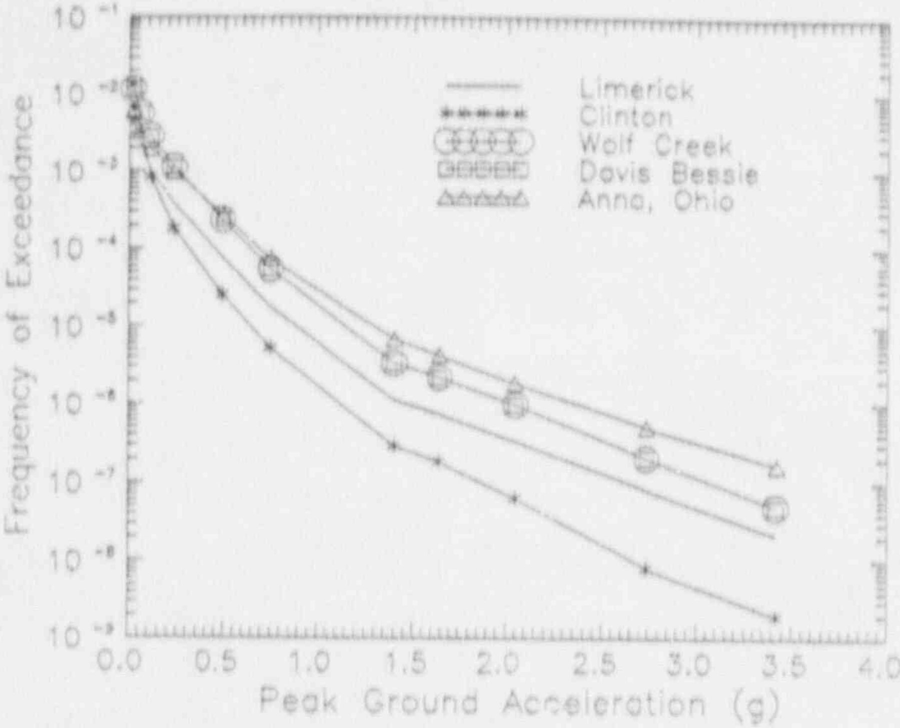

Figure 5-61 Mean site-specific seismic hazard curves for site category S2 for sites in the other areas.

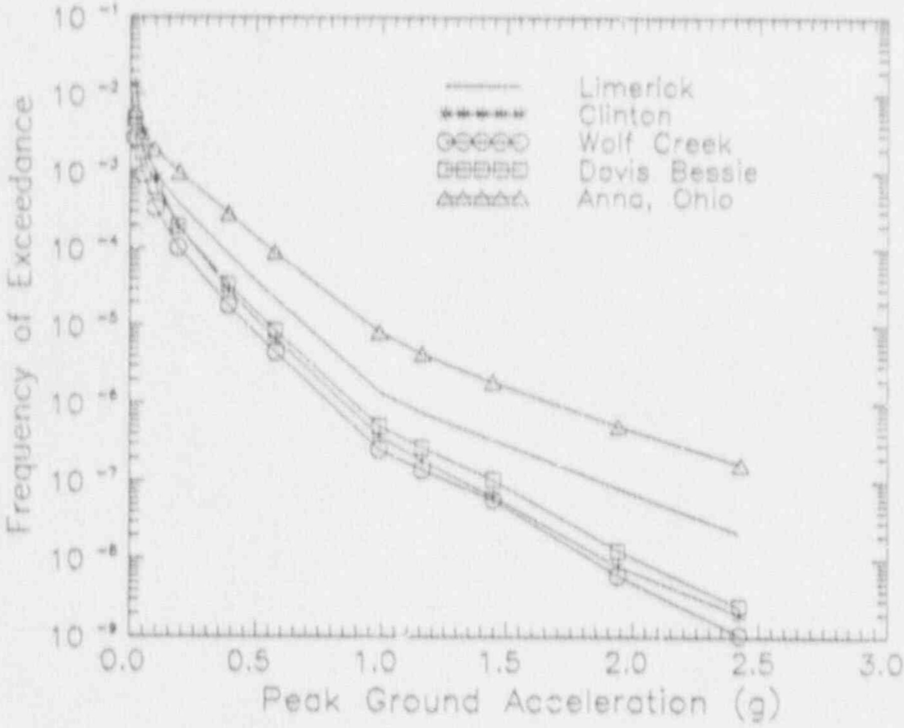

Figure 5-62 Mean site-specific seismic hazard curves for site category S3 for sites in the other areas.

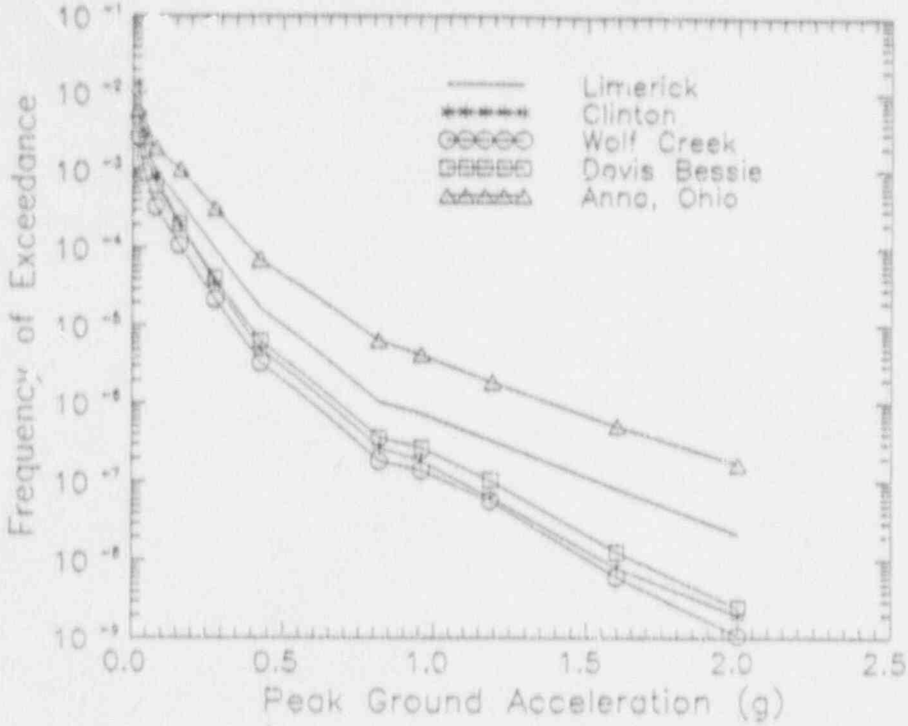

Figure 5-63 Mean site-specific seismic hazard curves for site category S4 for sites in the other areas.

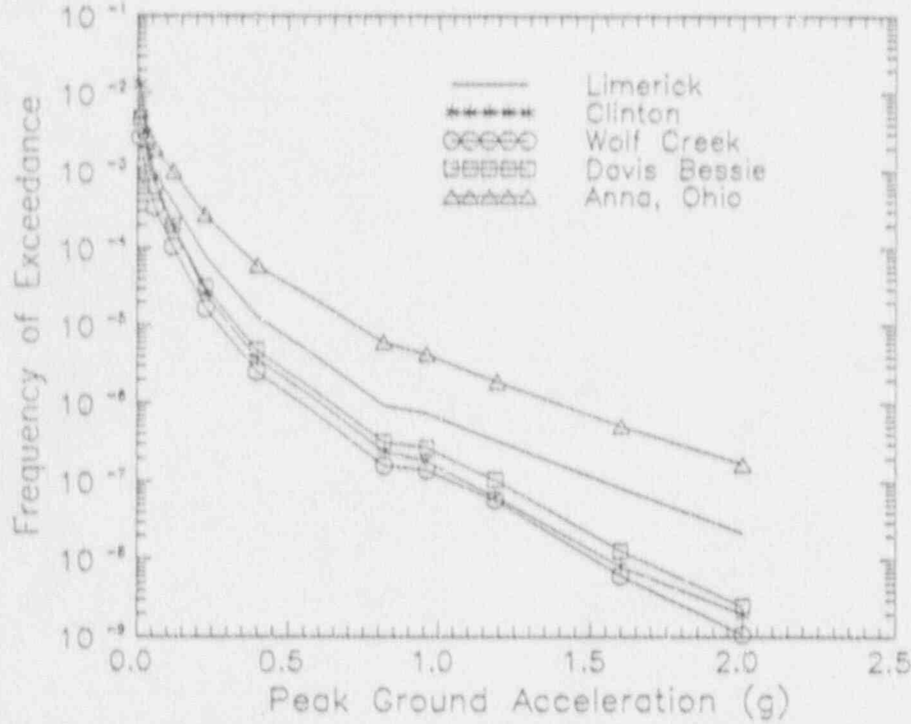

Figure 5-64 Mean site-specific seismic hazard curves for site category S5 for sites in the other areas.

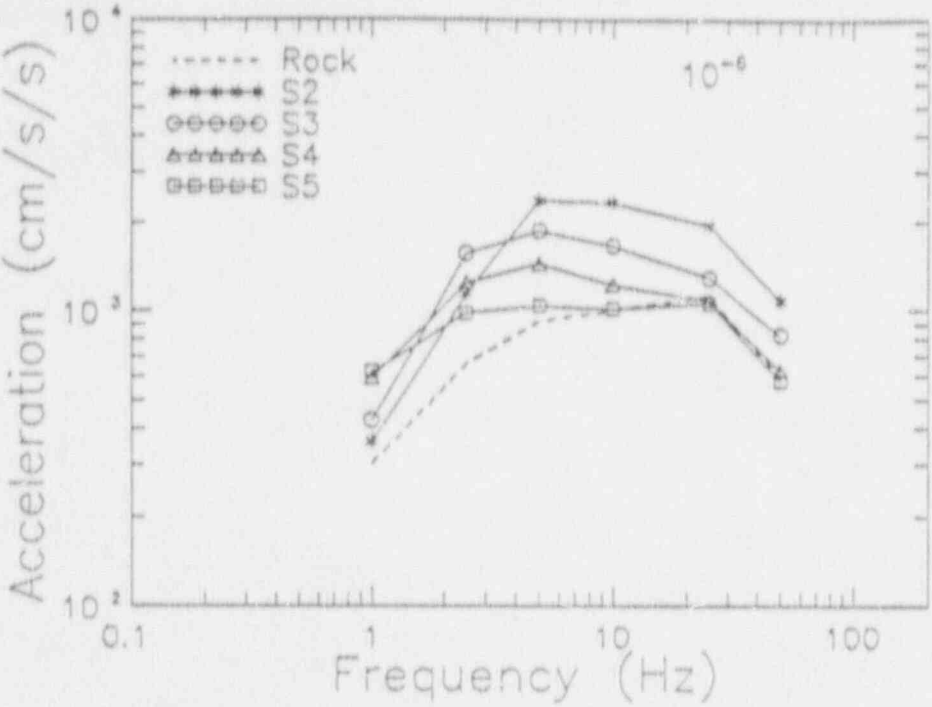

Figure 5-65 Average of the mean uniform-hazard response spectra for 57 sites and each site category.

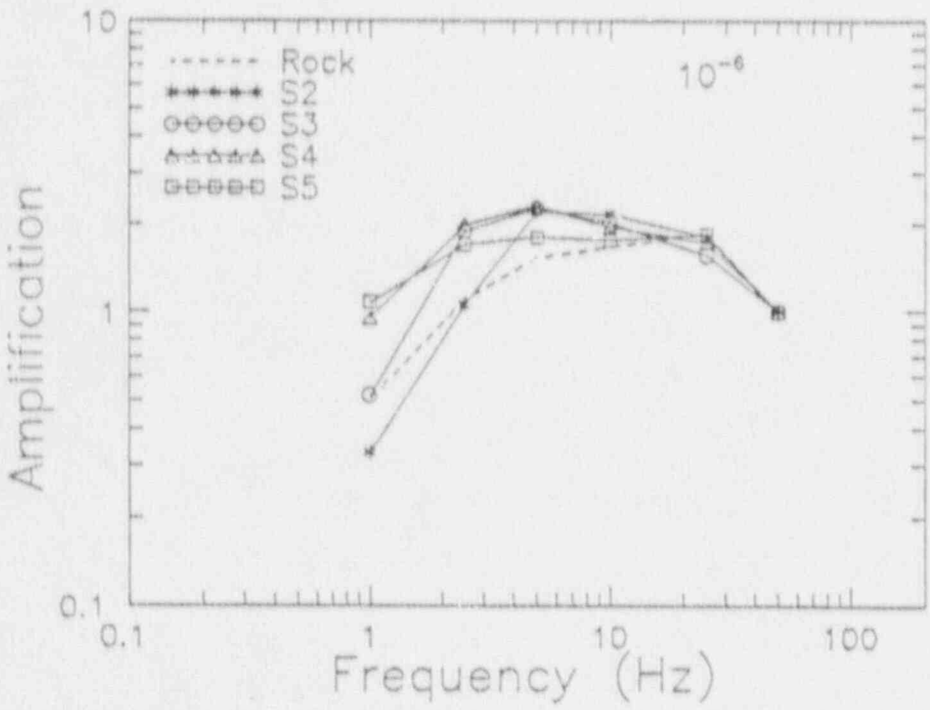

Figure 5-66 ALWR SH response-spectrum shape (normalized to 1.0 PGA) for each site category.

Section 6

ALWR PLANT CORE-DAMAGE FRAGILITY

6.1 Introduction

This section presents the basis for the mean core-damage fragility curves used in the ALWR seismic PRA presented in this report. Since an ALWR has not been constructed, and many of the plant components have been only designed conceptually, target fragility curves were developed which are believed, with high confidence, to be achievable. Fragility curves for the ALWR were developed from experience, drawn from past seismic PRAs and extrapolated to the ALWR plants. It is recognized that actual component specific structural capacities, based on installed hardware which has been reviewed during a walkdown to verify anchorage adequacy and for potential systems interactions, can not be presently developed. However, starting with the ALWR design Safe Shutdown Earthquake (SSE) PGA capacity, which is 0.3g, along with the knowledge of the plant design bases, the plant structural ultimate capacity can be indirectly inferred. It is assumed that a future ALWR plant will be walked down and the plant design bases reviewed, as part of the design process, to confirm the assumptions made in the fragility development.

The following subsection describes the basis for the mean core-damage fragility curve, assuming that the shape of the mean ground-response spectrum is given by the median-shape NUREG/CR-0098 curves (i.e., for rock and soil sites) (33). Generally, these shapes have been assumed in past seismic PRAs to represent uniform-hazard spectra across the dynamic frequency range of interest. As discussed in previous sections of this report the UHS shapes vary with the different soil conditions. Thus, the last subsection describes modifications to the mean core-damage fragility curve for different site conditions.

6.2 Basic Core-Damage Fragility Curve

The mean core-damage fragility curve has been developed using the fragility curves from past seismic PRAs determined for safety-related structures and equipment and the plant systems model, which logically relates the frequency of failure of these components through event and fault trees. The family of fragility curves for each component are defined by a median capacity and logarithmic standard deviation for randomness and uncertainty, β_r and β_u, respectively. Figure 6-1 shows an example family of fragility curves for one component. The 95th, 50th and 5th percentile curves shown represent the uncertainty in which the curve is correct, while each curve gives the fraction of failure as a function of the motion parameter (e.g., peak ground acceleration). The "S" shape of each curve reflects the inherent randomness in the component capacity, which is dominated by the ground motion variability.

Also shown in Figure 6-1 is the mean component fragility curve, which is the average of all fragility curves. In the risk analysis performed for the ALWR, the mean frequency of core damage is calculated using the mean core-damage fragility curve. The median capacity for each component along with the combined logarithmic standard deviation, β_c (i.e., $\beta_c = \sqrt{\beta_r^2 + \beta_u^2}$) and the plant system model is all that is required to calculate the mean core-damage fragility curve.

In past seismic PRAs, fragility curves were developed for the safety-related components where the design capacity (i.e., typically the SSE peak ground acceleration) is adjusted for the conservatisms (and non-conservatisms) in the various capacity and response parameters. Variabilities for each parameter are estimated which lead to the final values for β_r and β_u. For some components (e.g., piping, cable trays and ducting) knowing the design procedure, material properties, and code requirements the fragility curves can be indirectly inferred.

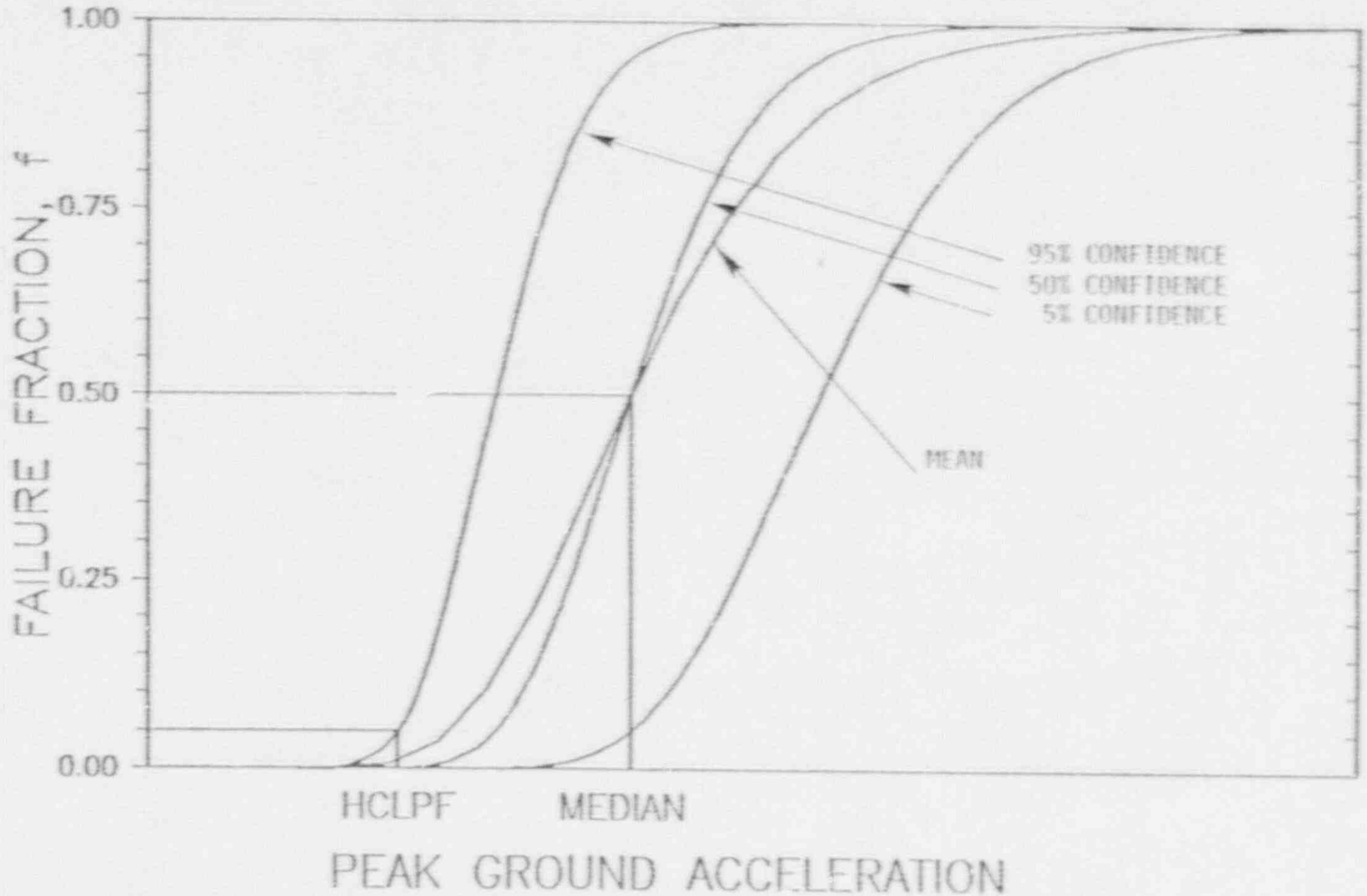

Figure 6-1 Example fragility curves for a single component.

This is a practical alternative to developing fragility curves for individual components which would be prohibitively expensive and would not be cost effective.

The approach used here is similar to the philosophy for developing generic fragility curves for classes of components, but examines instead the entire plant rather than individual or even classes of components. Results from past seismic PRAs are used to indicate the level of capacity which can be expected for a plant with a given design SSE. From studies of past seismic PRAs conducted for more modern EUS nuclear power plants (i.e., with post-1973 seismic design criteria) it has been found that the mean annual probability of core-damage caused by earthquakes is at least 40 times smaller than the mean annual frequency of exceedance of the plant design SSE level (34). Prior to the change in the NRC standard review plans and regulation guides around 1973, the procedures and criterion used in design lead to plants with varying capacities relative to the SSE level. Thus this relationship does not generally hold for older plants.

For the ALWR plant, which will be designed for modern seismic criteria and analyzed for a 0.3g PGA, the same level of seismic margin can be expected compared to recent modern nuclear power plants. In order to estimate what this margin is for modern plants, an estimate of the variability in the core-damage fragility curves for existing plants along with the rate at which typical hazard curves drop with increasing ground motion level is needed.

The determination of the variability in core-damage fragility curves is approached from two perspectives. First, it is assumed that the mean core-damage fragility curve can be represented by a lognormal distribution with a median capacity and a logarithmic standard deviation. This is an adequate approximation since only the central portion of the resulting fragility curve (i.e., within plus and minus 2 standard deviations of the median) are important when integrating it with the mean hazard curve to obtain the mean frequency of core-damage. In this sense the lognormal model is a reasonable choice.

Using this model, the objective here is to find the ratio of the median capacity of core-damage to the SSE design level and the logarithmic standard deviation. Reference 35 investigated 8 past seismic PRAs from which the median capacity and β_r and β_u for core-damage were calculated. Values of β_c can be calculated from this report and are found to range between 0.30 and 0.39.

This range of values can be confirmed from a different perspective using structure and equipment fragility data and inferring what the core-damage β_c value might be. Reference 4 lists estimated β_r and β_u values for structures and equipment from which β_c can be calculated. For structures β_c ranges from 0.36 to 0.59 and for equipment the range is 0.45 to 0.68. The core-damage fragility curve comes typically from several components in series. Starting with 4 identical components in series each with a β_c value of 0.5 it is found that the logarithmic standard deviation for the combined system is about 0.35. Similar calculations easily confirms the 0.3 to 0.4 range of values for β_c based on the results given in Reference 35. Table 6-1 gives some example results for a number of components and β_c values.

Table 6-1

Logarithmic Standard Deviation
Values For Identical Components in Series

Number of Components in Series	β_c For Individual Components		
	0.5	0.6	0.7
2	0.41	0.49	0.58
4	0.35	0.42	0.48
10	0.30	0.35	0.40

Hazard analysis for the EUS typically leads to a mean-hazard curve which plots in a log-log plane as a downward sloping curve as shown in Figure 6-2. The mean seismic hazard curve is expressed in the following form:

$$G(a) = ka^{-\kappa} \qquad (6\text{-}1)$$

where

$G(a)$ = frequency of exceedance

κ = exponent

a = peak ground acceleration

k = constant of proportionality

Typically κ values range from 2.5 to 3.0 and in some cases higher in the typical acceleration range which controls the mean core-damage frequency for EUS nuclear power plants (e.g. 0.5 to 0.9g, for example see Ref. 35).

Using the properties of the lognormal model it can be shown that the mean frequency of core-damage, $\bar{P}_f$ is related to the parameters of the hazard and fragility curves as follows:

$$\bar{P}_f = \bar{G}(\hat{a})e^{0.5\,\beta_c^2\,\kappa^2} \qquad (6\text{-}2)$$

where

$\bar{G}(\hat{a})$ = mean hazard curve evaluated at the median core-damage fragility value, $\hat{a}$

Using Eq. 6-1 and 6-2 with an assumed factor of 40 between the SSE frequency of exceedance and the mean frequency of core-damage the following relation is found for the ratio of $\hat{a}$ to the SSE value:

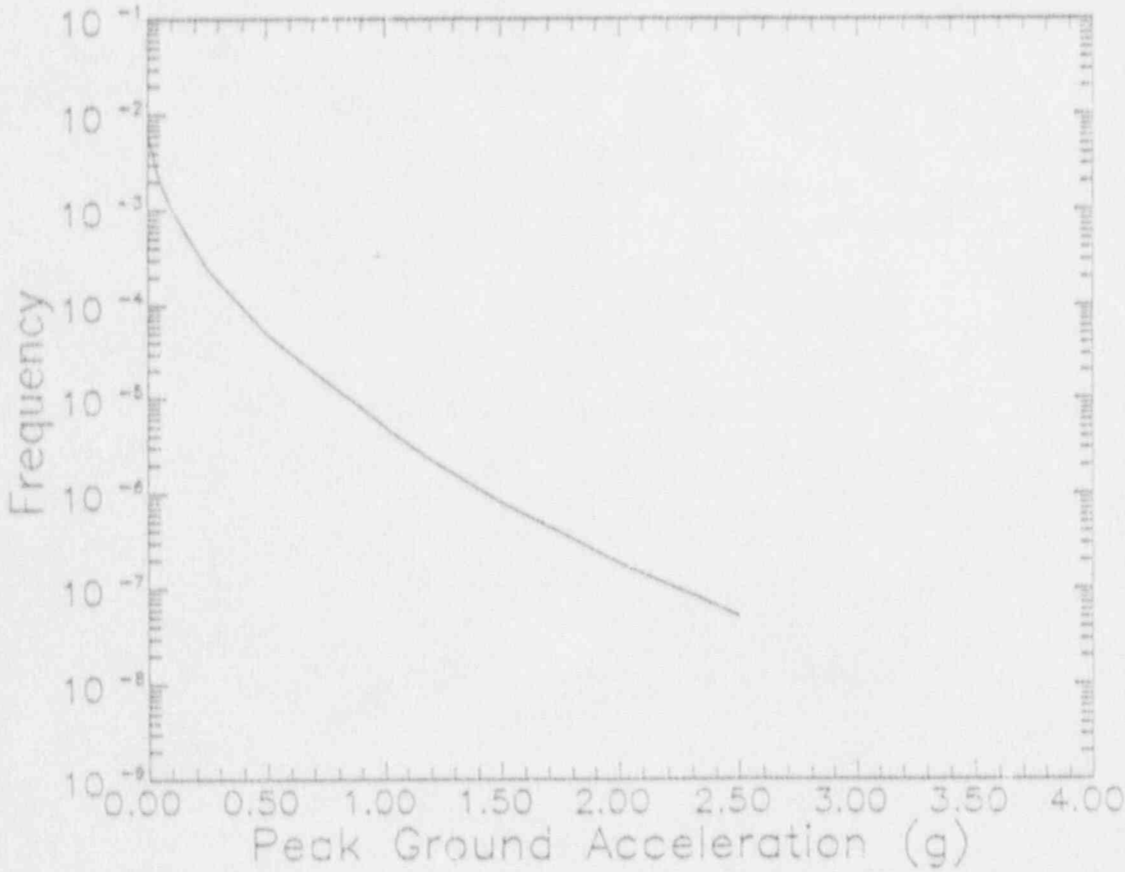

Figure 6-2 Example mean hazard curve for the EUS.

$$\frac{\hat{a}}{SSE} = \left[40e^{0.5\,\beta_c^2\,\alpha^2}\right]^{1/\alpha} \qquad (6\text{-}3)$$

Table 6-2 gives results for Eq. 6-3 for ranges of β_c and α values. For the typical values of β_c and α a ratio of 4 is easily justified.

A more direct approach is to look at the median values found in Reference 35 which came from a study of mean core-damage fragility curves for 8 seismic PRAs. Unfortunately, the SSE values which consisted of 1 value at 0.1g, 4 values at 0.15g and 3 values at 0.17g can not be paired directly with the median core-damage capacities which ranged from 0.3 to 0.92g. In addition, 5 of the 8 plants appear to have been designed using the pre-1973 criteria. Nevertheless the ratio of 4 between the SSE and the medians is consistent with the findings using Eq. 6-3.

Past seismic PRAs have typically used the NUREG/CR-0098 (36) median response-spectrum shape anchored to the PGA as the seismic input at the ground surface in the free field. Thus the finding that there is a factor of 4 between the SSE and $\hat{a}$ implicitly assumes this ground response-spectrum shape. For the ALWR which will be designed using a 0.3g SSE value, it is expected that a median capacity for the core-damage fragility curve of 1.2g is achievable. This conclusion assumes that the NUREG/CR-0098 shape anchored to the PGA is used as the ground response-spectrum shape.

6.3 Modification For Different Site Conditions and Attenuation Variability

The core-damage fragility curve for the ALWR plant, based on the NUREG/CR-0098 shape, should be modified to reflect site-specific UHS shapes. In calculating the mean core-damage frequency the "best" response spectral shape for each site is the mean UHS shape corresponding to a frequency of exceedance close to the mean frequency of core melt (i.e., the 10^{-6} per year value which is the desired target). Comparing the site-specific UHS shapes with the NUREG/CR-0098 shape in the dynamic frequency range of interest the

Table 6-2

Ratio of Median Core-Damage Capacity To SSE PGA

Hazard Curve Slope Exponent, α	Core-Damage Logarithmic Standard Deviation[1]				
	0.3	0.35	0.4	0.45	0.5
2.0	6.9	7.1	7.4	7.7	8.1
2.2	5.9	6.1	6.4	6.7	7.0
2.4	5.2	5.4	5.6	5.9	6.3
2.6	4.5	4.8	5.1	5.4	5.7
2.8	4.2	4.4	4.7	5.0	5.3
3.0	3.9	4.1	4.3	4.6	5.0
3.2	3.7	3.9	4.1	4.4	4.7
3.4	3.4	3.6	3.9	4.2	4.5
3.6	3.3	3.5	3.7	4.0	4.4
3.8	3.1	3.3	3.6	3.9	4.2
4.0	3.0	3.2	3.5	3.8	4.1

[1] β_c

median core-damage capacities can be modified to more accurately represent the plant capacity for the different site conditions.

In addition to site effects a second modification was made. This correction accounts for the differences between site-specific spectra developed in Reference 5 and spectra based on more realistic attenuation variability which varies as a function of magnitude (see Section 5).

Figure 6-3 show schematically the basis for the two modifications which were made for the effects of ground-response spectra. In Figure 6-3a the differences between the NUREG/CR-0098 spectrum and a site-specific spectrum (based on an analysis which used a constant ground motion variability and no truncation) are shown. The first adjustment is made for this difference.

In Figure 6-3b the difference between the site-specific spectra based on a constant attenuation variability is shown again relative to a line which connects the normalization point (i.e., PGA) with the spectral ordinate at 2.5 hz. This normalized value is based on a more realistic attenuation variability. It is assumed that the modification to the site-specific spectrum is linear with frequency between these two points.

The following two subsections describe the modifications for these two effects.

6.3.1 Effects of Different Site Conditions

Comparing the ALWR response spectra for each site category to the NUREG/CR-0098 spectra, adjustment factors were developed. Figure 6-4 shows the relationship between the ALWR ground-response spectra and the NUREG/CR-0098 spectra (i.e., for rock and soil sites).

The spectra have been normalized to the same PGA value since this is the parameter used in the hazard analysis. For components located in structures with fundamental frequencies in the 2-10 hz region the core-damage capacities for rock and site category S5 are increased, while for the other three site categories the capacities decrease slightly. Note that the relative amplitudes of the ground-response spectra for frequencies greater than 10 hz are not as significant to the component capacities, except as they influence the fundamental modes of the supporting structures.

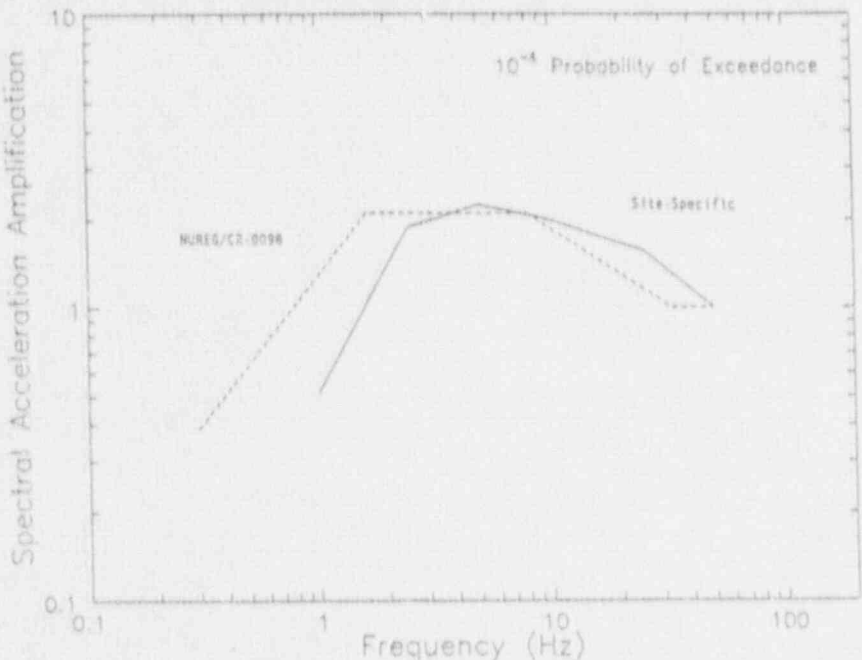

a. Relationship between NUREG/CR-0098 spectrum and site-spe .fic spectrum.

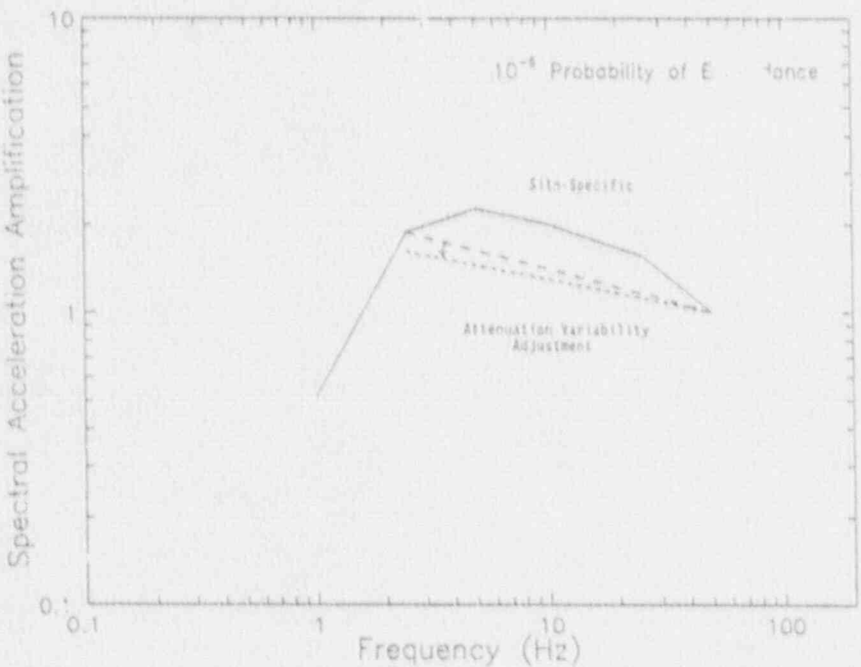

b. kelationship between site-specific spectrum and attenuation variability adjustment.

Figure 6-3 Modifications for site conditions and attenuation variability

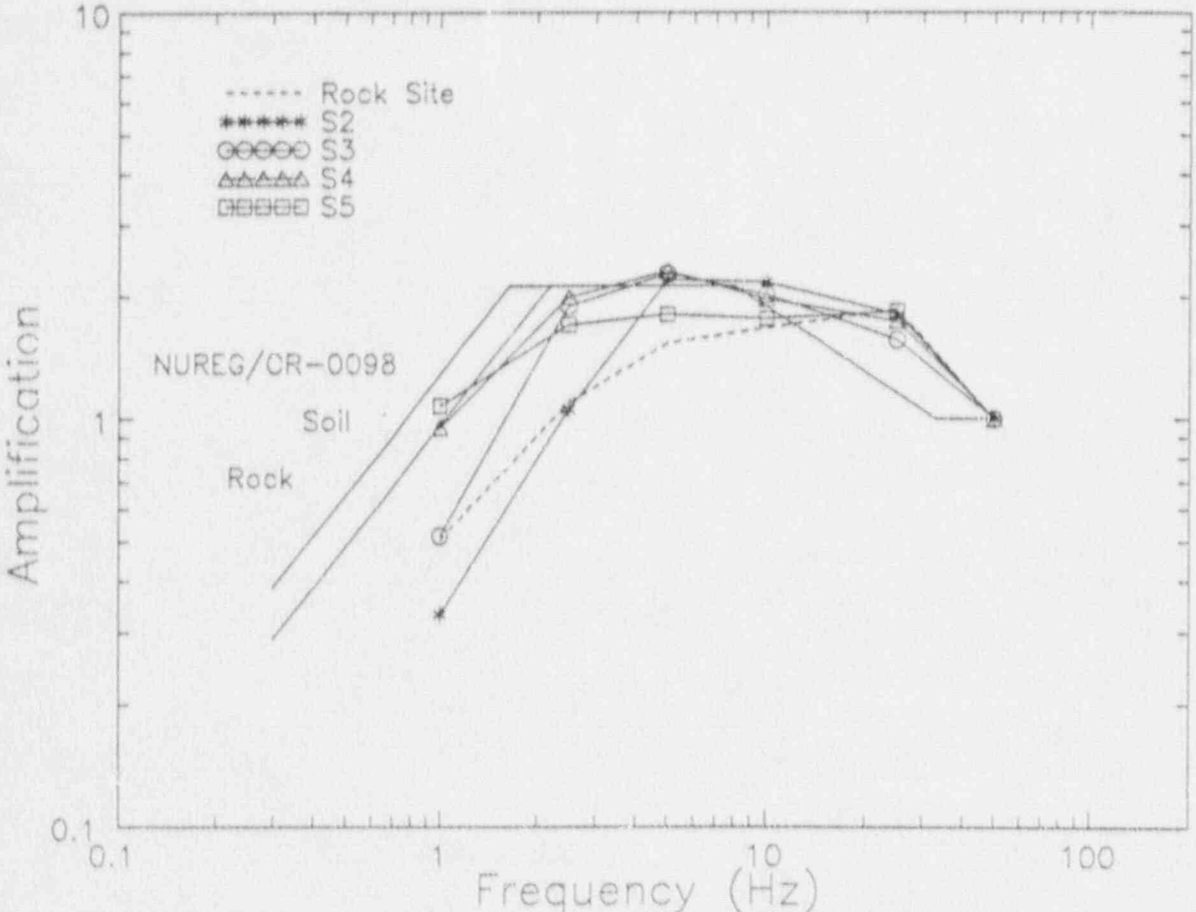

Figure 6-4 Comparison of NUREG/0098 and ALWR response spectra.

Table 6-3 gives the modified median core-damage capacities for the five site categories. The adjustment factors were determined based on the differences between the site and NUREG/CR-0098 spectra over the significant frequency range for each site category. Judgement was used in selecting the adjustment factors to reflect the range of values as a function of frequency and the possibility that input outside the assumed significant frequency range may contribute to the response. In general, the factors are on the conservative side.

Table 6-3

Modified Core-Damage Capacities For Site Specific UHS

Site Category	Significant Frequency Range (hz)	NUREG/CR-0098 Based Median Capacity (g)	Adjustment Factor	Modified Median Core Damage Capacity (g)
Rock	[illegible]-10	1.20	1.17	1.40
2	4-8	1.20	0.92	1.10
3	3-7	1.20	0.96	1.15
4	2-6	1.20	0.96	1.15
5	2-6	1.20	1.17	1.40

6.3.2 Effects of Attenuation Variability

Independent of the capacity adjustment in Table 6-3 new hazard analyses were conducted (see Section 5) where more rational values for the ground motion variability were used. Mean hazard values at the 10^{-6} frequency of exceedance level for spectral acceleration at 2.5 hz and at the PGA were calculated for locations corresponding to the five site categories. Ratios of the 2.5 hz to PGA values were calculated for the different site-specific hazard results. Average values for these ratios were then compared site by site to corresponding ratios for the spectra obtained in the EPRI/SOG analysis (see Section 5.6.2).

Table 6-4 gives the new modified median core-damage capacities for the five site categories. In Table 6-4 the effects of spectral shape as function of site condition, as well as the effects of the variability on ground motion, is included in the median capacities. The adjustment factors again reflect the significant frequencies of response and do not follow exactly the ratios, which are based only on the results at 2.5 hz relative to the PGA.

Table 6-4

Modified Core-Damage Capacities
For Spectral Shape and Attenuation Randomness

Site Category	Median Core[1] Damage Capacity (g)	Adjustment[2] Factor	Modified Median Core Damage Capacity (g)
Rock	1.40	1.07	1.50
2	1.10	1.18	1.30
3	1.15	1.13	1.30
4	1.15	1.13	1.30
5	1.40	1.07	1.50

[1]From Table 6-3

[2]For response spectrum differences due to ground motion variability

The median capacities in the last column in Table 6-4 were used as representative median capacities which are achievable for the EPRI site categories. A constant value of 0.40 was used for all sites for the combined logarithmic standard deviation. This value is representative of the value which likely will be found in future PRAs for the ALWR.

7.0 ALWR SEISMIC RISK CALCULATIONS

7.1 Introduction

In this section the regional- and site-specific seismic hazard results are combined with the ALWR core-damage fragility to estimate the seismic risk of core damage. The mean annual frequency of core damage is estimated for each site where site-specific calculations have been performed and for the 12,837 sites considered in the regional-hazard analysis. Using the regional hazard results, a core-damage risk map for the ALWR design is obtained. The risk estimates derived from the site-specific hazard results are used to calibrate the map. This process is repeated for each soil category.

The ALWR seismic risk estimates that are obtained from the site-specific and regional hazard calculations are used to determine the ALWR SH curve and to identify areas where the ALWR core-damage frequency may exceed the seismic-risk target.

In Section 7.2 the frequency of core-damage for the ALWR is estimated using the site-specific hazard curves as input for each site category. In Section 7.3 seismic risk calculations are performed using the regional-hazard results as input. The regional risk calculations are then compared to those obtained using the site-specific hazard curves. The comparison of these risk estimates provides a basis to calibrate the regional risk map. The risk map is used to identify regions where the ALWR seismic risk may exceed the target level. In Section 7.4 a map of the areas for each site category whe the ALWR seismic risk target may be exceeded is given.

7.2 Site-Specific Risk Calculations

The mean frequency of core-damage is computed using the site-specific hazard curves at each site. Table 7-1 shows the frequency of core-damage estimates for each site category.

Table 7-1

Mean Frequency of ALWR Seismic Core-Damage
SOG/EPRI Seismic Hazard

Site	Rock	S2	S3	S4	S5
			EPRI/SOG Site Category		
Seabrook	1.02-6	2.01-5	7.76-6	2.24-6	1.03-6
Pilgrim	3.76-7	8.38-6	3.20-6	8.8[illegible]-7	3.99-7
Maine Yankee	3.85-7	7.78-6	3.01-6	8.72-7	4.06-7
Millstone	3.87-7	8.09-6	3.10-6	8.88-7	4.09-7
New England	2.07-6	4.59-5	1.67-5	4.35-6	1.86-6
Virginia 1	1.57-6	2.61-5	1.03-5	3.24-6	1.58-6
Virginia 2	5.87-7	1.04-5	4.00-6	1.21-6	5.78-7
Surry	1.28-7	2.76-6	1.03-6	2.82-7	1.26-7
North Anna	5.30-7	1.12-5	4.30-6	1.23-6	5.66-7
New Madrid 1	4.10-7	1.84-5	6.63-6	1.36-6	4.85-7
New Madrid 2	3.30-6	4.33-5	1.70-5	5.66-6	2.84-6
New Madrid 3	4.39-5	3.80-4	1.57-4	6.06-5	3.28-5
New Madrid 4	2.23-5	2.02-4	8.23-5	3.15-5	1.69-5
Arkansas	9.56-8	2.31-6	8.56-7	2.25-7	9.69-8
Catawaba	3.86-7	7.34-6	2.88-6	8.56-7	4.04-7
Oconee	5.06-7	9.57-6	3.69-6	1.09-6	5.16-7
Watts Bar	5.94-7	1.26-5	4.86-6	1.38-6	6.34-7
Sequoyah	8.28-7	1.46-5	5.68-6	1.71-6	8.12-7
Charleston 1	5.73-6	6.50-5	2.61-5	9.21-6	4.73-6
Charleston 2	3.72-7	6.46-6	2.46-6	7.33-7	3.42-7
Charleston 3	1.33-6	1.76-5	6.99-6	2.35-6	1.18-5
Charleston 4	2.81-7	6.39-6	2.33-6	6.07-7	2.60-7
Vogtle	2.48-7	4.39-6	1.67-6	4.93-7	2.30-7
Summer	3.29-7	5.75-6	2.20-6	6.54-7	3.06-7
Limerick	3.41-7	6.53-6	2.52-6	7.38-7	3.44-7
Clinton	8.62-8	2.00-6	7.43-7	1.95-7	8.36-8
Wolf Creek	5.59-8	1.31-6	5.00-7	1.36-7	6.07-8
Davis Besse	1.12-7	2.51-6	9.57-7	2.63-7	1.17-7
Anna, Ohio	2.33-6	2.74-5	1.10-5	3.79-6	1.92-6

A review of the results in Table 7-1 indicates the following ... each site category:

Category	Number of Sites Exceeding 10^{-6}
Rock	9
S2	29
S3	25
S4	15
S5	9

Based on the results for rock sites, the Charleston, New Madrid and New England areas are regions where the relatively high rates of seismic activity produce risk estimates that exceed the target seismic risk level of 10^{-6}. Other areas where the risk target is exceeded is the Giles County area of Virginia and the Anna, Ohio area. The same observations can be made for the category S5 sites. For category S4 sites the same general areas produce high risk estimates that exceed the 10^{-6} level, however the number of sites in an area that exceed the target is larger. For example, the 10^{-6} risk level is exceeded at 3 of 4 sites in the Virginia area. This is attributed to the lower-median capacity (1.30g versus 1.50g) of the ALWR at S4 sites. Also for category S4 sites, in the Piedmont area the Watts Bar and Sequoyah sites are added to the list where the target level is exceeded.

For the category S2 sites the 10^{-6} risk level is exceeded at all sites. This is due to the relatively high-amplification factors for S2 sites (see Fig. 5-66) and the corresponding reduction in the median ALWR capacity to 1.30g from 1.50g for rock. At category S3 sites the results are nearly the same, only 4 sites do not exceed the risk goal. These sites are located in the mid-western states; Arkansas, Clinton, Wolf Creek, and Davis Besse.

7.3 Regional Seismic Risk Calculations and Comparison to Site-Specific Results

Using the hazard curves generated in the regional-seismic hazard analysis, the ALWR mean frequency of core damage is calculated at each site in the regional grid. The risk calculations are performed for each site category and corresponding ALWR core-damage fragility curve. Figures 7-1 to 7-5 identify areas on a grid map where the frequency of core-damage exceeds 10^{-6}, based on the regional-seismic hazard input. (Recall, the regional-risk estimates must be calibrated with the site-specific results in order to make a final determination of locations where the target risk level of 10^{-6} may be exceeded.) The map in Figure 7-1 also indicates the sites where site-specific hazard calculations were performed.

Table 7-2 lists the calculated mean-annual frequency of core damage derived from the regional-seismic hazard results for the locations where site-specific risk estimates are available. The comparison between the site-specific seismic-risk estimates and the regional calculations is quite good. For the results on rock sites, the regional risk estimates are within a factor of 2 of the site-specifc estimates at 18 sites and w thin a factor of 3 at 23 sites. The regional-risk estimates typically deviate from the site-specific result in areas of known high seismic activity, such as in the Charleston and New Madrid areas. As discussed in Section 5 this can be attributed to the fact that the maximum magnitude values used in the seismic hazard assessment are low for these regions.

For the soil sites, the regional- and site-specific results are closer (than for rock sites) with the exception of category S5 soils where only 13 of the regional-risk estimates are within a factor of 2 of their site-specific counterpart. When the regional-risk estimates deviate from the site-specific results, they are as likely to overestimate as underestimate the frequency of core damage.

7.4 Identifying High Seismic Hazard Areas

By systematically comparing the site-specific and regional-seismic risk

Table 7-2

ALWR Mean Frequency of Seismic Core-Damage
Regional Seismic Hazard

Site	Rock	S2	S3	S4	S5
			EPRI/SOG Site Category		
Seabrook	8.92-7	1.49-[illegible]	5.76-6	1.75-6	1.43-6
Pilgrim	8.69-7	1.32-5	5.14-6	1.62-6	1.34-6
Maine Yankee	3.18-7	5.91-6	2.25-6	6.56-7	5.27-7
Millstone	3.16-7	5.83-6	2.25-6	6.64-7	5.36-7
New England	3.57-6	5.45-5	2.09-5	6.49-4	5.35-6
Virginia 1	1.42-6	2.13-5	8.30-6	2.63-6	2.18-6
Virginia 2	6.69-7	1.00-5	3.87-6	1.22-6	1.01-6
Surry	1.50-7	2.19-6	1.23-6	3.26-7	2.51-7
North Anna	5.65-7	9.53-6	3.64-6	1.09-6	8.85-7
New Madrid 1	2.47-6	5.02-5	1.85-5	5.04-6	3.94-6
New Madrid 2	4.17-7	9.32-6	3.40-5	8.99-7	6.94-7
New Madrid 3	1.60-5	2.28-4	8.96-5	2.88-5	2.41-5
New Madrid 4	7.20-6	1.05-4	4.09-5	1.30-5	1.08-5
Arkansas	1.08-7	1.85-6	7.00-7	2.01-7	1.60-7
Catawaba	6.06-7	9.36-6	3.60-6	1.12-6	9.25-7
Oconee	8.58-7	1.56-5	5.86-6	1.70-6	1.37-6
Watts Bar	1.08-6	1.70-5	6.62-6	2.06-6	1.70-6
Sequoyah	6.57-7	1.11-5	4.25-6	1.28-6	1.05-6
Charleston 1	7.22-7	1.14-5	4.38-6	1.35-6	1.11-6
Charleston 2	5.05-7	7.85-6	3.03-6	9.42-7	7.77-7
Charleston 3	4.03-7	6.60-6	2.53-6	7.74-7	6.32-7
Charleston 4	2.59-7	4.53-6	1.72-6	5.08-7	4.11-7
Vogtle	4.07-7	6.65-6	2.56-6	7.83-7	6.41-7
Summer	7.12-7	1.07-5	4.18-6	1.32-6	1.10-6
Limerick	5.61-7	8.68-6	3.34-6	1.04-6	8.54-7
Anna, Ohio	1.37-6	1.80-5	7.13-6	2.37-6	2.01-6
Clinton	5.24-7	7.66-6	2.95-6	9.37-7	7.81-7
Wolf Creek	3.31-7	4.90-6	1.89-6	5.99-7	4.96-7
Davis Besse	2.61-7	4.38-6	1.69-6	5.10-7	4.16-7

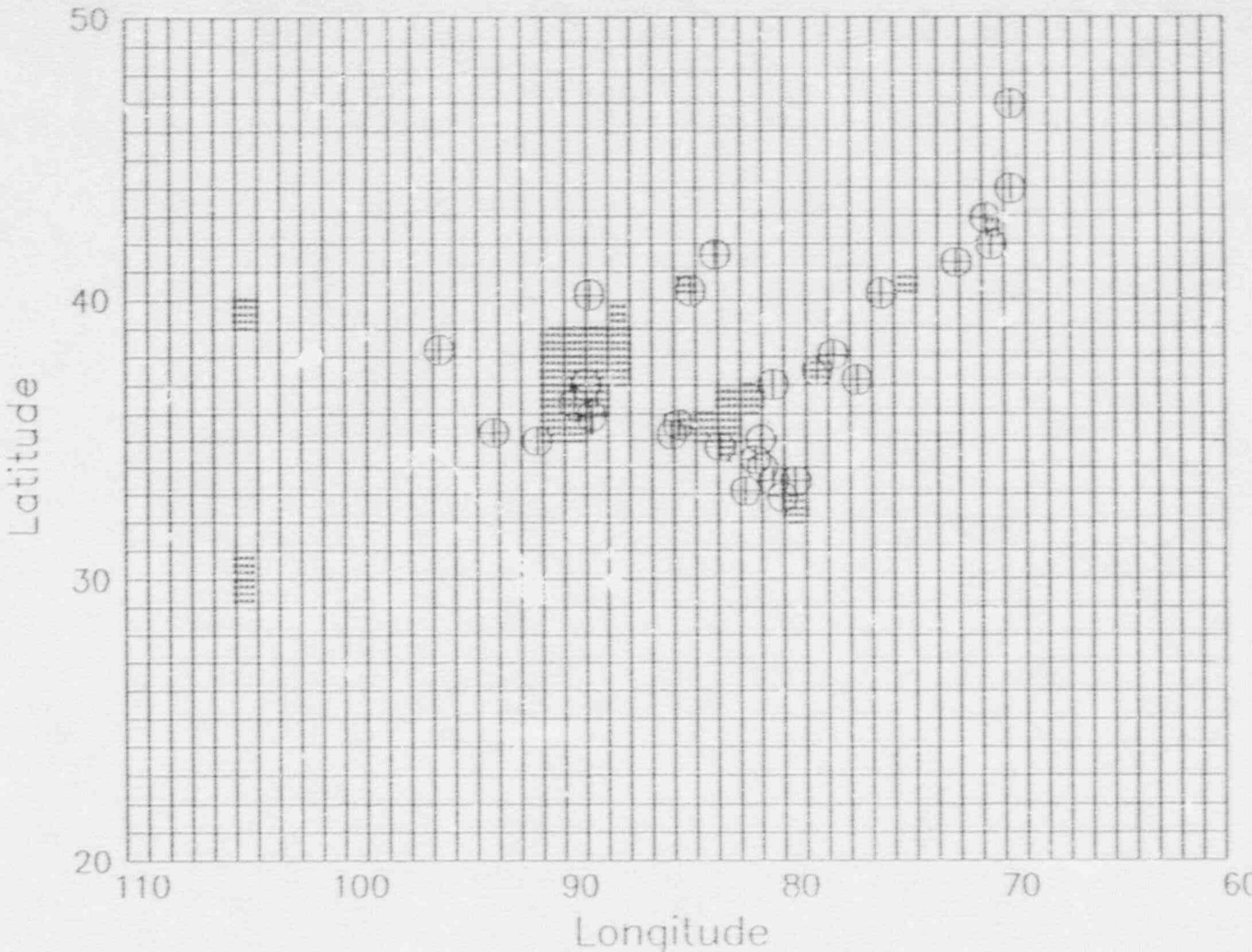

Figure 7-1. Map of areas where the target seismic risk level is exceeded, based on the regional seismic hazard calculations results for rock sites. The circles denote locations where site-specific hazard calculations were performed.

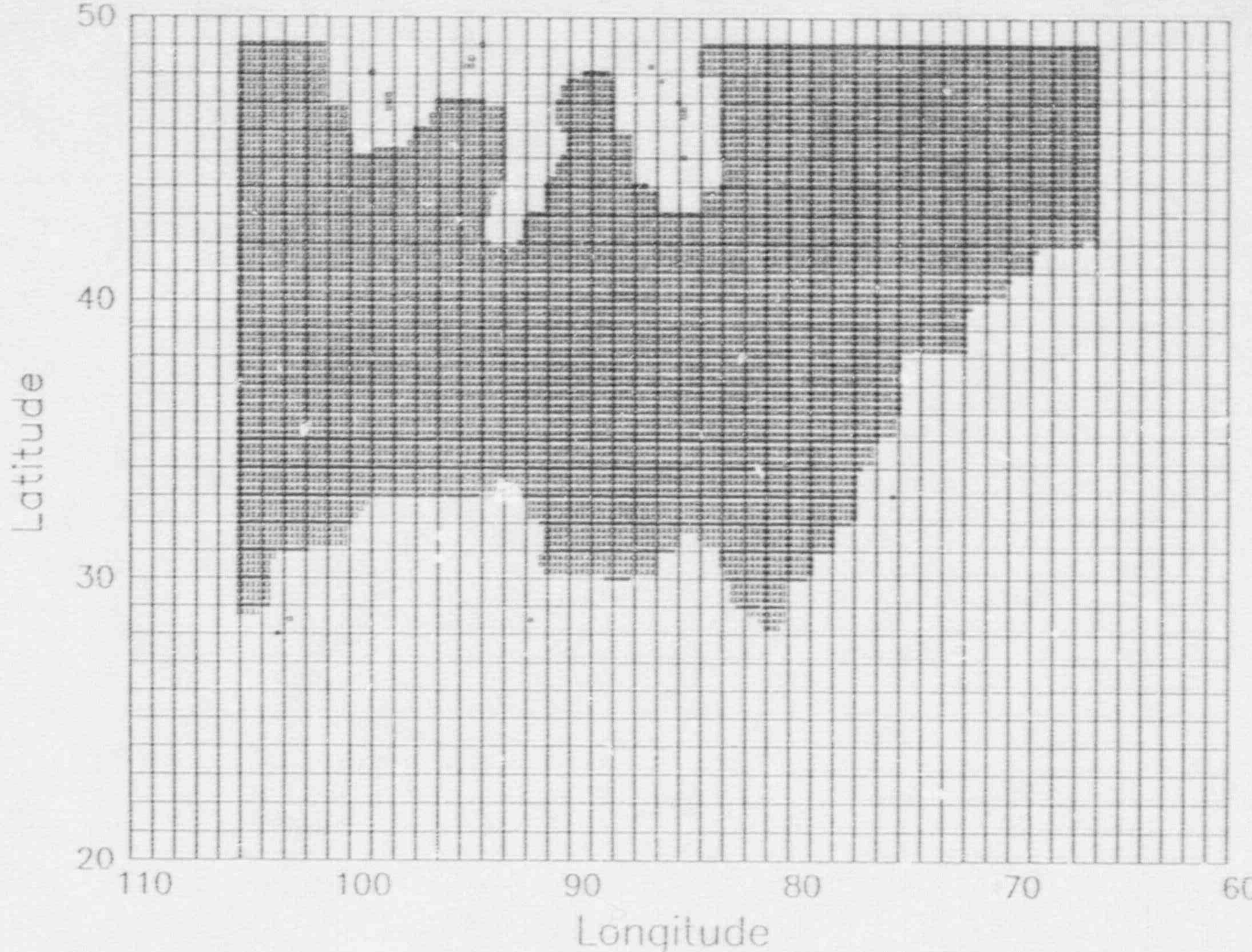

Figure 7-2. Map of areas where the target seismic risk level is exceeded, based on the regional seismic hazard calculations results for S2 sites.

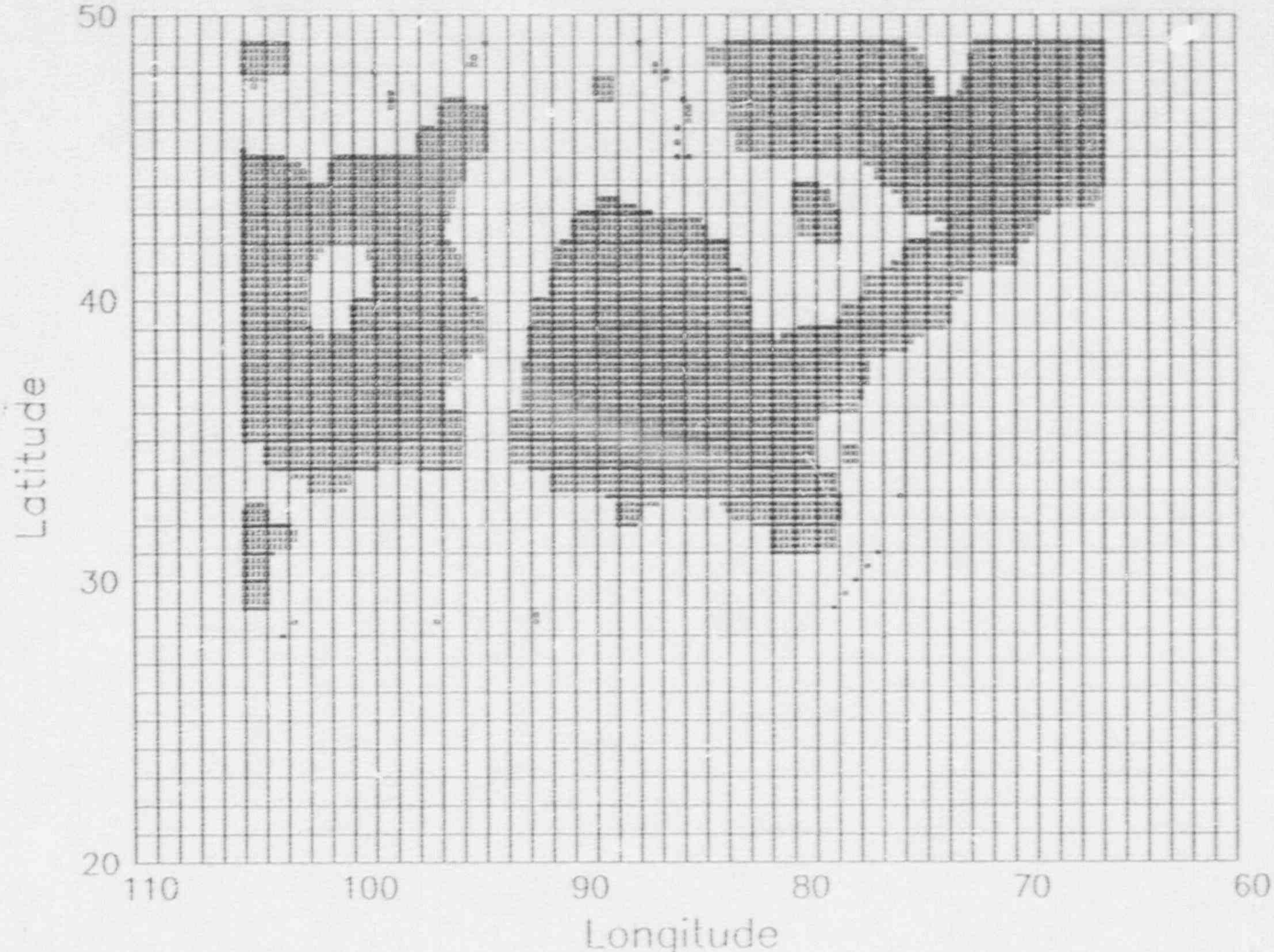

Figure 7-3. Map of areas where the target seismic risk level is exceeded, based on the regional seismic hazard calculations results for S3 sites.

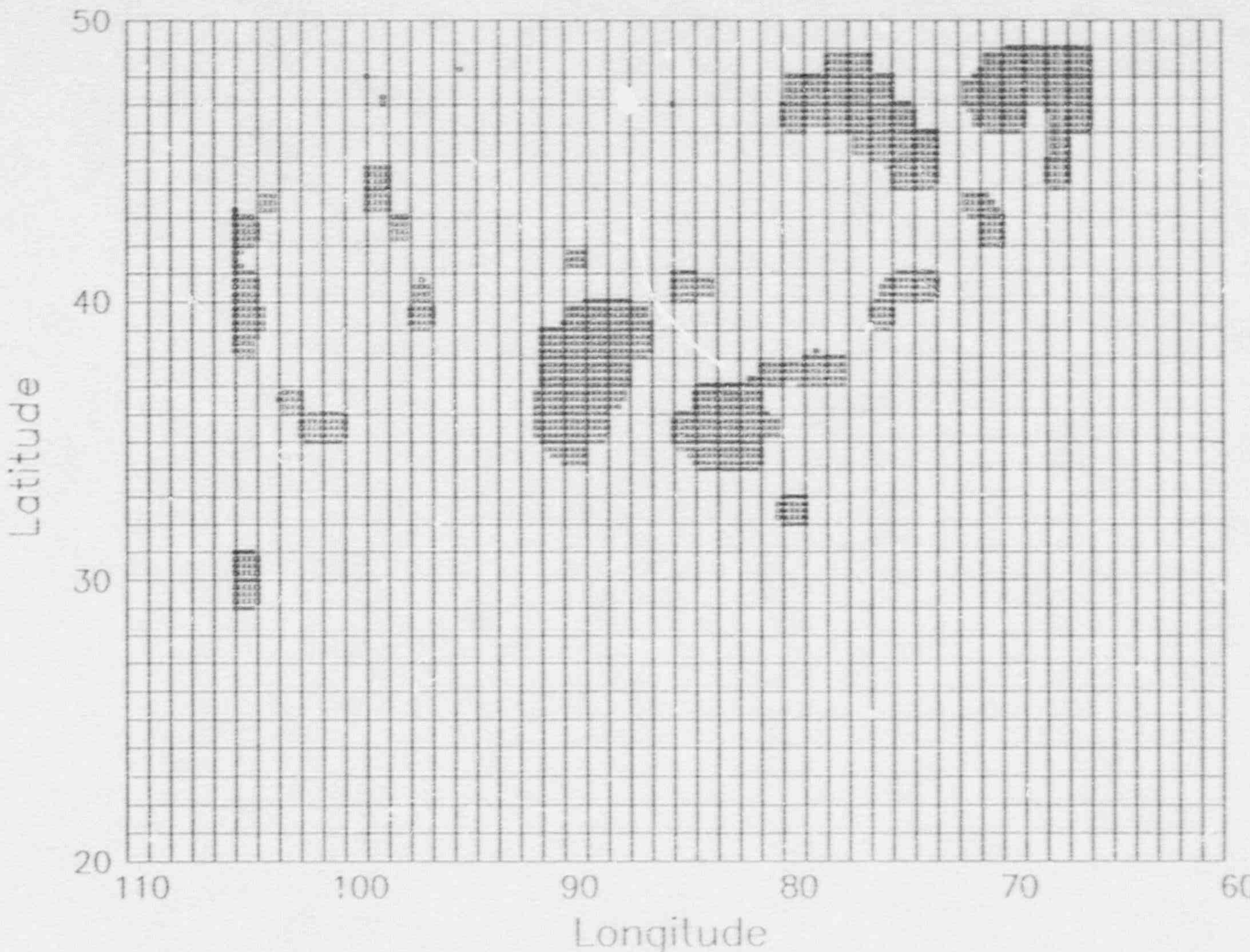

Figure 7-4. Map of areas where the target seismic risk level is exceeded, based on the regional seismic hazard calculations results for S4 sites.

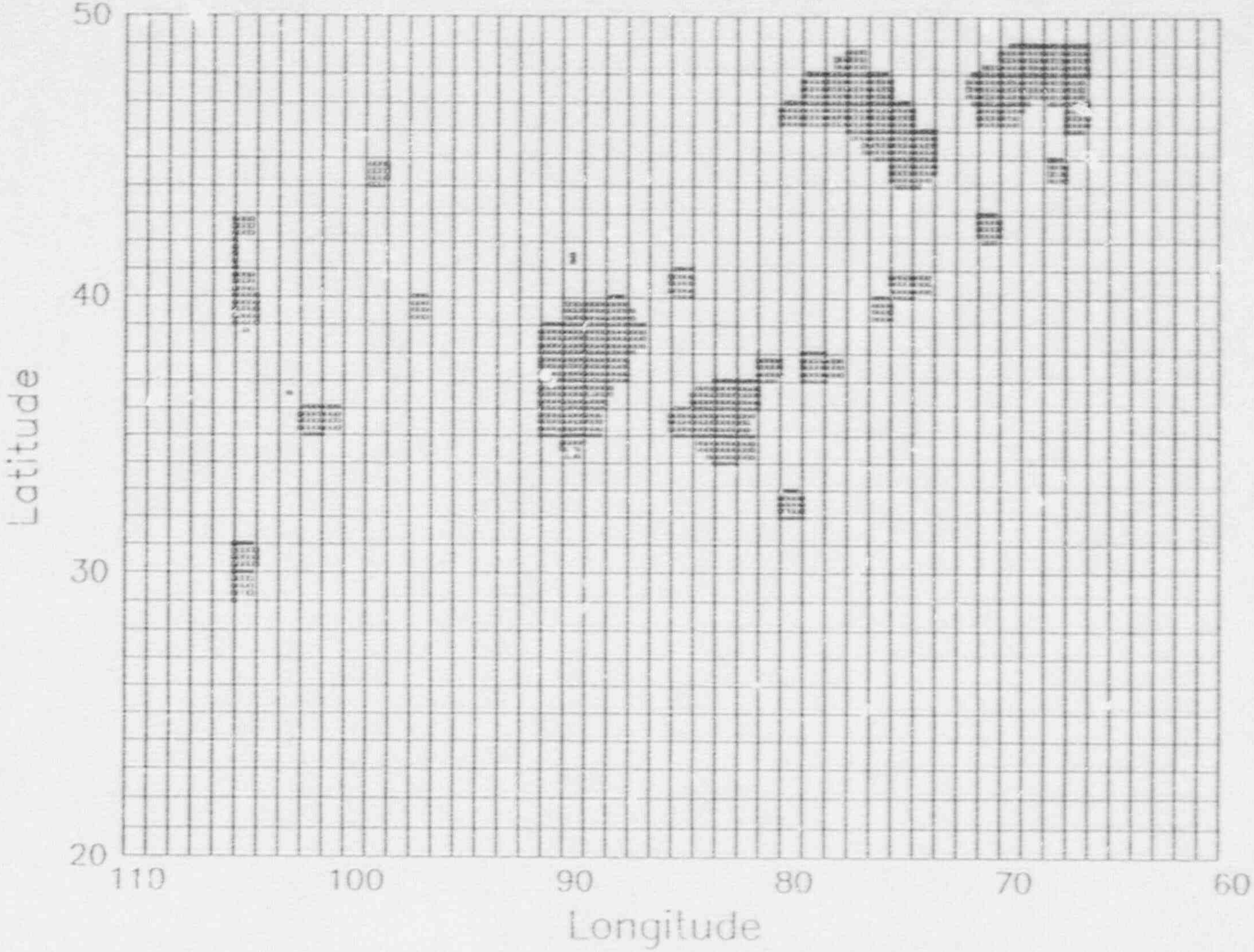

Figure 7-5. Map of areas where the target seismic risk level is exceeded, based on the regional seismic hazard calculations results for S5 sites.

estimates, areas where the target ALWR seismic level may be exceeded are identified.

The basis, in order of preference, to calibrate the regional risk map consists of the following steps:

1. Direct comparison with the site-specific risk results,
2. Comparison with EPRI/SOG results at existing nuclear power plant sites (5), and
3. Comparison of m_{max} values assigned by the EPRI/SOG Earth Science Teams to those used in the regional hazard calculation.

Once the general areas where the ALWR seismic risk is expected to exceed the target risk level were identified, the spatial distribution of the regional risk estimates was used to define the area bounds. This process was carried out for each site category.

The results of this process define the areas where the ALWR seismic risk target may be exceeded. These results are reported in Section 8. The map for site category S2 requires special mention. For category S2 the site-specific risk estimates indicate that the frequency of core damage exceeds 10^{-6} at each of the 29 sites. Furthermore, the map of the regional-risk calculations suggests the ALWR target level risk will be exceeded nearly everywhere in the EUS. By examining the seismic hazard results obtained in the EPRI/SOG seismic hazard project (5) for sites where site-specific calculations are absent in this study, a further calibration of the regional hazard results can be made. A comparison of the EPRI/SOG results and those produced in this study indicate they are comparable to about 1.0g. This comparison is particularly useful in the gulf coastal area and in the southeast. In the midwest (i.e., Nebraska, Oklahoma, Iowa, Kansas, etc.) a comparison of the EPRI/SOG Earth Science Team m_{max} values and those assigned in the regional hazard calculations provided a basis to calibrate the results in this area.

The conclusion of this assessment is that the regional-hazard results overestimate the seismic hazard and thus the ALWR seismic risk in the southeast, gulf coast and midwest areas. In most of the remaining parts of the EUS, the seismic hazard and ALWR seismic risk is well defined by the regional and site-specific calculations. As a result, for category S2 sites, large areas are identified where the ALWR target seismic risk level may be exceeded. Similar comparisons were made for category S3 sites, however, the areas where the ALWR target risk level may be exceeded are not as extensive.

8.0 ALWR SEISMIC HAZARD

8.1 Introduction

The results of the previous sections are used to define the ALWR SH for each site category which includes:

- ALWR mean seismic hazard curve,
- ALWR response-spectrum shape,
- Consideration of the hazard/fragility interface.

These topics are discussed in the following sections.

8.2 ALWR Seismic Hazard Curve

Recall from Section 2 that the ALWR SH curve is defined as a mean hazard curve, which integrated with the ALWR mean core-damage fragility curve equals a target risk level of 10^{-6}. To determine the ALWR SH for each site category, the mean-core damage frequency estimates obtained using the site-specific hazard curves were reviewed. For each soil category a site was identified whose risk estimate was equal to or approximately equal to the target level. The mean hazard curve for this site was scaled such that the mean frequency of core damage would exactly equal 10^{-6}. This defined the ALWR SH curve. The ALWR SH curves for each site category are shown in Figure 8-1 and are listed in Table 8-1.

Other features of the ALWR SH are:

- the ALWR SH is defined in terms of peak ground acceleration. The PGA is the mean of the two-horizontal components of ground motion, and
- motion occurs at the ground surface.

The PGA is used to scale the ALWR ground response-spectrum shape to determine the seismic hazard at individual spectral values. Because the seismic hazard

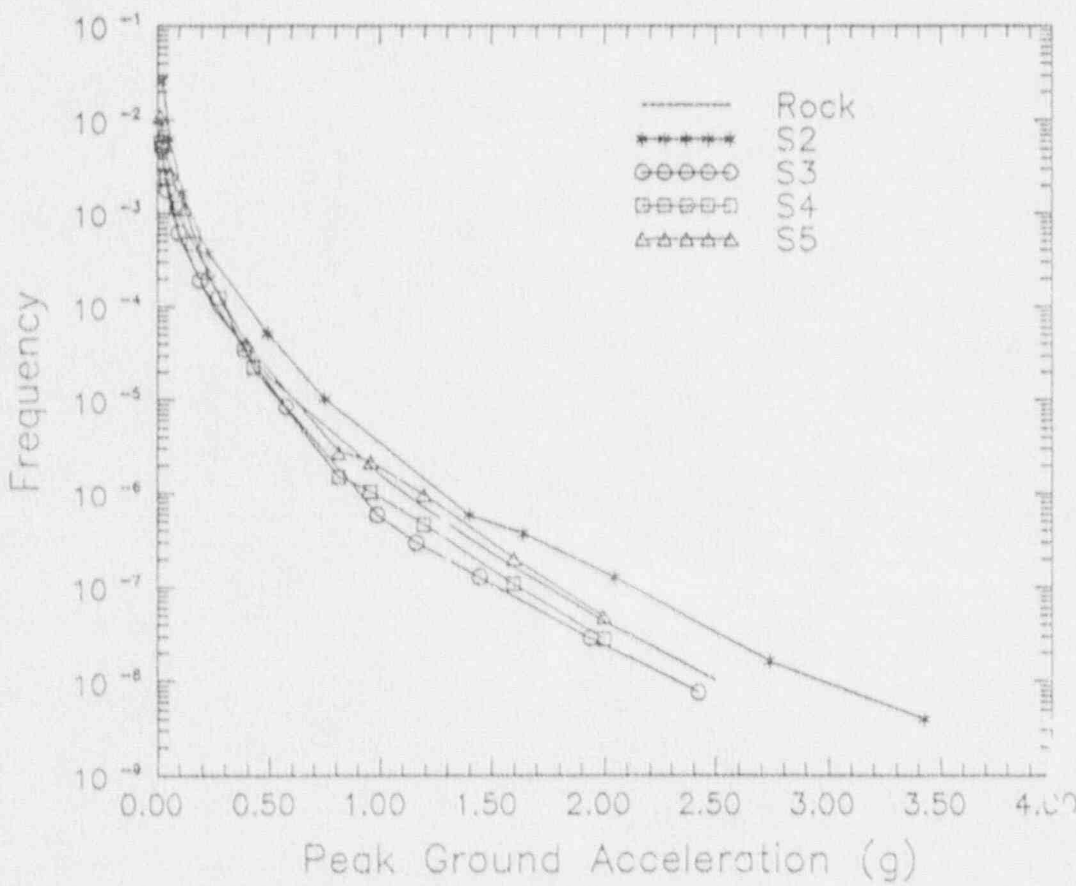

Figure 8-1 ALWR seismic hazard curves for each soil category in the EUS. (see Figures 8-2 to 8-6 for areas where the seismic hazard may exceed the ALWR SH.)

Table 8-1

ALWR Seismic Hazard Curves For Each Site Category

Rock		S2		S3		S4		S5	
PGA (g)	Exceedance Frequency	PGA (g)	Exceedance Frequency	PGA (g)	Exceedance Frequency	PGA (g)	Exceedance Frequency	PGA (g)	Exceedance Frequency
0.010	7.478-3	0.023	2.513-2	0.019	5.165-3	0.016	5.820-3	0.012	1.102-2
0.026	3.390-3	0.057	6.364-3	0.048	1.764-3	0.041	2.464-3	0.031	5.396-3
0.051	1.493-3	0.114	1.656-3	0.097	6.239-4	0.081	1.138-3	0.061	2.698-3
0.102	5.265-4	0.230	3.611-4	0.195	1.896-4	0.164	4.770-4	0.123	1.131-3
0.254	9.450-5	0.493	5.147-5	0.389	3.491-5	0.280	1.214-4	0.229	2.292-4
0.502	1.725-5	0.753	1.041-5	0.577	8.519-6	0.427	2.230-5	0.402	3.926-5
1.021	1.455-6	1.399	5.865-7	0.991	5.879-7	0.817	1.489-6	0.817	2.727-6
1.198	7.140-7	1.642	3.711-7	1.162	2.988-7	0.959	1.045-6	0.959	2.176-6
1.493	2.363-7	2.046	1.277-7	1.448	1.284-7	1.195	4.647-7	1.195	9.666-7
2.000	4.372-8	2.739	1.628-8	1.940	2.856-8	1.600	1.060-7	1.600	2.011-7
2.499	1.028-8	3.424	3.950-9	2.424	7.679-3	1.999	2.826-8	1.999	4.825-8

is defined as the motion at the ground surface, the base input motion must consider soil-structure interaction effects and deconvolution due to structure embedment as part of the fragility analysis.

8.3 Ground Response Spectrum and Soil Effects

The ALWR response-spectrum shape is defined as the average 10^{-6} UHS (over a wide range of sites) for the EUS. The response spectra are defined for each site category and are paired with the corresponding ALWR SH curve. Figure 8-2 shows the ALWR response spectrum shapes for each soil category. The spectral values are listed in Table 8-2.

The UHS are derived from ground motion models that define a smooth response spectrum shape. To incorporate the peak-to-valley variability in actual earthquake response spectra, a logarithmic standard deviation of 0.20 should be used (19). This variability is incorporated in the seismic fragility assessment.

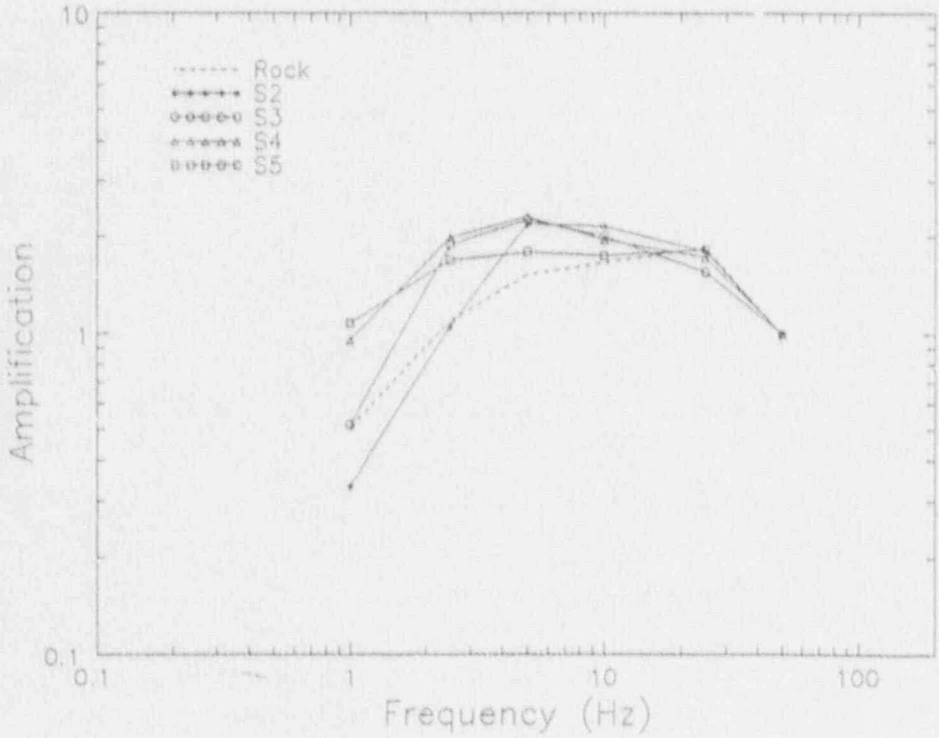

Figure 8-2 ALWR ground response spectrum shapes for each site category.

Table 8-2

ALWR Response Spectra For Each Soil Category

Frequency (hz)	Soil Category Rock	S2	S3	S4	S5
1.0	0.504	0.332	0.516	0.951	1.078
2.5	1.097	1.055	1.893	1.991	1.702
5.0	1.532	2.192	2.268	2.307	1.801
10.0	1.668	2.15[illegible]	2.014	1.961	1.755
25.0	1.862	1.804	1.563	1.736	1.838
5C.0*	1.000	1.000	1.000	1.000	1.000

* Assumed frequency at which response spectra return to PGA

8.4 Site-Specific Hazard Evaluations

In certain areas, the mean-seismic hazard may exceed the ALWR SH curve. As a result the mean frequency of core damage may exceed the 10^{-6} target level at these locations. In this case a site-specific hazard calculation may be required. Figures 8-3 to 8-7 show the areas where the frequency of core damage may exceed the ALWR target risk level for each soil category, respectively.

A site-specific seismic hazard assessment must be performed for all potential sites located west of 105°W longitude.

8.5 Hazard/Fragility Interface

In a seismic PRA an approach must be defined to interface the hazard and fragility parts of the analysis. A requirement is that the method chosen should effectively characterize the potential of seismic ground motion to damage ALWR structures and equipment. The hazard/fragility interface establishes the method used to describe the ground motion hazard and the parameter used to define component fragilities.

In the ALWR seismic risk assessment the seismic hazard is characterized in terms of a single seismic hazard curve and a ground response spectrum shape. Because earthquakes of different size generate ground motions with differing characteristics, engineers prefer that seismic hazard be deaggregated with respect to earthquake size (19). In this way the potential of earthquakes of different magnitude to damage structures and equipment can be evaluated. However, in seismic design/analysis and in PRA applications the seismic hazard curve is presented in an aggregated format. (The ground motions generated by all magnitude earthquakes are combined into a single seismic hazard curve.)

In the ALWR seismic risk assessment, the hazard/fragility interface is defined in the following terms:

- Seismic hazard curve - a single mean hazard curve expressed in terms of the mean-peak horizontal ground acceleration. The hazard is estimated for events greater than magnitude 5.0. The seismic hazard curve includes the total variability in ground motion. This variation incorporates the randomness of earthquake source characteristics and ground motion attenuation.

- Ground Response Spectrum - UHS for EUS defined in terms of the mean shape and the peak-to-valley variability.

- Seismic Fragility - structure and component capacities are defined in terms of the mean peak horizontal ground acceleration and are evaluated using the ALWR ground response spectrum shape.

Expressing the seismic hazard input in this format provides a practical, but generally conservative characterization of the seismic hazard.

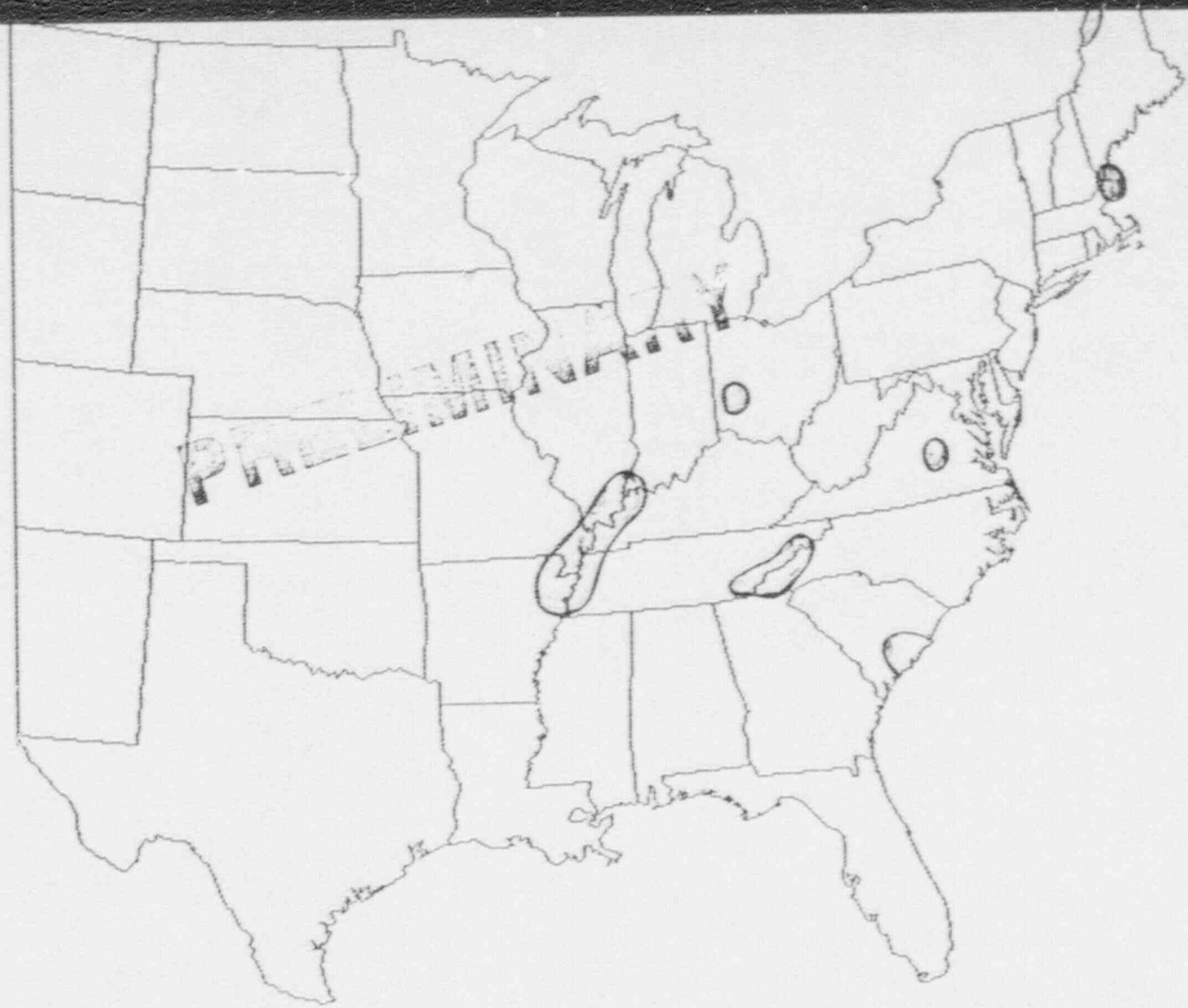

Figure 8-3 Areas in the EUS where the ALWR seismic risk may be greater than 10^{-6} per year for rock site conditions. Site-specific hazard assessments may be required for plants located in these areas.

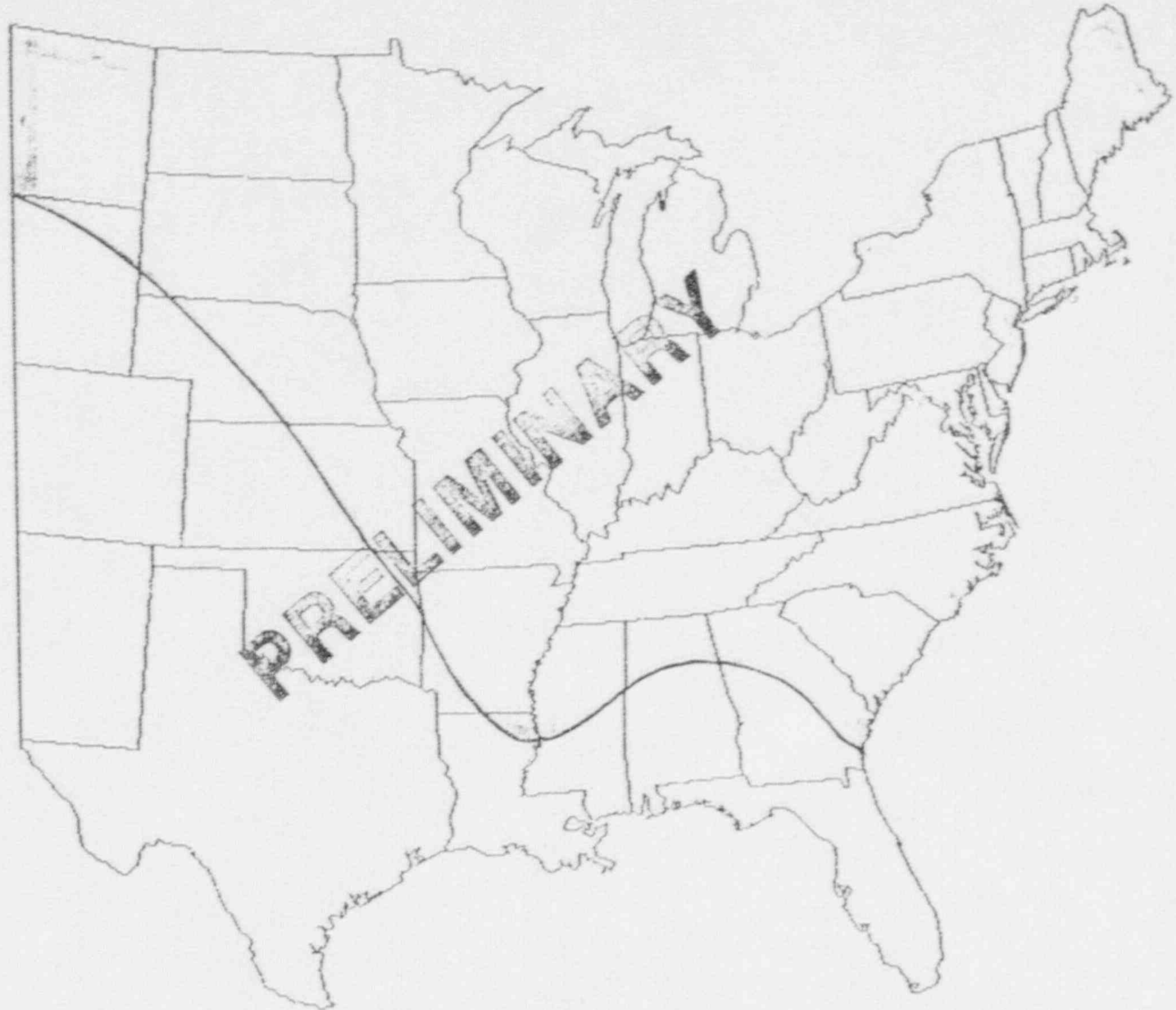

Figure 8-4 Areas in the EUS where the ALWR seismic risk may be greater than 10^{-6} per year for soil category S2 sites. Site-specific hazard assessments may be required for plants located in these areas.

Figure 8-5 Areas in the EUS where the ALWR seismic risk may be greater than 10^{-6} per year for soil category S3 sites. Site-specific hazard assessments may be required for plants located in these areas.

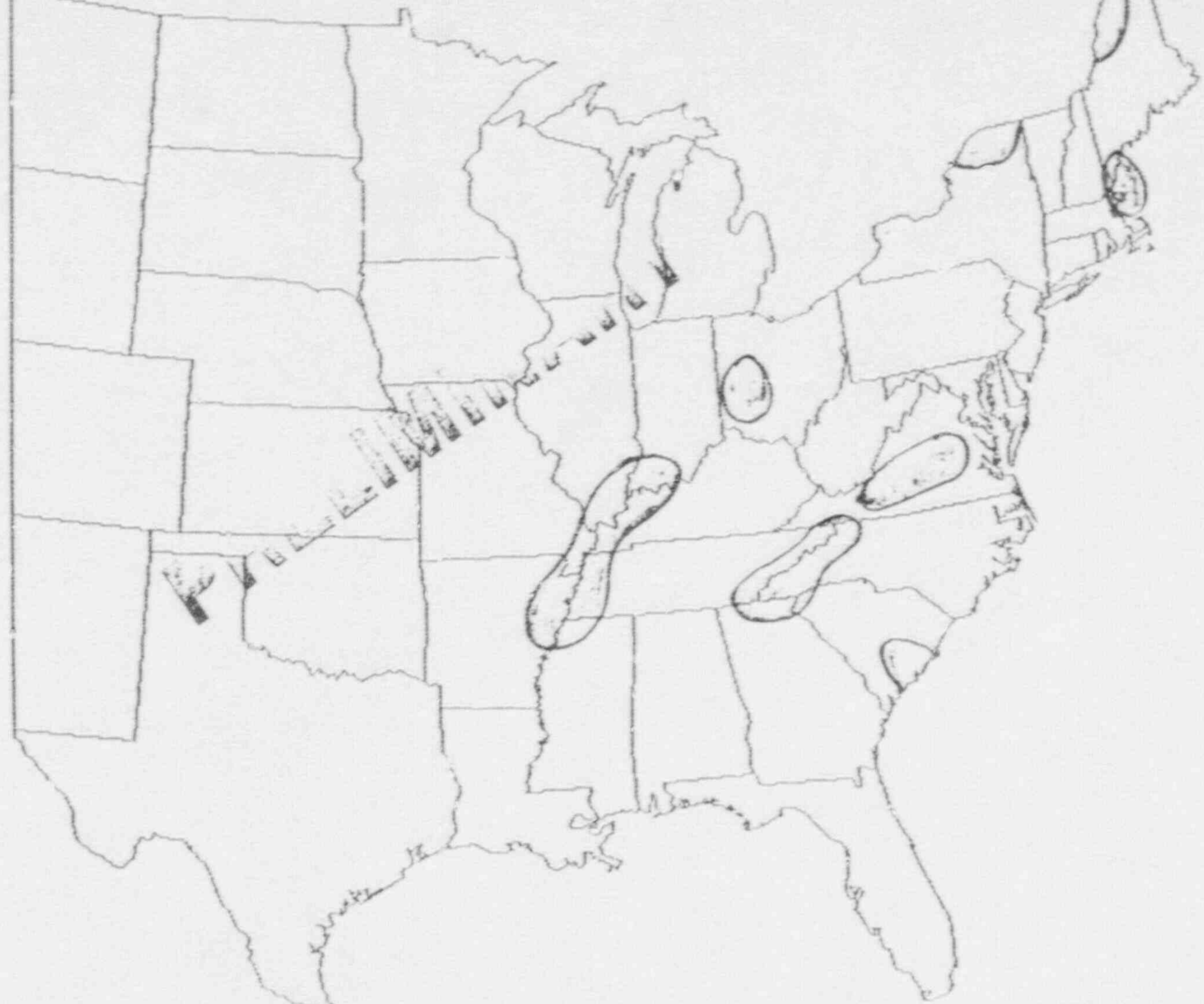

Figure 8-6 Areas in the EUS where the ALWR seismic risk may be greater than 10^{-6} per year for soil category S4 sites. Site-specific hazard assessments may be required for plants located in these areas.

Figure 8-7 Areas in the EUS where the ALWR seismic risk may be greater than 10^{-6} per year for soil category S5 sites. Site-specific hazard assessments may be required for plants located in these areas.

REFERENCES

1. S. T. Algermissen, D. M. Perkins, P. C. Thenhaus, S. L. Hanson, and B. L. Bender, "Probabilistic Estimates of Maximum Acceleration and Velocity in Rock in the Contiguous United States," U.S. Geological Survey, Open-File Report 82-1033, 1982, p. 99.

2. R. K. McGuire, et. al., "Seismic Hazard Methodology for the Central and Eastern United States," NP-4726, Volume 1, Part 1. Methodology. Electric Power Research Institute, Palo Alto, California, Revision 1, November 1988.

3. D. L. Bernreuter, J. B. Savy, R. W. Mensing and J. C. Chen, "Seismic Hazard Characterization of 69 Nuclear Plant Sites East of the Rocky Mountains, Methodology Input Data and Comparisons to Previous Results for Ten Sites," Volume 1-8, prepared for U.S. Nuclear Regulatory Commission, Lawrence Livermore National Laboratory, NUREG/CR-5250, UCID-2157, January 1989.

4. R. K. McGuire, et. al., "Seismic Hazard Methodology for the Central and Eastern United States," NP-4726, Volume 3. Revision 1, User's Manual, Electric Power Research Institute, Palo Alto, California, 1988.

5. Electric Power Research Institute, "Resolution of the Charleston Earthquake Issue," NP-6395-D, Palo Alto, California, April 1989.

6. Risk Engineering, Inc. "Engineering Models of Earthquake Ground-Motion for Eastern North America," NP-6074. Electric Power Research Institute, Palo Alto, California, October 1988.

7. C. A. Cornell, Memo to B. Ellingwood, R. P. Kennedy, and J. W. Reed, 1988.

8. B. Ellingwood, "Presentation to NRC Fragility Evaluation Committee," Electric Power Research Institute, Palo Alto, California, March 1988.

9. Western Geophysical Corporation, "Seismic Hazard Methodology for the Central and Eastern United States," NP-4726, Volume 5: Tectonic Interpretations, Electric Power Research Institute, Palo Alto, California, July 1986.

10. Dames and Moore, Inc., "Seismic Hazard Methodology for the Central and Eastern United States," NP-4726, Volume 6: Tectonic Interpretations, Electric Power Research Institute, Palo Alto, California, July 1986.

11. Law Engineering Testing Company, "Seismic Hazard Methodology for the Central and Eastern United States," NP-4726, Volume 7: Tectonic Interpretations, Electric Power Research Institute, Palo Alto, California, July 1986.

12. Woodward Clyde Consultants, "Seismic Hazard Methodology for the Central and Eastern United States," NP-4726, Volume 8: Tectonic Interpretations, Electric Power Research Institute, Palo Alto, California, July 1986.

13. Bechtel Group, Inc., "Seismic Hazard Methodology for the Central and Eastern United States," NP-4726, Volume 9: Tectonic Interpretations, Electric Power Research Institute, Palo Alto, California, July 1986.

14. Rondout Associates, Inc., "Seismic Hazard Methodology for the Central and Eastern United States," NP-4726, Volume 10: Tectonic Interpretations, Electric Power Research Institute, Palo Alto, California, July 1986.

15. D. M. Boore, and G. M. Atkinson, "Stochastic Prediction of Ground Motion and Spectral Response Parameters at Hoard-Rock Sites in Eastern North America," Bulletin of the Seismological Society of America, Vol. 77, No. 2, 1987.

16. O. W. Nuttli, Appendix C-A. Seismic Hazard Characterization of the Eastern United States, Volume 2: Questionnaires. Letter to D. Chung, Lawrence Livermore National Laboratory, UCID-20421. Prepared for the U.S. Nuclear Regulatory Commission, April 1985.

17. D. L. Bernrueter, J. C. Chen and J. B. Savy, "Development of Site-Specific Response Spectra," NUREG/CR-4861, UCID-20980, Lawrence Livermore National Laboratory, Prepared for the U.S. Nuclear Regulatory Commission, March 1987.

18. N. A. Abrahamson, "Statistical Properties of Peak Ground Accelerations Recorded by the SMART 1 Array," Bulletin of the Seismological Society of America, Vol. 78, No. 1, February, 1988.

19. Pacific Gas and Electric Company, "Final Report of the Diablo Canyon Long Term Seismic Program," Docket Nos. 50-275 and 50-323, San Francisco, California, July 1988.

20. I. M., Idriss, "Evaluating Seismic Risk in Engineering Practice," Procledings of the Eleventh International Conference on Soil Mechanics and Foundation Engineering, San Francisco, California, August 12-16, 1985, A.A. Balkema/Rotterdam, Boston, 1985.

21. Row, III, L.W., "An Earthquake Strong-Motion Data Catalog for Personal Computers, SMCAT, User Manual, Release 1.0," World Data Center for Solid Earth Geophysics, National Geophysical Data Center, National Oceanic and Atmospheric Administration, Boulder, Colorado, 1988.

22. J. N. Brune, "Tectonic Stress and the Spectra of Seismic Shear Waves from Earthquakes," Journal Geophysical Research, Vol. 75, 1971.

23. McGarr, A. "Upper Bounds on Near-Source Peak Ground Motion Based on a Model of Inhomogeneous Faulting," Bulletin of the Seismological Society of America, Vol. 72, No. 6, December, 1982.

24. T. C. Hanks and D. A. Johnson, Geophysical Assessment of Peak Accelerations," Bulletin of the Seismological Society of America, Vol. 66, No. 3, June, 1976.

25. N. N. Ambraseys, "Dynamics and Response of Foundation Materials in Epicentral Regions of Strong Earthquakes," Proceedings of the Fifth World Conference on Earthquake Engineering, Rome, Italy, 1973.

26. K. W. Campbell, "Near-Source Attenuation of Peak Horizontal Acceleration," Bulletin of the Seismological Society of America, vol. 71, 1981.

27. G. M. Atkinson, "Attenuation of Strong Ground Motion in Canada From a Random Vibrations Approach," Bulletin of the Seismological Society of America, Vol. 74, No. 6, December 1984.

28. W. B. Joyner and D. M. Boore, "Peak Horizontal Acceleration and Velocity From Strong-Motion Records Including Records From the 1979 Imperial Valley, California Earthquake," Bulletin of the Seismological Society of America, Vol. 71, No. 6, December 1981.

29. K. W. Campbell, "Progress Report, Near-Source Estimation of Strong Ground Motion For the Eastern U.S.," Prepared for U.S. Nuclear Regulatory Commission, 1985.

30. Risk Engineering, Inc., "EQHAZARD Primer," prepared for Electric Power Research Institute, Palo Alto, California, Draft, November, 1987.

31. M. W. McCann, Jr., A. C. Boissonnade and H. Hadidi-Tamjed, "Development of Seismic Hazard Input for the Advanced Light Water Reactor Seismic PRA," prepared for Electric Power Research Institute, May 1988.

32. M. W. McCann, Jr. and J. W. Reed, "Lower-Bound Magnitude for Probabilistic Seismic Hazard Assessment," EPRI NP-6496, Electric Power Research Institute, Palo Alto, California, October 1989.

33. Nuclear Regulatory Commission, "Development of Criteria for Seismic Review of Selected Nuclear Power Plants," by N. M. Newmark and W. J. Hall, NUREG/CR-0098, May 1978.

34. The Industry Degraded Core Rulemaking Program, "IDCOR Position Paper on Treatment of External Events Within the Severe Accident Policy," April, 1987.

35. Risk Engineering, "A Decision Framework and Approaches for Using Seismic Hazard Results to Resolve Issues of Nuclear Plant Seismic Safety," prepared for Electric Power Research Institute, Palo Alto, California, May 1988, Draft.

36. R. P. Kennedy and M. K. Ravindra, "Seismic Fragilities for Nuclear Power Plant Risk Studies," Nuclear Engineering and Design, Vol. 79, No. 1, May 1984.